Aus der Klinik und Poliklinik für Diagnostische und Interventionelle Radiologie der Universitätsmedizin der Johannes Gutenberg-Universität Mainz

und der Klinik für Diagnostische und Interventionelle Radiologie, Kemperhof, Akademisches Lehrkrankenhaus der Universitätsmedizin der Johannes Gutenberg-Universität Mainz

Quantifizierung und Standardisierung von epikardialem Fettgewebe in der Diagnostik der koronaren Herzkrankheit

Quantification and Standardization of Epicardial Adipose Tissue in Diagnostic of Coronary Artery Disease

Inauguraldissertation

zur Erlangung des Doktorgrades der

Medizin

der Universitätsmedizin

der Johannes Gutenberg-Universität Mainz

Vorgelegt von

Andrej Dobrovolskij

aus Vilnius, Litauen

Mainz, 2024

Wissenschaftlicher Vorstand: Univ.-Prof. Dr. Hansjörg Schild

Tag der Promotion: 12. März 2025

Table of contents

List of abbreviations

AF – atrial fibrillation

AIVG – anterior interventricular groove

ANOVA – analysis of variance

AUC – area under the receiver operating characteristic curve

BAT – brown adipose tissue

BMI – body mass index

BSA – body surface area

CAD – coronary artery disease

CCS – coronary calcium score

CD – cluster of differentiation

COVID-19 – Coronavirus disease 2019

cm^3 – cubic centimeter

CMR – cardiac magnetic resonance

CT – computed tomography

EAT – epicardial adipose tissue

ECG – electrocardiogram

EISNER – Early Identification of Subclinical Atherosclerosis by Non-invasive Imaging Research

et al. – and others

FFA – free fatty acids

g – gram

IIVG – inferior interventricular groove

IL – interleukin

ISL –interventricular septum length

kg – kilogram

LAD – left anterior descending coronary artery

LAVG – left atrioventricular groove

LCX – left circumflex coronary artery

LVFW – left ventricular free wall

m^2 – square meter

MACE – major adverse cardiac event

MCP-1 – monocyte chemoattractive protein-1

MESA – Multiethnic Study of Atherosclerosis

mg – milligram

MHz – megahertz

mm – millimeter

MRI – magnetic resonance imaging

ms – millisecond

PAI-1 – plasminogen activator inhibitor-1

PET – positron emission tomography

RAVG – right atrioventricular groove

RCA – right coronary artery

ROC – receiver operating characteristic

RVFW – right ventricular free wall

SIVG – superior interventricular groove

SPECT – single-photon emission computed tomography

SSFP – steady state free precession

TNF-α – tumor necrosis factor – α

T1IR – inversion recovery prepared T1 weighted gradient echo sequence

UCP – unique uncoupling protein

vs. – versus

WAT – white adipose tissue

18F-FDG – 18F-Fluorodeoxyglucose

18F-FDG-PET–CT – 18F-Fluorodeoxyglucose Positron Emission Tomography – Computed Tomography

List of figures

List of tables

1 Introduction and goals of research

1.1 Burden of cardiovascular diseases and coronary artery disease

Cardiovascular diseases are the main cause of death worldwide. According to World Health Organization, an estimated 17.9 million people die from cardiovascular diseases annually, which represents approximately 1/3 of all global deaths (1). Coronary artery disease (CAD) is an important health condition that is responsible for approximately 7.4 million deaths per annum across the globe (2). In Germany, the CAD mortality rate lies in the middle-risk zone and is approximately 350 cases per 100000 (3). CAD remains the main cause of morbidity and mortality in both developing and developed countries (4). In 2013, World Health Organization and its member states aimed to reduce the premature mortality rate from cardiovascular diseases by 25% by the year 2025 (5).

The search for novel cardiovascular risk factors that significantly contribute to CAD, continues to this day. The aim of this search targets more sensitive measures for cardiovascular risk stratification as well as therapeutic targets for treatment and prevention of CAD (6).

1.2 Nomenclature, morphology and physiology of adipose tissue

Cardiovascular diseases are associated with excessive adiposity (7). Obesity is defined as a body mass index (BMI) ≥30 kilogram/square meter (kg/m^2). It stands for one of the preventable causes of increased morbidity and mortality in western societies. Furthermore, obesity is one of the CAD risk factors that could be modified (8). One way of lowering the risk of major adverse cardiac events (MACE) is reduction of adipose tissue depots (9). In addition, recent studies have revealed that not only the amount of adipose tissue, but also its distribution is important for the occurrence of cardiovascular diseases, including CAD. Unfortunately, BMI alone fails to take into consideration variations in quality and distribution of adipose tissue (10). Therefore, diverse secretome profiles and depot-specific differences of adipose tissue subgroups are important to understand the association of adiposity with cardiovascular diseases (11).

Adipose tissue contains several cell types – mature adipocytes, preadipocytes and stromal cells (blood cells, endothelium, immune cells). Adipose tissue is grouped according to physiology, embryological origin and morphology. Currently it is divided into white adipose tissue (WAT) and brown adipose tissue (BAT). The differences between WAT and BAT are listed in Table 1 (12).

Properties	White adipose tissue	Brown adipose tissue
Location	subcutaneous, visceral	deep cervical, supraclavicular, interscapular
Function	energy reserve	production of heat
Lipid droplets	large, single	small, multiple
Amount of mitochondria	+	+++
Expression of UCP1	-	+++
Effect on CAD	Promoting	suppressing

Table 1. Heterogeneity of adipose tissue. Abbreviations: CAD – coronary artery disease, UCP – unique uncoupling protein

BAT continues to be a subject of intense scientific research since its purpose has not been yet fully understood. BAT arises from dermomyotome precursor cells and expresses the unique uncoupling protein 1 (UCP1) on the inner mitochondrial membrane (13). This suggests certain correspondence with skeletal muscle cells, whose development is based on similar pathways (14). BAT has high vascularization and innervation; it is found in small deposits. BAT expresses an abundant supply of mitochondria. Therefore, brown fat dissipates energy in the form of heat, as a result of circumvent adenosine triphosphate (ATP) production. This process is called non-shivering thermogenesis (15). Moreover, BAT coordinates the metabolic rate of the body, protecting it from stressful hemodynamic states such as hypoxia (16). In adults BAT is present within the neck and cranial chest areas (17). Reduced BAT function is closely connected to cardiovascular risk, obesity and impaired metabolic conditions (18). Finally, BAT has also been shown as a potential therapeutic target in severe cases of obesity (19).

WAT is responsible for mechanical protection of the body and organs, fat storage, it acts as an energy source. White fat derives from mesodermal stem cells (20). According to anatomical allocation, WAT is classified into subcutaneous and visceral fat tissues (21).

Visceral adipose tissue is defined as a fat of trunk and abdomen which primarily covers internal organs. In contrast, subcutaneous adipose tissue is present mainly on hips, thighs and under the skin in hypodermis (22). Subcutaneous adipose tissue is found to be less metabolically or lipolytically active. Therefore, it is associated with lower cardiovascular risk than visceral adipose tissue (23).

There is solid evidence that visceral adipose tissue provides a much higher cardiovascular risk than peripheral subcutaneous fat (24). Anti-inflammatory functions of the continuously expanding visceral fat eventually shift to pathophysiologic pro-inflammatory state (25). Visceral adiposity is associated with systemic inflammatory and metabolic changes that determine the development of cardiovascular diseases (26). The relationship between cardiovascular risk and adipose tissue is not only determined by the quantity of the latter, but more importantly by the location in which it is stored (27). As an illustration, abdominal adipose tissue is the largest visceral fat depot in the human body. As a result, it is significantly associated with the risk of cardiac events (28-30).

1.3 Epicardial adipose tissue as a novel cardiovascular risk factor

Visceral adipose tissue surrounding the heart muscle, which is directly connected to coronary arteries, is of special concern. This fat deposit is named epicardial adipose tissue (EAT). EAT has emerged as a new modifiable cardiometabolic risk factor besides abdominal depots of visceral adipose tissue. In contrast to visceral abdominal adipose tissue, EAT represents a small portion of total body fat (31).

EAT is identified as a visceral WAT, it has direct contact with the myocardium. As a result, epicardial fat interacts with the heart in a more direct way. EAT is located between myocardium and visceral pericardium, it covers more than three quarters of the surface of the heart (32). Larger epicardial fat depots are located in the areas of coronary grooves, cardiac apex and over the right ventricular free wall (RVFW) (6). EAT does not only directly contact with coronary arteries and myocardium, but also has the same blood supply as the heart muscle (32).

EAT shows unusual biochemical properties and is actively participated in the energy and lipid homeostasis (33). Functions of EAT include the mechanical protection of coronary arteries from the arterial pulse wave during contraction of the heart muscle, thermoregulation and the storage of the free fatty acids (FFA) for the consequent application in the heart muscle during energy demand (34). In addition, EAT produces a bright spectrum of biological active molecules which systemically regulate vascular smooth muscle tone. During physiological conditions these substances protect the human body from atherogenesis and inflammation

(35,36). Molecules produced by EAT interact with the body systemically as they are directly secreted into coronary arteries (37).

Excess of EAT leads to its hypoxia. As a result, EAT begins to produce large quantities of various pro-inflammatory cytokines and vasoactive peptides (mainly interleukin (IL) 6, tumor necrosis factor – α (TNF-α), angiotensin II, plasminogen activator inhibitor-1 (PAI-1)) (6, 34-36 38-40, 41, 42). The adipokine concentration in pericoronary epicardial fat is much higher than that of subcutaneous adipose tissue (43). All pro-inflammatory substances independently facilitate the production of atheromatous plaques in coronary vessels and thus, the progress of CAD (6). Atherosclerotic process in coronary arteries is additionally promoted by endothelial dysfunction, local proliferation of smooth muscle cells, increased oxidative stress, plaque instability, apoptosis and neovascularization (44).

1.4 Quantification and indexation of epicardial adipose tissue

In the past years, the accurate quantification of EAT has been allowed, as a result of rapid progress in non-invasive imaging techniques. The size of epicardial fat depots may be measured using different radiological modalities – above all transthoracic echocardiography, computed tomography (CT) and cardiac magnetic resonance (CMR) imaging. Nonetheless, recent literature reviews have suggested CMR to be the gold standard in evaluation of the size of EAT depots (6, 45, 46). EAT are estimated by measuring thickness on different sites and volume (45, 47, 48). CMR and CT rank superior to echocardiography since cross-sectional imaging techniques allow the volumetric quantification of EAT. Although echocardiography can only provide measurements of EAT thickness, it is non-invasive, cheap and easy to perform as a screening test (49).

Recently, non-invasively quantified increased epicardial fat depots have demonstrated a relationship with the presence and progression of CAD, coronary plaque burden measured with coronary calcium score (CCS), subclinical atherosclerosis, MACE, myocardial ischemia, metabolic syndrome, atrial fibrillation (AF) and lipotoxic cardiomyopathy (50-61). Overall, observational studies in patients undergoing coronary angiography have suggested a positive association between increased EAT measurements and the presence of CAD (45). Recent meta-analysis conducted by Nerlekar and others (et al.) demonstrated that incorporation of EAT measurements into the clinically performed radiological imaging would have the potential to improve patient risk stratification (62). Furthermore, ultrasound EAT thickness measurements over the RVFW and in the anterior interventricular groove (AIVG) were shown to be valuable variables in identification of individuals with CAD (63, 64). Finally, it has been demonstrated that larger EAT depots might be associated with plaque instability in patients with CAD. Authors speculated that specific threshold of EAT could exist, above which epicardial fat would facilitate changes of coronary plaque composition (65).

Because there is no guideline-advocated technique for EAT quantification, individual studies are subject to authors discretion and experience (62). This generates confusion and increases the need for standardized evaluation techniques of epicardial fat depots in clinical practice. EAT holds the potential to be a strong marker for cardiovascular risk assessment, as well as a possible therapeutic target to reduce the burden of cardiovascular diseases (51, 62).

EAT is regarded as a better predictor of CAD than commonly known estimators of adiposity such as BMI (61, 66, 67). Unfortunately, there is a lack of research in terms of the comparison between different quantification methods of EAT in prediction of CAD patients. It is not clear whether EAT thickness measured at a single point could be comparable with the volumetric assessment of epicardial fat. Occasional EAT and CMR studies published to date have analyzed small samples of subjects, authors did not perform receiver operating characteristic curve (ROC) analysis with EAT measurements (68-70). As a result, the representation of small study population is doubtful to determine reference values of EAT size in prediction of CAD.

Most of the published studies presented EAT thickness measurements over the RVFW (45, 48, 61, 71, 72). Nonetheless, Hirata et al. introduced a novel echocardiographic EAT thickness measurement in the area of AIVG. Authors suggested that it could be a better prognostic parameter for predicting coronary lesions than thickness measurement over the RVFW. Researchers validated EAT values on CT images by calculating EAT volume in some patients of the study sample (49). In another example, Wang et al. recommended to measure EAT thickness in the left atrioventricular groove (LAVG). Authors suggested that LAVG EAT thickness could offer a more accurate metabolic risk prediction than other EAT thickness measurements. Unfortunately, authors did not evaluate gathered EAT values in respect to CAD (73). Finally, the meta-analysis conducted by Nerlekar et al. proposed a complete volumetric assessment of epicardial fat rather than linear EAT thickness measurements (62). Some authors indicated that the difficulty in standardizing measurement locations limits the determination of possible EAT reference values (45). Although CMR modality has been viewed as a gold standard for evaluation of adipose tissue, it was to this day rarely employed in quantification of EAT in CAD patients (54, 68-70, 74-77). EAT thickness over the left ventricular free wall (LVFW) was never quantified in CAD patients using CMR modality.

Fewer studies are available on the topic of EAT indexation. The effect of anthropometric EAT variability is assumed to play an important role in identifying individuals with increased cardiovascular risk (78). Besides various non-indexed EAT depots measurements, some authors derived EAT amounts indexed to body surface area (BSA) or to BMI (79, 80). As an illustration, Shmilovich et al. in their study concluded that BSA-indexed EAT volume significantly predicted MACE in patients with CAD (80). Moreover, Nakazato et al. showed that BMI, body weight and waist circumference exhibited moderate relationship with epicardial fat volume – changes in these parameters were associated with the size variations of EAT depots (81). Finally, Saad et al. demonstrated that BSA- and BMI-indexed, as well as non-indexed EAT volume, have an equivalent predictive power in prediction of significant CAD (79). Generally, EAT volume was to this day rarely indexed in clinical studies. EAT thickness was on the other hand never indexed to this day. As a consequence, there were no studies published on the topic of possible advantages of indexed EAT thickness measurements in comparison to non-indexed counterparts in identification of individuals with CAD. Furthermore, no studies indexed EAT with anthropometric heart measurements such as interventricular septum length (ISL).

1.5 Goals of research

In this study we aimed to compare predictive powers of various EAT measurement techniques in identification of patients with CAD. Moreover, this study aimed to answer whether indexed EAT measurements bring advantage in comparison to non-indexed counterparts in prediction of CAD. To achieve these goals, the study aimed to accomplish the following tasks:

1. Assessment of EAT ability to predict CAD.
2. Identification of the most effective EAT measurement technique (indexed or non-indexed) in prediction of CAD.
3. Determination of reference cut-off values of the most effective EAT measurement techniques in prediction of CAD.
4. Analysis of possible connection between EAT measurements and CAD severity.

2 Literature review

2.1 Nomenclature of thoracic adipose tissue

The nomenclature of thoracic adipose tissue varied from study to study, especially during the first years of research on the topic of EAT. Fortunately, in the following years the terminology became more consistent and uniform, allowing to avoid possible confusion when addressing histologically different types of adipose tissue (36, 45, 48, 82-89). Table 2 shows short definitions of different thoracic fat deposits surrounding the heart.

Fat deposits	Definition
Paracardial fat	Mediastinal adipose tissue outside the parietal pericardium
Pericardial fat	Thin layer of adipose tissue between visceral and parietal pericardium
Epicardial fat	Adipose tissue located between visceral pericardium and myocardium without adjacent fascial plane
Pericoronary fat	Part of epicardial fat directly surrounding the coronary arteries

Table 2. Nomenclature of thoracic adipose tissue surrounding the heart.

The anatomy and distribution of thoracic adipose tissue is displayed in Figure 1.

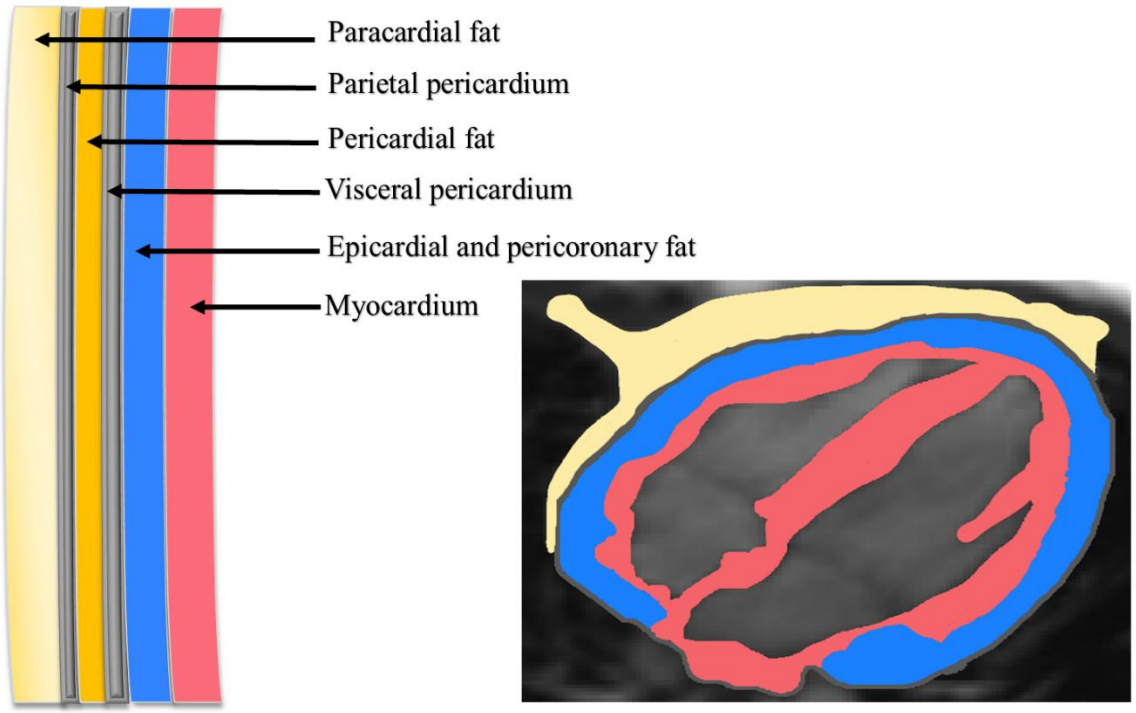

Figure 1. Anatomy and distribution of thoracic adipose tissue surrounding the heart.

Paracardial adipose tissue (mediastinal or intrathoracic fat) – is a fat deposit that exists outside the parietal pericardium (71, 90). It covers approximately 80% of the heart and constitutes

between 20-50% of the cardiac mass (91). Paracardial fat derives from the primitive thoracic mesenchyme, unlike EAT, which evolves from splanchonopleuric mesoderm (92). In contrast to EAT, paracardial adipose tissue is supplied by the branches of internal thoracic artery such as pericardiacophrenic artery (93). Paracardial fat depots differ from EAT in molecular and biochemical properties (66, 94). Gene expression in paracardial adipose tissue is closer to WAT. There is evidence that the release rate of FFA by paracardial fat is twice as lower as by EAT (95). Authors, estimating the paracardial adipose tissue, consider pericardium, bronchi and aorta as the posterior limit, and chest wall as the anterior limit (45).

Pericardial fat describes the very thin layer of fat tissue that is located between visceral and parietal layers of pericardium (88).

Pericoronary adipose tissue is an EAT which directly surrounds adventitia of the coronary vessels without separating fascial layer between vascular wall and fat tissue. Pericoronary fat is most prominent around the proximal portions of coronary arteries (96, 97). It contains vasa vasorum – a system of small blood vessels that supply the larger arteries and veins. Perivascular adipose tissue is referred to as a beige fat. It contains BAT markers such as UCP1. However, the amount of UCP1 is considerably lower in pericoronary fat as compared to brown adipocytes (35, 98).

2.2 Epicardial adipose tissue

2.2.1 Anatomy, vasculature and embryology

EAT is situated between the epicardial surface of the heart and the visceral surface of pericardium. Pericardium is seen on radiological modalities as a thin layer (1-4 millimeter (mm)) around the heart (99). Epicardial fat deposits are enclosed by the pericardial sac and directly surround coronary vessels without separating fascial layer (32).

In healthy individuals, the mass of EAT averages 100 g. EAT represents 20% of the total weight of the heart and it covers approximately 80% of the heart surface (91, 100). EAT is divided into pericoronary epicardial fat which encloses the coronary arteries; myocardial adipose deposits in the heart muscle; and epicardial fat which is found over the myocardium (42). EAT is most concentrated in the areas of atrioventricular and interventricular grooves at both ventricles, extending to the apex of the heart (35, 101). As a result, coronary arteries, which travel through the area of the cardiac grooves, are covered within EAT. Smaller epicardial fat deposits are located on the free walls of the atria and ventricles as well as around the atrial appendages (71). In some cases, EAT may cover the entire cardiac surface as the volume of epicardial fat increases (102). The number of adipocytes per gram (g) in EAT is increased in comparison to other fat depots, and the size of adipocytes is significantly smaller (103).

Coronary arteries supply both EAT and myocardium. No fascia or aponeurotic tissue separate EAT from coronary artery wall or the myocardium. As a result, EAT, heart muscle and coronary vessels are in direct contact with one another. This enables a setting of local close interaction between the coronary vessels and EAT (32).

Both EAT and visceral adipose tissue (including omental and mesenteric fat) have a common origin (42, 104). EAT derives from splanchnopleuric mesoderm – BAT cells migrated from septum transversum (67). Human data reveal that vascular and cardiac adipose tissues are brown during early stages of life (85). They maintain brown properties in adulthood despite whitening with age (105). In newborns both vascular and cardiac fat deposits consist of multilocular, UCP1 positive adipocytes. However, during the course of childhood (1–8 years), EAT cells shift to unilocular, UCP1 negative adipocytes with only small remaining islands of

UCP1 positive cells (82). Nevertheless, the amount of BAT markers (such as UCP1) in adult EAT remains higher than in other thoracic or ectopic fat deposits (106, 107).

The most traditional activator of BAT cells along with the browning process of WAT is hypothermia (108). Activated WAT cells are called beige (brown in white) adipocytes. They were first discovered in cold-acclimated mice (19). Beige cells contain multiple lipid droplets with triglycerides as wells as countless mitochondria (109). They are characterized by the positive expression of UCP1 (110). It should be noted that both beige and active BAT cells offer protection from metabolic disease and atherogenic process – reinducing a brown phenotype in cardiac and vascular adipose tissue alleviates local inflammation and hypoxia of the adjacent vascular wall (106).

EAT consists of more than adipocytes and pre-adipocytes – it involves nodal and nervous tissue (ganglia, interconnecting nerves) (31). Immune, vascular and stromal cells (lymphocytes cluster of differentiation 3- (CD3-), macrophages CD68-, mast cells) have been identified as resident cells in EAT as well (102).

2.2.2 Physiologic functions

EAT serves a number of physiologic functions, it plays an important role in primary functions of the heart (84). First of all, EAT acts as an energy source to the cardiomyocytes which have high demand for energy. Epicardial fat is responsible for the oxidation of FFA, converting them into lipid storage units, which serve as the main energy source to the contractile function of the heart (39). This process is responsible for about 50-70% of the energy production in the heart muscle (111). EAT is able to synthesize, incorporate and break FFA down at a very high rate (112). Therefore, it is considered that epicardial fat depots could perform as a shield between local vessels and the heart muscle, absorbing excessive intravascular FFA, and thus protecting the myocardium from lipotoxicity (94). EAT is notable to have the highest rate of FFA metabolism and lipogenesis of all known adipose tissue depots due to the presence of thermogenic genes (113). Moreover, epicardial fat is known to have lower rate of glucose utilization in comparison to other adipose depots (33). Finally, the amount of saturated fatty acids in the human EAT is higher and the amount of unsaturated fatty acids is lower in comparison to subcutaneous adipose tissue (103).

EAT, being a visceral fat deposit, acts as a topic gland and serves as a major source of different chemokines, biomolecules and cytokines, which are all called adipokines (33). Adipokines participate in the regulation of otherwise produced cytokines as well as in the lipid and glucose-insulin metabolism (114). Some of the substances show anti-inflammatory, anti-thrombotic and anti-atherogenic properties. Most important beneficial adipokines are adiponectin, adrenomedullin, omentin and UCP1 (6, 34, 35, 39, 41). Other substances, such as TNF-α, IL-1β, -6, -8, PAI-1, resistin, angiotensin II, leptin and monocyte chemoattractive protein-1 (MCP-1) are pro-inflammatory mediators (36, 38, 40, 42, 115, 116). All above listed adipokines are secreted in EAT by adipocytes as well as stromal pre-adipocytes, fibroblasts, mast cells, lymphocytes and macrophages (117).

Anti-atherogenic substances produced by EAT in healthy individuals participate in regulation and maintenance of vascular tone, preserve blood pressure and proper contractive ability of the heart muscle (118). It has been shown that adiponectin, adrenomedullin and omentin secreted by epicardial fat wield anti-atherogenic, anti-inflammatory and anti-diabetic effects in coronary vessels (119). Adiponectin is one of the most important anti-inflammatory adipokines generated by EAT. It increases insulin sensitivity, decreases circulating FFA in blood as well as intracellular triglyceride concentration in muscles and liver (45). The amount of adiponectin is lower in obese individuals with increased cardiovascular risk. It is inversely linked with the extent of visceral, epicardial and pericardial fat (120).

Table 3 shows important pro- and anti-inflammatory adipokines produced by epicardial fat and their main functions.

Adipokines	Main functions
Anti-inflammatory adipokines	
Adiponectin	• Transport and oxidation of FFA • Decrease of fat storage in EAT • Increase of insulin sensitivity • Vasodilation • Prevention of monocyte adhesion to endothelium
Adrenomedullin	• Antioxidant • Vasodilation • Inhibition of pro-inflammatory pathways and endothelial cell apoptosis • Elevation of cardiac output
Omentin	• Inhibition of fibrosis • Suppression of foam cells
UCP1	• Aid in mitochondrial release of heat • Anti-inflammatory brown adipose tissue properties
Pro-inflammatory adipokines	
TNF-α, IL-1β, IL-6, IL-8	• Induction of lipolysis • Mobilization of immune cells • Promotion of apoptosis • Inhibition of anti-inflammatory adipokines • Elevation of endothelial cell permeability • Insulin resistance
Visfatin	• Vascular remodeling and inflammation • Marker of visceral adipose tissue • Mobilization of immune cells
Resistin	• Thrombosis • Angiogenesis • Insulin resistance • Vascular remodeling and inflammation
Angiotensin II	• Mobilization of macrophages • Promotion of fibrosis • Vasoconstriction
Leptin	• Angiogenesis • Platelet aggregation • Proliferation of smooth muscle cells • Elevation of endothelial cell permeability • Destabilization of atheromatous plaques

Table 3. Adipokines secreted by epicardial adipose tissue and their roles. Abbreviations: EAT – epicardial adipose tissue, FFA – free fatty acids, IL – interleukin, TNF – tumor necrosis factor, UCP – unique uncoupling protein

EAT does not only contact directly with coronary arteries and myocardium, but also has the same blood supply as the latter. Therefore, secreted adipokines may interact with the body systemically (37). Presently, two interaction mechanisms have been described – paracrine and vasocrine (22). Pro-atherogenic adipokines, secreted by pericoronary EAT during paracrine

signaling, diffuse directly to the adjacent vascular wall and the heart muscle via interstitial fluid ("outside to inside" mechanism). Alternatively, vasocrine signaling suggests that pro-inflammatory adipokines, secreted from EAT, directly enter the vessels of closely located vasa vasorum (67).

EAT, as a result of the proximity to coronary vessels, mechanically protects them against the torsion induced by heart contraction and arterial pulse wave (100). EAT functions as an additional protective anatomic layer for the total heart mass in the event of mechanical injury. Moreover, epicardial fat provides space for the arterial wall expansion during the early stages of atherosclerosis (121).

EAT serves as an immune barrier, protecting the heart muscle and coronary arteries from pathogenic and inflammatory substances (122). Epicardial fat depots contain immune and stromal cells (lymphocytes CD3-, macrophages CD68-, mast cells and other) (102).

Finally, EAT expresses thermogenic genes which are associated with brown and beige adipose tissue (123). Therefore, epicardial fat is able to protect the heart during ischemia or hypothermia by providing direct heat to the heart muscle (33). Moreover, larger distribution of thermogenic EAT around the coronary vessels suggests that it may be involved in maintaining normal myocardial temperature by heating blood in coronary arteries on the way to the heart muscle (124).

2.2.3 Dysfunction and transition to pathological inflammatory state

Although EAT is essential for the heart muscle, it has been noted over the past decades that growing epicardial fat depots promote the risk of cardiovascular diseases. Greater EAT depots have been described as clinical markers of excessive visceral adiposity (125). Increase in the size of EAT, for instance among obese patients, is associated with increased CCS, CAD, subclinical atherosclerosis, metabolic syndrome, cardiac arrhythmias, lipotoxic cardiomyopathy (50-60). Recently, EAT has become a new target for numerous prevention strategies of cardiovascular diseases (126).

In states of positive energy balance, FFA are transformed into triglycerides in the blood and then stored in adipocytes (36). During both overnutrition and ageing, WAT increases in the size by hypertrophy of mature adipocytes and hyperplasia of adipocyte precursors (20). Similar to this, lipid droplets in BAT gather fat, becoming hypertrophic and eventually exceeding the vascular supply. These changes are defined by failure to store triglycerides, increased lipolysis and inflammation (41). As a result, adipocytes become impaired, leading to cell apoptosis, rarefaction of capillary vessels and fibrosis (127).

To further describe the transition phase, the process of "brown to white" transdifferentiation of EAT in patients with cardiovascular diseases is represented by decrease of thermogenic genes and upregulation of WAT adipogenesis (128). This remodeling of adipose tissue results in a systemic chronic inflammatory state since the phenotype of adipose cells shifts from a protective to inflamed profile (10). An increased incorporation and oxidation of FFA in the heart muscle eventually leads to the development of cardiac lipotoxicity (also known as cardiac steatosis) (129). As a result, adipose tissue infiltrates the myocardium, thus, further predisposing to various pathologic cardiovascular conditions (31). Interestingly, advanced chronic inflammation impairs the differentiation process of small and immature adipose cells into large adipocytes, rich in intracellular fat (100).

Finally, excess of EAT causes its hypoxia, leading to a diminished mitochondrial function and adrenergic signaling (130, 131). As a consequence, epicardial fat is invaded by greater numbers of T-lymphocytes and macrophages, resulting in a shift of a metabolic profile to the inflammatory state (132). Preadipocytes are capable of differentiation into macrophages as well (133). Inflamed and large adipose cells manifest insulin resistance and greater release of FFA into the bloodstream (67). Thus, EAT becomes dysfunctional (131).

2.3 Modalities used to quantify epicardial adipose tissue

Accurate estimation of EAT depots could serve as a prognostic tool for identification of patients with CAD and other cardiovascular diseases (125). The size of epicardial fat depots may be measured using different radiological modalities: transthoracic echocardiography, CT and CMR. EAT depots are estimated by measuring EAT thickness in different locations and volume (45, 47, 48). Several important properties of non-invasive imaging modalities, used for EAT assessment, are listed in Table 4.

Imaging modality	Spatial resolution	EAT measurements	Cost	Strengths	Limitations
Cardiovascular magnetic resonance	+++ (gold standard)	Thickness, area, volume, proton density fat fraction	+++	• No radiation • No iodinated contrast media • Can be coupled with spectroscopy	• Low accessibility • Time consuming • Less tolerable by patients
Cardiac computed tomography	+++	Thickness, area, volume, attenuation	++	• CAD evaluation • Assessment of perivascular adipose tissue	• Radiation exposure • Intravenous contrast when appropriate
Positron emission tomography – computed tomography	++	Radiotracer uptake (metabolic and inflammatory activity)	+++	• High sensitivity • Functional examination	• Radiation exposure • Interference caused by the radiotracer distribution in blood and surrounding tissues
Transthoracic echocardiography	+	Thickness (limited to RVFW and AIVG)	+	• Readily available • No radiation • No contrast media	• Volumetric quantification not possible • Variable imaging quality • Limited by the quality of acoustic window • Poor reproducibility

Table 4. Imaging modalities used for assessment of epicardial adipose tissue quantity and quality. Abbreviations: AIVG – anterior interventricular groove, CAD – coronary artery disease, EAT – epicardial adipose tissue, RVFW - right ventricular free wall

Incorporation of EAT assessment in clinical praxis has the potential to improve patient risk stratification in detection of cardiovascular diseases (61). Non-invasive quantification of EAT might improve identification of early subclinical CAD among high-risk patients without visible coronary lesions. In subjects with stable CAD, EAT measurements could help to recognize individuals with higher risk of experiencing a MACE (134). Nevertheless, further studies are required to confirm these assumptions (62).

2.3.1 Transthoracic echocardiography

In 2003, EAT thickness has been first described and measured by Iacobellis et al. with the transthoracic two-dimensional echocardiography (135). Patients are placed in the left lateral decubitus position and echocardiography is performed during several (usually three) cardiac cycles (136). A sector probe is used for the examination (2-3 MHz (megahertz), spatial resolution – 0.5 mm). EAT is defined as an echo free space between the external wall of the myocardium and the visceral layer of the pericardium (Figure 2). Echocardiographic thickness of EAT is measured in parasternal long and short axis views over the RVFW in at least two locations, since it contains the highest adipose tissue thickness, followed by the anterior wall

(137). The ultrasound beam is directed perpendicularly with the aortic annulus as a landmark (138). Epicardial fat should not be confused with pericardial fluid (139).

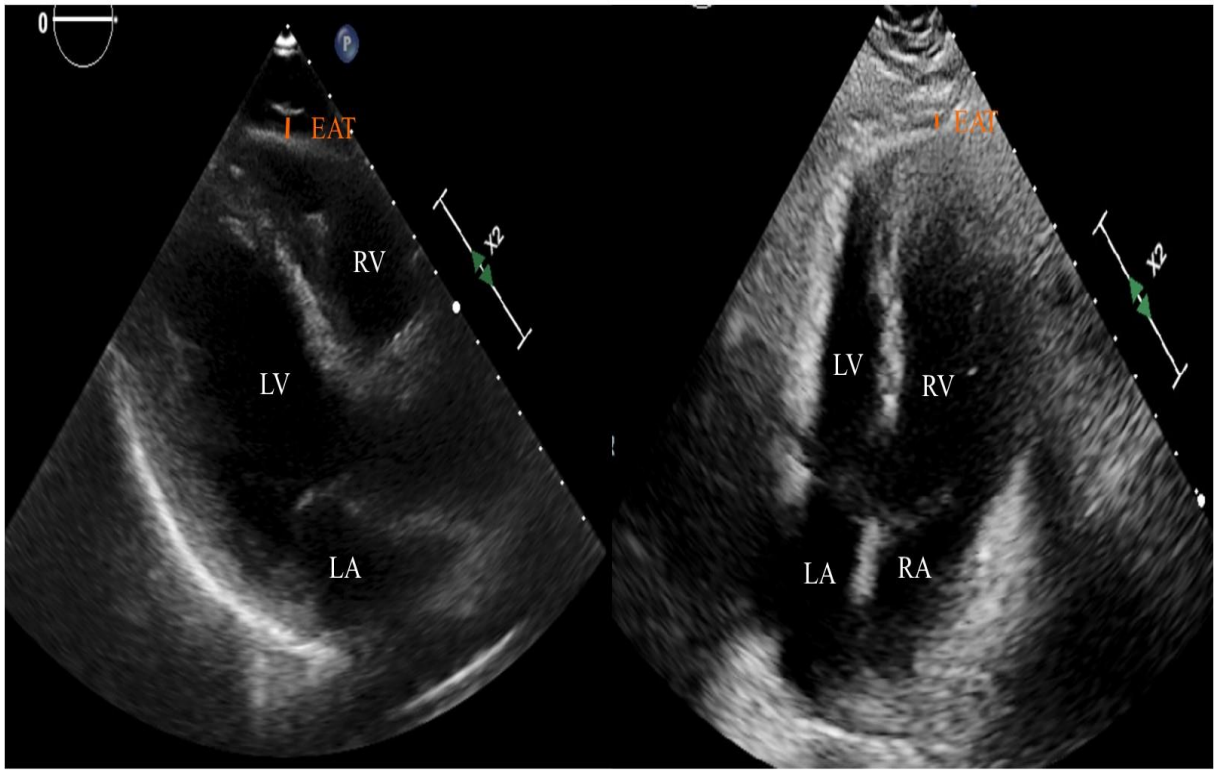

Figure 2. Echocardiographic measurements of epicardial adipose tissue thickness on the right ventricular free wall and in the area of anterior interventricular groove. Abbreviations: EAT – epicardial adipose tissue, LA – left atrium, LV – left ventricle, RA – right atrium, RV – right ventricle

Hirata et al. described another approach of visualizing EAT thickness in the area of AIVG (Figure 2). A linear probe was used for the examination (7.5 MHz, spatial resolution – 0.1 mm). The high-frequency linear probe allowed more precise EAT thickness measurements. Interestingly, this method related to the EAT volume, quantified on CT images, beyond of the EAT thickness measurements over the RVFW (49).

One important debatable issue concerns the time of cardiac cycle which could be used for echocardiographic EAT thickness assessment. Some authors suggested measurements of EAT thickness during systole to prevent possible compression of epicardial fat depots during diastole (139, 140). Other researchers recommended performing epicardial fat measurements in diastole to coincide with other imaging modalities, such as CT or CMR (141, 142).

Echocardiographic estimation of EAT thickness over the RVFW is the most commonly described approach. In addition, transthoracic ultrasound permits sufficient assessment of pericardial space. Echocardiography is described as an accessible, cheap and easily reproducible non-invasive method of EAT quantification in daily practice (64).

On the other hand, this modality has shown some disadvantages. It is capable of delivering only a linear measurement of EAT thickness at a single location (49, 143). Therefore, echocardiographic measurements have proven not possible to comprise a true representation of the overall EAT volume (82). Three-dimensional echocardiography could provide volumetric measurements of EAT in the future. Furthermore, some cases have revealed a difficult task for investigators to distinguish between epicardial and thoracic fat depots. Another important issue is referred to discrepancies in the measurement location, as a result of spatial variations in the echocardiographic window along the right ventricle and the great vessels (45). Thus, the

two-dimensional assessment of EAT thickness with ultrasound might under- or overrepresent the true size of epicardial fat due to changes in probe angulation (49). Finally, imaging quality was shown to be highly dependent on the individual acoustic window of the examined subject, which could be unsatisfactory in obese patients, as a result of fat impedance (144).

Echocardiographic EAT thickness measurements showed good correlation with the measurements, obtained from CMR images (r=0.91, p=0.001) (145). Iacobellis et al. published an excellent intra- and interobserver reliability of this modality with intraclass correlation coefficients of 0.98 and 0.9, respectively (146). On the other hand, Saura et al. presented poor echocardiographic reliability results with an intra- and interobserver intraclass correlation of 0.625 and 0.605, respectively (147). Of course, evidence of the poor correlation of a single EAT thickness measurement over the RVFW with EAT volume, quantified on CT images, has also been published (48). Further research is needed to address these controversies.

2.3.2 Computed tomography

Multi-detector CT (16 or more detectors) offers high spatial resolution and three-dimensional views. CT images permit evaluation of coronary arterial calcifications, degree of vessel stenosis and high-risk vulnerable plaque characteristics (88). Non-contrast cardiac CT is commonly applied for estimation of CCS, whereas coronary CT angiography is defined as one of the primary modalities for the diagnosis of coronary stenosis (148). Coronary CT angiography additionally allows characterization of coronary plaques and identification of high-risk properties (149). Unfortunately, several limitations complicate the assessment of coronary arteries on CT images. First of all, multiple dense calcifications frequently restrict the assessment of artery lumen (150). Furthermore, arrhythmias, tachycardia, motion artefacts and foreign bodies may further limit the quality of CT investigation (151). Therefore, additional predictors of CAD besides CCS and vessel changes in coronary CT angiography would be important to be examined. Epicardial fat depots could be an alternative marker of the CAD risk.

Electrocardiogram-gated (ECG-gated) CT – both coronary CT angiography and non-contrast CCS – allows measurement of EAT thickness and volume (48). However, lower availability and high cost are disadvantages of CT in comparison to echocardiography. Moreover, CT modality includes exposure to ionizing radiation. Lastly, in some cases it may be difficult to recognize the pericardium in lean individuals (66).

Cardiac CT images are generally obtained prospectively in CCS examination using ECG tracing. During CT scan, radiation exposure is found at a predetermined phase of the cardiac cycle. CT images are commonly reconstructed in slices of 2-3 mm thickness (152). On the other hand, CT angiography requires the use of contrast media in addition to ECG tracing. This method allows reconstruction of images with more detail and slices less than 1 mm (153). Remarkably, significantly lower values of EAT volume measurements have been obtained on CT angiography images in comparison to native CCS scan in the same patients. On the contrary, cardiac cycle phase did not influence EAT volume measurements acquired on cardiac CT angiography images (154).

Adipose tissue on CT images is defined through distinct attenuation values, obtained both with and without contrast media (range of -30 to -190 Hounsfield units) (155). Fat voxels within this attenuation range between epicardial surface of the heart and visceral pericardium are defined as EAT. CT modality allows to measure the exact amount of EAT in various locations (152). Researchers have been mostly measuring EAT thickness around the main coronary arteries and over the RVFW (156). Pericoronary EAT thickness is estimated perpendicular to the heart surface at the level of the three main coronary arteries (right coronary artery (RCA), left anterior descending coronary artery (LAD) and left circumflex coronary artery (LCX)) in the areas of atrioventricular and interventricular grooves. In contrast, volumetric assessment of the epicardial fat depots requires the following steps – limits of the heart and pericardium are manually marked at 5-10 slices; pericardium is then outlined at intervals to exclude the

paracardial adipose tissue (30). The superior heart limit slice is commonly selected at the split of the pulmonary artery (48). Anatomical reference for the inferior border of the heart is the lowest slice of the myocardium with the passing posterior descending artery (157). EAT volume is calculated as the sum of EAT areas, taking into account slice thickness and interslice gap (158). As a model, Figure 3 demonstrates the outlined EAT area on native CT image suitable for CCS measurements.

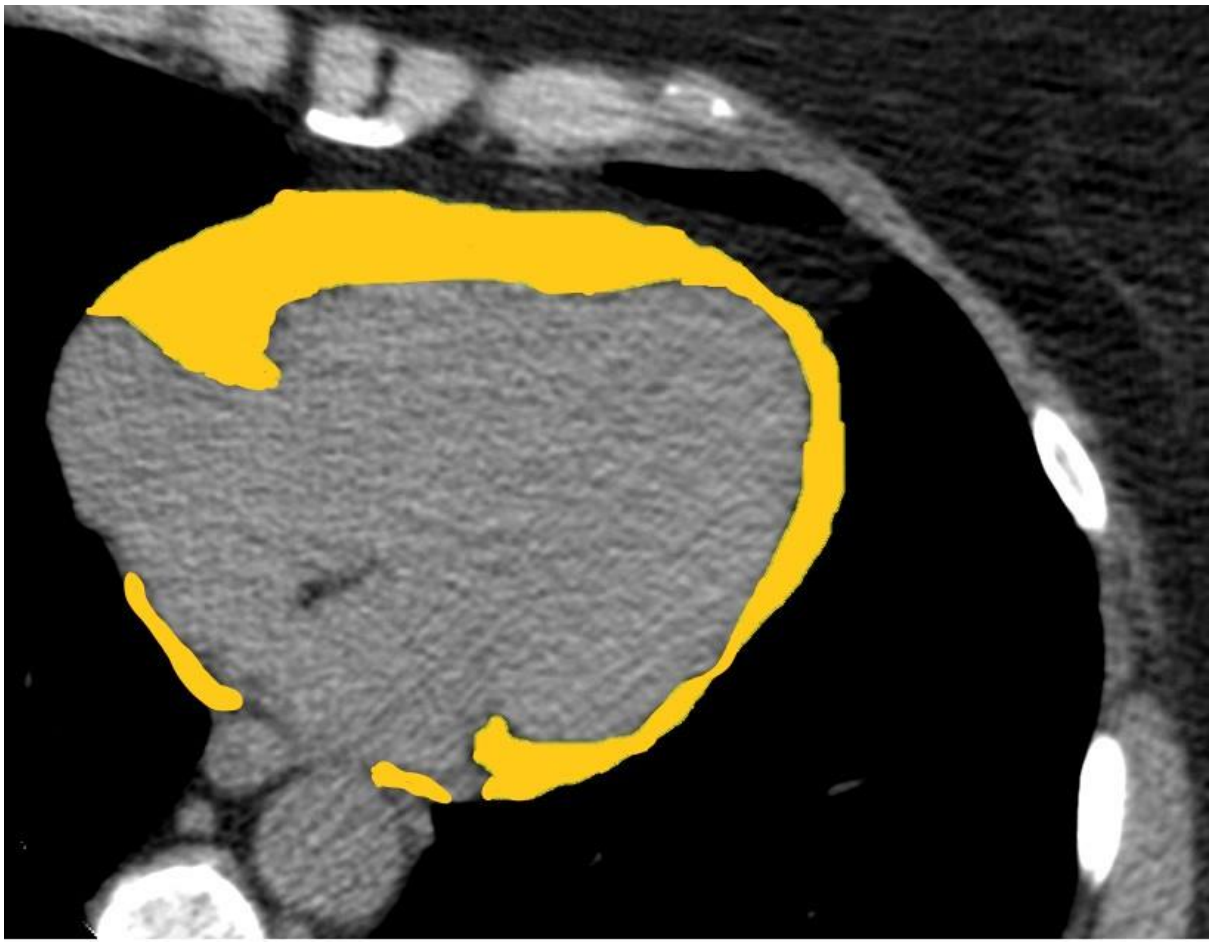

Figure 3. Epicardial adipose tissue area measured on native computed tomography image. Fat voxels between epicardial surface of the heart and pericardium are defined as EAT (yellow color).

The process of volumetric EAT quantification can be manual or semi-automated. Semi-automated techniques of EAT estimation are being developed on the basis of CT attenuation thresholds (78, 152, 159, 160). Although semi-automated approaches are being actively investigated, they still lack a firm and fast solution (161-163). First of all, these techniques require appropriate tools at the workstation to quantify the EAT volume. The operator should define the craniocaudal margins of the chest area with epicardial fat depots. Then the operator identifies the area of interest by manually outlining the pericardium at each cross-section. The next step involves software recognition of the outlined area with the content within with density values between -30 and -190 Hounsfield units. Median filtering is applied to limit noise. Finally, software calculates the volume of fat tissue from the number of fat voxels inside the pericardial contour. At the same time, the mean EAT density is estimated as an expression of the mean fat attenuation in Hounsfield units. In general, high interscan reproducibility for the semi-automated methods of EAT measurements was reported – correlation coefficients ≥0.98 for the same CT scanner (164).

Both semi-automated and manual processes of EAT volume quantification require extremely long processing times. Furthermore, vendor specific software algorithms of semi-automated

techniques present differences in epicardial fat size values (62). Deep learning could provide fast and fully automated estimation of EAT depots. Quantification of EAT on CT images could be implemented along with CCS in a clinical practice as a possible way of improving the cardiovascular risk assessment (165).

Intra- and interobserver variability of EAT volume measurements is reported to be higher than that of EAT thickness measurements (intraclass correlation coefficient of 0.95 versus (vs.) 0.87 (156) and interobserver agreement of 0.96 vs. 0.58 (166)). Kim et al. demonstrated poor correlation results between echocardiographically measured EAT thickness and CT quantified EAT volume (167).

Several authors calculated EAT mass – EAT volume values multiplied by the specific weight of adipose tissue (0.92 gram/cubic centimeter (g/cm^3)) (76, 168). Unfortunately, EAT mass values did not bring advantage in comparison to EAT volume measurements, it took one additional unnecessary step to calculate EAT mass. Finally, complicated comparison of EAT mass measurements with the studies, which employed volumetric EAT estimation, was another disadvantage of this quantification method of epicardial fat depots.

CT modality allows measurements of the EAT attenuation (density, expressed in Hounsfield Units) around the coronary arteries (96). Density of fat tissue is defined by the size and differentiation of adipocytes. The greater size or the higher differentiation level of adipocytes, the more fat molecules they contain, the less dense they will appear on CT images (lower Hounsfield Units value). In addition to this, EAT attenuation is dependent on the presence or absence of contrast media as well as inflammatory condition of the adipose cells. EAT attenuation is considered to be the indicator of adipose tissue quality, which could offer additional information to the quantity of epicardial fat depots (169).

In early stages of CAD, EAT density was found to be lower in stable low- to high-risk patients. Franssens et al. investigated EAT attenuation of 140 patients from SMART cohort (Secondary Manifestations of ARTerial disease). Authors reported an independent association between the lower EAT density and an adverse metabolic profile as well as positive CCS (170). Similar results achieved Abazid et al. in 609 low- to intermediate-risk asymptomatic patients – EAT density was lower in individuals with coronary artery calcifications, and these results were independent of EAT volume (171).

In contrast, Mahabadi et al. discovered that advanced CAD patients, who suffered from myocardial infarction, had significantly higher EAT density in comparison to stable CAD patients. This finding suggests that inflammatory activity of EAT could be considerably increased in individuals who suffer from acute coronary syndrome (172). On the other hand, Hell et al. were unable to report the positive association between EAT attenuation and induced myocardial ischemia on single-photon emission computed tomography (SPECT) (173). Nevertheless, Goeller et al suggested that increased EAT attenuation could be a sign of a coronary plaque progression as well as of an active coronary inflammation (174). Finally, increase of EAT density in advanced CAD patients was more profound around RCA, as a result of anatomically larger EAT quantities on the right side of the heart (175).

Recently, a new innovative qualitative method of pericoronary EAT analysis has been presented – fat attenuation index. This standardized measurement stands for attenuation (density) degree of adipose tissue in the perivascular region. Fat attenuation index acts as a detector of coronary inflammation around vulnerable plaques and can only be calculated on coronary CT angiograms. As mentioned before, throughout chronic coronary inflammation pro-inflammatory cytokines eventually stop the differentiation of preadipocytes into mature adipocytes. As a result, this measurement is inversely associated with the size and differentiation of adipose cells (176).

Fat attenuation index has been validated as an indicator for cardiovascular risk assessment. This measurement was significantly increased around culprit lesions in acute myocardial infarction patients vs. subjects with stable CAD as well as compared with healthy individuals. Following 5 weeks after myocardial infarction, high fat attenuation index persisted around the

culprit lesions as a consequence of longitudinal changes in coronary inflammation (176, 177). In the CRISP-CT (Cardiovascular RISk Prediction using Computed Tomography) study, increased fat attenuation index (with cut-off value of 70 Hounsfield Units) around RCA and LAD predicted cardiac and all-cause mortality (177).

2.3.3 Cardiac magnetic resonance

CMR imaging, which is considered the “gold standard” modality for visualization of adipose tissue and total body fat, offers excellent image resolution and can be used to measure EAT (46, 178). CMR has been validated as a reproducible, accurate and reliable method for the evaluation of EAT (141, 179).

Estimation of epicardial fat depots with CMR involves morphological analysis with sequences that allow definition of the fat (black blood sequences) and functional (bright blood) sequences. EAT is quantified at the end of the diastole. EAT can be measured at a single point (thickness); in addition, volumetric quantification can be performed. Epicardial fat volume is calculated applying the modified Simpson method. Similar to quantification on CT images, contours of EAT are traced on short axis slices; adipose tissue areas are added to calculate EAT volume, taking into account slice thickness and interslice gap (158). As an illustration, Figure 4 shows the outlined EAT area on a CMR image, acquired using a segmented steady state free precession (SSFP) algorithm.

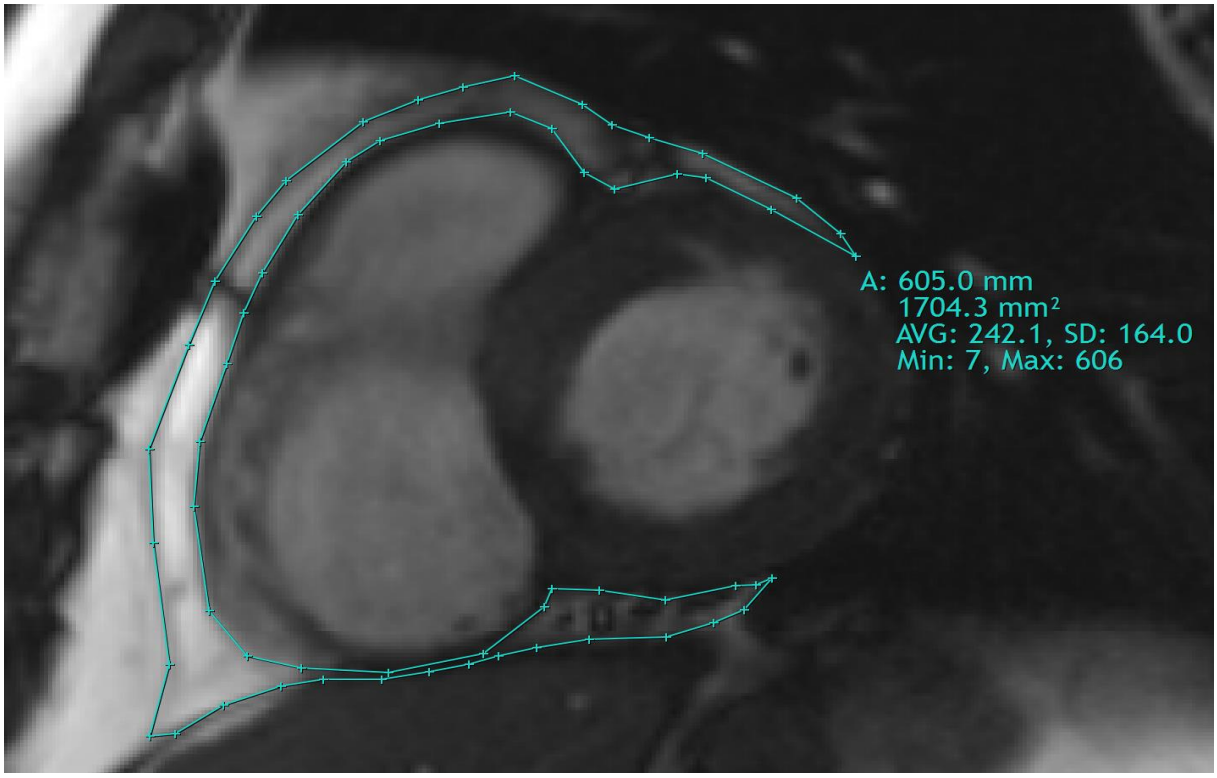

Figure 4. Epicardial adipose tissue area measured on cardiac magnetic resonance image, acquired using the segmented steady state free precession algorithm. Area of the epicardial fat is outlined using area measurement tool. Abbreviations: A – area, AVG – average, Min – minimum, Max – maximum, mm – millimeter, mm^2 – square millimeter, SD – standard deviation

In addition to quantification of epicardial fat depots, CMR is considered to be the reference modality for examination of ventricular volumes and the cardiac mass. CMR can be performed

with free breathing, mild arrhythmias are generally not a problem for image assessment (180). Furthermore, this modality is free from radiation exposure, use of contrast media is not necessary (178). Although image resolution of CMR is superior in comparison to CT, CMR is far more expensive and less available, which is a significant disadvantage of this modality. Long training time of medical staff is another drawback (181). Application of CMR is also limited in obese or claustrophobic patients, as a result of long scan time, as well as in patients with incompatible implanted devices (35).

2.3.4 18F – Fluorodeoxyglucose Positron Emission Tomography – Computed Tomography

18F-Fluorodeoxyglucose Positron Emission Tomography – Computed Tomography (18F-FDG-PET–CT) becomes increasingly important in the detection of infection or inflammatory diseases such as sarcoidosis (182). In addition, this modality is capable of non-invasively determining the inflammatory activity of EAT (88). This imaging method maps local absorption of 18F-Fluorodeoxyglucose (18F-FDG) within specific areas of interest (183). The number of glucose transporters in a cell as well as the cellular metabolic status are related to the degree of 18F-FDG uptake. Cells with increased metabolic activity along with inflammatory cells express an increased number of glucose transporters. Furthermore, the activity of glucose transporters is facilitated by pro-inflammatory cytokines and growth factors (184).

Increased EAT uptake of 18F-FDG has been observed on PET-CT images, as a result of CAD (185). In a study by Mazurek et al., pericoronary EAT showed higher standardized uptake values of 18F-FDG in CAD patients (in comparison to non-CAD controls as well as to other non-cardiac adipose tissue depots). Furthermore, uptake of 18F-FDG correlated with the severity of CAD (186). Pericoronary EAT attenuation, measured on CT images, correlated with uptake values of 18F-FDG in identifying inflamed adipose tissue around high-risk coronary plaques (176, 186, 187). ECG-gated 18F-FDG-PET–CT, as a novel method, allowed more detailed assessment of pericoronary EAT and coronary plaque composition. Ohyama et al. reported that increased pericoronary EAT volume along with the 18F-FDG uptake values were significantly connected to vasospastic angina (188).

Unfortunately, 18F-FDG-PET–CT is highly expensive and not widely accessible. Moreover, lower spatial resolution and high background noise limit the quantitative estimation of epicardial fat depots. Finally, 18F-FDG-PET–CT includes exposure to high amounts of ionizing radiation (88, 96).

2.4 Distribution and changes of epicardial adipose tissue in healthy individuals

Many different factors, involving age, race, gender, weight, heart mass, have been connected with variations of EAT distribution around the heart (126).

EAT in neonates consists primarily of brown fat cells; the main function of epicardial fat is thermogenesis. Mature EAT cells in adults become more responsive to environmental and metabolic changes; the main function of EAT shifts from thermogenesis to the energy storage (189). EAT grows with age – individuals older than 65 years have approximately 20% thicker epicardial fat depots (78, 155, 190). During ageing process, the lean body mass decreases, and the fat mass increases with the redistribution of adipose tissue to viscera and trunk (191). These transitions develop at a different rate between male and female persons, with a higher grade of redistribution seen in older women (192).

In general, people with black skin color suffer less from central obesity than those with white skin (193). Both visceral and epicardial fat tissues are smaller in individuals with black skin color (194, 195). Moreover, EAT volume is higher in Caucasians in comparison to Blacks, Hispanics or Asians (78). It is worth noting that among individuals with chest pain symptoms, EAT thickness over the RVFW has been reported to be higher in people with white skin color (196).

It is not yet clear how gender impacts the amount of EAT. Epicardial fat thickness is inclined to be insignificantly less prominent in females than males. However, EAT volume and mass have been shown to be significantly higher in males (78, 168). One study of the Framingham cohort data demonstrated a stronger correlation of the EAT size with cardiovascular risk factors in women than in men (30). On the other hand, other studies of the same cohort have not been able to detect this association (80, 90).

BMI, weight and waist circumference have shown a positive moderate link to the size of EAT depots over an interval of approximately 5 years. A decrease of total body weight (>5%) have been connected to reduction or stability of EAT, whereas epicardial fat have progressed with weight gain and BMI (81). On the other hand, EAT seems to correlate more closely with visceral fat mass compared to total fat mass (93).

EAT is positively correlated with the heart mass. In fact, autopsy studies have described a constant fat–muscle ratio which exists in each ventricle. The mass of adipose tissue surrounding the heart reaches on average 100 g in lean and fit individuals (91).

EAT thickness at different heart locations ranges between 1 and 15 mm in healthy individuals. Epicardial fat thickness over the RVFW generally amounts 5-7 mm in lean and fit persons (71). Furthermore, normal EAT thickness in the atrioventricular and interventricular grooves is considered to be 10-14 mm (197). EAT thickness measurements, carried out on CMR images, seem to be similar to those measured during autopsies in the same location (168, 198).

As an illustration, in a study with 573 healthy postmenopausal women the average EAT thickness in the right atrioventricular groove (RAVG) (RCA area) was 17±4 mm, in the AIVG (LAD area) – 6±2 mm and in the LAVG (LCX area) – 11±3 mm (199). Moreover, the mean echocardiographic EAT thickness of 5±2 mm was reported in 356 asymptomatic individuals by Nelson et al. (72).

Epicardial fat volume varies similar to EAT thickness. For example, on CT images quantified EAT volume was determined as high with 139.4 cm^3 for men and 119 cm^3 for women in healthy 3312 individuals from Framingham Heart Study (200). Other authors evaluated the same cohort and reported similar high EAT volume measurements – 110±41 cm^3 in women and 137±53 cm^3 in men (30). Bertaso et al. in their systematic review considered EAT volume below 125 cm^3 as normal in low-risk populations (45).

2.5 Pathophysiological role of epicardial adipose tissue in the development of coronary artery disease

Overall, CAD is caused by a decrease of blood supply to the heart muscle, as a result of plaque remodeling and growth in coronary arteries (201). Sudden death, acute coronary syndrome (unstable angina, myocardial infarction) and stable angina are all clinical presentations of CAD (4).

In general, studies, regarding the importance of epicardial fat depots in CAD pathogenesis, attempt to answer a common question whether inflamed EAT triggers the development of coronary plaque or only promotes the existing vascular pathology (89, 202). Recently and more commonly, CAD pathogenesis is proposed by the “outside to inside” model, as a result of the increased activity of different pro-inflammatory cytokines rather than by the traditional model,

in which vascular endothelium is damaged by the formation of coronary plaques and hypertension (203). Inflamed and enlarged EAT disposes of its brown fat properties, facilitates oxidative stress in the heart muscle, lowers contractile function of cardiomyocytes, boosts local and systemic inflammation (83). Pro-inflammatory adipokine synthesis as well as chronic systemic inflammation are both viewed as important modulators of atherogenesis in CAD pathogenesis (87, 204).

The expression of genes, encoding thermogenic activation and fat browning proteins in EAT, is downregulated in patients with CAD (96). Several studies have repeatedly demonstrated that impaired EAT in CAD patients expresses significantly less protective anti-atherogenic adipokines (adiponectin or adrenomedullin) compared to healthy individuals (205-207). Moreover, intracoronary amount of adiponectin and adrenomedullin are proved to be lower in patients with chronic CAD (119). In these circumstances, the beneficial paracrine effects of epicardial fat are lost (208). Iwayama et al. revealed that EAT may play a significant role during early stages of CAD in non-obese patients. Authors have found that adiponectin concentration in pericardial fluid was lower in CAD patients compared with healthy controls. Furthermore, non-obese CAD patients have displayed significantly greater EAT volume (209).

EAT around coronary arteries, in both asymptomatic and symptomatic CAD patients, expresses higher levels of pro-inflammatory cytokines, vasoactive and angiogenic peptides in comparison to subcutaneous adipose tissue (6, 34-36, 38-42). These substances mediate oxidative stress and arterial inflammation through an “outside to inside” mechanism (42). Enlarged adipocytes produce FFA at an increased rate, FFA activate local macrophages, resulting in an enhanced synthesis of TNF-α (210). TNF-α activates lipolysis and the expression of numerous different pro-inflammatory genes, such as MCP-1, intracellular adhesion molecule-1, IL-1, IL-6, angiotensin II, PAI-1, resistin, leptin (211). The results of numerous studies indicate that pro-inflammatory cytokines, derived in EAT, are well associated with coronary plaque vulnerability in CAD patients (201). Interestingly, decreased adiponectin/leptin ratio in epicardial fat depots is considered to be an additional novel risk factor of CAD (212).

In EAT generated pro-inflammatory adipokines influence the progression of atherosclerotic plaque via two main mechanisms: paracrine and vasocrine (213). Pro-atherogenic adipokines, secreted by pericoronary EAT during paracrine signaling, diffuse directly to the adjacent vascular wall and the heart muscle via interstitial fluid (“outside to inside” mechanism) (67). As a result, pro-inflammatory adipokines interact locally with endothelium, atherosclerotic plaque components in coronary arteries and vascular smooth muscle cells (214). Paracrine mechanism applies to smaller arteries, as a consequence of the diffusion process which is only possible through thin vessel walls (215).

Alternatively, vasocrine signaling suggests that pro-inflammatory adipokines, secreted from EAT, directly enter the vessels of closely located vasa vasorum (216). The rate of substance entry into the vessel depends on the thickness of the vascular wall. Because of this, vasocrine signaling is compatible with medium and larger caliber arteries. Thus, molecules are transported downstream into the arterial wall where they influence cells in and around atherosclerotic plaques (93, 217).

Dysfunctional EAT attracts more macrophages (218). This leads to a constant cycle of inflammation state in and around epicardial fat depots (219). Furthermore, inflammatory properties of EAT are greatly exacerbated by severe body conditions, such as myocardial infarction or cardiac surgery (218). Coronary vessels, which lie in EAT without separating fascial layer, are affected as well. As a result, apoptosis of vascular smooth muscle cells and the awakening of the fibrous layer are both induced (87, 220). This generates vascular inflammation of the adventitia, which advances inward to the intima, eventually leading to coronary plaque formation (42, 221).

Lipotoxicity is another pathophysiological mechanism which accelerates formation of the coronary atherosclerotic plaques (222). High FFA production by inflamed adipocytes leads to fat accumulation in vascular plaques. Therefore, the formation of atheromatous plaques in

coronary vessels is facilitated and, thus, the progress of CAD (6). Moreover, EAT is considered an insulin-resistant fat because of lower glucose utilization rate in comparison to other visceral fat compartments (223).

During later coronary atherosclerotic plaque formation phases, EAT continues its contribution to the inflammation around and within the plaque (217). Thin fibrous layer of the plaque is at this stage densely infiltrated with macrophages and mast cells, as a result of higher surface expression of numerous adhesion molecules (224). Macrophages produce large quantities of metalloproteinases. These molecules play a major part in the breakdown of extracellular matrix components and in structural changes within the vascular wall (225). Consequently, plaque rupture begins in this location (226).

In response to decreased vascular density and hypoxia, recruited macrophages express platelet derived growth factors as well as hypoxia inducible factors, which promote formation of new capillary vessels (132). Above all, these mediators provoke neoangiogenesis near coronary vessels, around EAT including vasa vasorum. In the beginning, neovascularization reduces effects of hypoxia on the subsequent thickening of the vascular intimal layer during early stages of the coronary plaque formation (227). At the same time, new vessels facilitate transportation of harmful pro-inflammatory cytokines from EAT to the vascular intima of fatty plaques (201). Furthermore, macrophages continue to shift from EAT into coronary plaques via new vessels, where they become foam cells. Over the long term, neoangiogenesis is closely related with coronary plaque hemorrhage (228).

Epicardial fat depots in CAD patients present higher quantities of reactive oxygen species, as a marker of a total oxidative stress and inflammation (229, 230). Moreover, EAT displays elevated resistin secretion in individuals with CAD (231). Resistin impairs contractile function and reduces glucose uptake in the myocardial cells, increases endothelial cell permeability (232, 233). In addition, EAT in CAD patients exhibits lower levels of catalase. Catalase is an antioxidant which converts hydrogen peroxide into oxygen and water, thus reducing oxidative stress (234). More importantly, EAT assessed with PET-CT shows increased uptake of 18F-FDG than other visceral fat depots in patients with CAD. This marker is acknowledged as an indicator of local inflammation. It is especially elevated in and around stenotic coronary vessel areas (186).

As an illustration of inflammatory properties of EAT, epicardial fat probes, collected during cardiac surgery from individuals with significant CAD, were considerably infiltrated with inflammatory cells (T and B lymphocytes, macrophages, dendritic and mast cells). Hirata et al. revealed a higher concentration of inflammatory M1 in comparison to anti-inflammatory M2 macrophages in EAT samples, acquired from patients with advanced CAD during cardiac surgery (43). Inflammatory features of EAT were unrelated to the clinical parameters of examined patients, such as BMI, diabetes or statin therapy (42, 235). Furthermore, approved systemic inflammation factors, such as low-density lipoprotein cholesterol concentration in blood, did not directly interact with EAT (65).

Specific mechanical effects of coronary atherosclerotic plaques on epicardial fat deposits have been observed. Growing coronary atherosclerotic plaque leads eventually to a disproportionate extension of the vascular wall (121). EAT is thought to play a permissive role in vessel expansion, as a result of its compressibility. On the other hand, myocardium is not compressible, therefore, vascular wall surrounded only by the heart muscle cannot expand (32).

Finally, segments of coronary arteries called myocardial bridges, which are circumferentially surrounded by myocardium and clear of any epicardial fat deposits, are free from atherosclerotic plaques, and, therefore, are immune to atherosclerosis. This phenomenon has been observed in both humans and animals (93, 236). In contrast, Chandalia et al. have suggested that EAT is not necessary for the development of coronary atherosclerotic lesions. Patients with generalized lipodystrophy and complete absence of adipose tissue still presented evidence of CAD (237). All in all, authors around the world have acknowledged that the thicker

epicardial fat depots around coronary arteries, the greater inflammatory activity EAT presents, the more risk CAD has to develop (42).

2.6 Distribution and changes of epicardial adipose tissue in patients with coronary artery disease

A connection between the size of EAT and the development of CAD becomes more evident in adulthood (238). Overall, a direct association between the amount of EAT and the presence of CAD has been identified in patients undergoing both CT and coronary angiography (61, 114, 239). Moreover, EAT has been able to predict atherogenesis and the severity of atherosclerosis in coronary vessels (78, 142, 240). Patients with unstable angina have shown increased EAT measurements in comparison to individuals with stable CAD symptoms (45, 136). In addition to this, EAT measurements have been able to effectively predict high-risk coronary plaques and myocardial ischemia (64, 90). Finally, EAT thickness measurements on the RVFW have identified an impaired myocardial flow reserve (estimated in Rb-82-PET) with the very high area under the curve (AUC) – 0.945 (241).

Due to the anatomic proximity of major coronary vessels to epicardial fat deposits, it is expected that changes in EAT could play an important role in the development of CAD (35). As an illustration, Mancio et al. carried out a meta-analysis which involved 41534 individuals. In low to intermediate cardiovascular risk subjects, EAT was independently related to obstructive CAD, myocardial ischemia and MACE (134).

Most thickness measurements of epicardial fat in literature were conducted over the RVFW with echocardiography. A volumetric estimation of EAT is another most common described method using cross-sectional imaging techniques (61). Despite varying results, a systematic review by Bertaso et al. suggested that EAT thickness over 5 mm and EAT volume over 125 cm^3 could both serve as a possible cut-off value of increased epicardial fat depots in low-risk populations with CAD (45).

Pericoronary adipose tissue thickness, measured on CT images, was increased in CAD patients as well as associated with CCS, diabetes and arterial hypertension (242). Coronary vessels with either calcified or mixed plaques showed increased pericoronary EAT, supporting a link between the excess of EAT and atherosclerosis. After calculating the average pericoronary EAT thickness around three main coronary arteries, it was revealed to be greater around coronary vessels with obstructive atherosclerosis (243).

Important evidence of causal relationship between epicardial fat and coronary atherosclerosis was generated in a pig model. A local EAT resection around LAD interrupted the progression of atherosclerotic plaque within the vessel, however, only at the site of resection (244).

A strong connection between EAT density, measured on CT images, and subclinical atherosclerosis along with MACE has been reported (86). Goeller et al. investigated 456 healthy participants of the prospective Early Identification of Subclinical Atherosclerosis by Non-invasive Imaging Research (EISNER). Authors revealed that lower EAT density as well as increased EAT volume are linked to early coronary plaque formation, inflammation and consequent MACE (245).

In the next subsections, the relationship between EAT and different coronary plaque characteristics along with the outcomes of CAD will be discussed more closely.

2.6.1 Coronary artery calcium

The amount of coronary artery calcifications is quantified via CCS on non-contrast ECG-gated CT images. CCS provides information about the total burden of coronary atherosclerosis in examined subject (246). This measurement is a broadly accessible and reliable variable of defining the risk of MACE (247). Patients are generally divided into groups of low, middle and high risk of developing a significant CAD in the future (248).

Multiple recent studies have revealed that EAT volume could be an independent predictor of subclinical coronary atherosclerosis in healthy subjects (30, 61, 171, 195, 239, 245, 249-253). 1155 healthy individuals from the Framingham Heart Study underwent CT imaging for estimation of paracardial and epicardial fat volume as well as CCS. After adjustment for cardiovascular risk factors, authors have found that epicardial fat depots, but not paracardial adipose tissue, were related to CCS (30). On the other hand, a smaller sample of 201 healthy participants of the EISNER study revealed positive associations of CCS with both EAT and paracardial adipose tissue (152).

6814 individuals, free from cardiovascular diseases at baseline, were analyzed in the Multiethnic Study of Atherosclerosis (MESA). This study showed a strong association between CCS and epicardial fat volume around proximal coronary artery boundaries, even after adjustments for BMI and waist circumference (195). The association persisted even in those patients who developed incidental CAD during a 5-year follow-up (66). Another MESA cohort study revealed a significant connection between pericoronary fat deposits and CAD in 398 patients, even after adjustments for conventional cardiovascular risk factors (254). Despite the published results, it is important to stress that only pericoronary, but not total EAT volume, was measured in MESA cohort studies.

Mahabadi et al. evaluated the Heinz Nixdorf Recall study cohort of 3367 subjects. A strong link was found between both CCS onset or progression and EAT volume in patients with absent or low CCS at a baseline. Furthermore, study results were more pronounced in young and lean individuals. In addition, findings were independent from BMI and traditional cardiovascular risk factors (250). Bos et al. studied the Rotterdam cohort (2298 participants); authors concluded that the independent association of larger EAT volume measurements and intracoronary calcifications was more prominent in men than in women (255).

Smaller studies showed consistent results. Djaberi et al. assessed 190 patients; authors reported significantly larger EAT volume in individuals with CCS over 10 compared to subjects with normal coronaries without calcifications (252). Ahmadi et al. confirmed the previous results– EAT, measured on CT images, was higher in both females and males with greater CCS (256). In addition, the relation between CCS an EAT volume was reported to be independent of the abdominal visceral fat size (253).

Follow-up studies achieved similar results. Yerramasu et al. measured EAT volume and CCS after approximately 3 years, following the initial CT scan in asymptomatic diabetic patients without CAD. Epicardial fat volume was an independent indicator of the presence and severity of CCS (50). Comparable results were obtained from the EISNER cohort study – in asymptomatic patients with intermediate cardiovascular risk both EAT volume and CCS increased over the course of 3-5 years (257).

Finally, EAT thickness, measured in a group of autopsied cases around main coronary arteries, was associated with coronary atherosclerosis. Epicardial fat thickness was also greater at the incision points on the right side of the heart (258).

2.6.2 Non-calcified coronary artery plaques

A presence of coronary calcifications stands for an advanced stable CAD (67). Absence of calcified plaques in coronary arteries is mostly a sign of a good prognosis. On the other hand, CAD, caused by non-calcified plaques, represents an active vulnerable process that can result in terminal cardiovascular events (259).

Generally, published studies revealed consistent positive conclusions regarding the association of epicardial fat depots and non-calcified coronary plaques. Ito et al. have demonstrated that EAT volume could significantly predict an obstructive coronary non-calcified CAD in symptomatic patients, independently of traditional CAD risk factors and anthropometric measurements of obesity (260). Oka et al. displayed similar findings in 357 individuals who received CT angiography. EAT volume in this study was identified as an independent predictor of non-calcified low-density coronary plaques with the positive remodeling after adjustments for visceral fat, BMI and CCS (261). Comparable results revealed Konishi et al. – authors measured EAT volume on coronary CT angiography images of 210 patients. Authors found that EAT, but not abdominal waist circumference, was significantly and independently associated with the presence of all types of coronary plaques (non-calcified, mixed, calcified). No significant EAT volume difference was observed between patients with different coronary plaque properties (262). Mahabadi et al. in the same way demonstrated a significant independent connection between pericoronary EAT and the presence of coronary plaque, irrespective of plaque type (90).

On the other hand, Alexopoulos et al. showed that EAT volume significantly differed between different coronary plaque features. Authors revealed that EAT volume was significantly greater in patients with mixed and non-calcified coronary plaques compared to individuals with calcified atherosclerosis or absent coronary plaques (78). It is a very important finding since mixed and non-calcified plaques have been linked to a higher incidence of MACE (263). Hwang et al. confirmed the results of Alexopoulos et al. as they followed 122 asymptomatic individuals over the course of 5 years. Authors revealed that BSA-indexed EAT volume, measured on CT images, was considerably higher in those patients, who developed non-calcified coronary plaques, in comparison to healthy individuals or those who featured only calcified atherosclerosis (240). Moreover, Okada et al. analyzed epicardial fat depots and coronary plaques in non-obese persons. In this study, increased EAT volume was associated with severe narrowing coronary plaques (not necessarily calcified). The results have indicated an important role of EAT in CAD progression in subjects with little accumulation of visceral fat (264).

In general, published findings suggested that greater EAT depots could appear before the development of coronary atherosclerotic plaques and their vulnerability (243). As a result, EAT could be an additional indicator of risk stratification for patients developing CAD before the appearance of visible damage signs to coronary arteries.

2.6.3 Significant coronary artery stenosis and high-risk plaque

High-risk coronary plaque includes one or more of the following features: low-attenuation plaque, positive remodeling, spotty calcification and the napkin ring sign (59). Instable high-risk coronary plaques can more often lead to the acute coronary syndrome, as a result of a higher rupture risk (265). Therefore, it is crucial to be able to predict the presence of high-risk coronary plaques due to the significance of early intervention (65).

A meta-analysis, conducted by Nerlekar et al. with 3772 patients, demonstrated some important findings. First of all, the increase of EAT measurements was significantly associated with the presence of high-risk coronary plaque features. Secondly, volumetric EAT quantification showed a stronger association with high-risk plaque features than linear EAT

thickness measurements (62). In another study a virtual histology intravascular ultrasound was used to assess coronary plaques and their high-risk features. Authors reported a strong correlation between increased EAT thickness, measured with transthoracic echocardiography, and coronary plaque instability (63). Nakanishi et al. followed up 517 CAD patients for approximately 4 years; a second CT scan was performed within 2 years after the first scan. Authors evaluated changes in EAT volume. CAD patients, which showed the significant increase of EAT volume during follow-up, more frequently developed high-risk coronary plaques despite comprehensive management of cardiovascular risk factors (266). Ito et al. performed optical coherence tomography on coronary plaques. The results of the study demonstrated a strong connection between high EAT volume measurements, quantified on CT images, and the features of coronary plaque instability (267). Shan et al. performed multivariate regression analysis which identified the EAT volume variable as an independent risk factor for instable high-risk coronary plaques. Authors suggested that the detection of increased EAT volume in native heart CT scan could be sufficient to initiate contrast enhanced examination of coronary arteries to be able to recognize high-risk plaque features, independently from the result of CCS. Lower EAT measurements could be an acceptable reason to cancel contrast enhanced CT scan to avoid possible side effects of contrast agent or excessive radiation (65).

Several studies with patients who underwent coronary CT angiography, identified greater EAT depots as a possible independent risk factor for the formation of significant (>50%) coronary stenosis (59, 61, 260, 268-271). Nakazato et al. presented a relation between high EAT volume and the appearance of both relevant coronary stenosis and myocardial ischemia (271). In addition to this, Iwasaki et al. reported a steep increase of EAT volume measurements in patients with severe coronary artery sclerosis and stenosis (269). EAT volume in individuals with high-risk stenotic coronary lesions, was approximately twice as high in comparison to subjects without CAD (270). Moreover, Rajani et al. confirmed the independent association between increased EAT depots and greater coronary stenosis (>70%) after adjustments for cardiovascular risk factors (58). Mahabadi et al. observed 2.5-fold odds increase of the coronary plaque presence per each doubling of pericoronary EAT volume. This discovery was not related to the type of coronary plaque (272). Hajsadeghi et al. presented a gradual rise of BSA-indexed EAT volume from individuals with no coronary obstruction to non-obstructive CAD – to obstructive CAD (266). Finally, authors, which applied widely used Gensini score for quantifying angiographic atherosclerosis, showed an independent association of EAT with CAD severity (61, 142, 273-275).

Several postmortem studies presented a significant connection between epicardial fat depots and the degree of coronary stenosis. Silaghi et al. measured EAT in 56 random human cadavers. Results of the study demonstrated significantly increased EAT areas on both anterior and posterior surfaces of the heart in subjects with CAD. Moreover, EAT areas on the anterior surface of the heart significantly correlated with the score of coronary stenosis (276). Sequeira et al. compared EAT thickness and volume measurements in 116 deceased subjects with different grades of coronary stenosis (absent, <50%, ≥50% stenosis). Published findings revealed increased EAT volume in subjects with significant (≥50%) coronary stenosis, even after controlling for BMI. In comparison, analysis of EAT thickness measurements showed no significant differences (277).

2.6.4 Major adverse cardiovascular events

The term MACE refers to a certain clinical endpoint used for outcome evaluations; MACE include cardiovascular death, myocardial infarction, stent thrombosis or repeat revascularization. Greater epicardial fat depots have been independently associated with MACE on different occasions (65, 66, 278, 279).

In a study from the EISNER registry, MACE patients demonstrated larger epicardial fat depots compared to event-free individuals. Moreover, increased EAT volume together with high CCS values improved prediction of MACE in the study population (51). One more work from the EISNER registry showed increased EAT volume in subjects with inducible myocardial ischemia on SPECT images. Of note, EAT attenuation values did not differ between ischemic and non-ischemic individuals (173). Two other studies showed similar results – EAT volume presented a strong relationship with the induced ischemia of the heart muscle, measured by both SPECT and PET (52, 157). Lu et al. concluded that greater EAT volume could significantly predict MACE probability in patients following coronary intervention, after adjustments for clinical, demographic and angiographic variables. Authors reported the cut-off value of EAT volume of 125.2 cm^3 as an independent predictor of MACE in the study population (201). Furthermore, researchers announced a significant higher risk of MACE with an approximately two-fold increase in EAT volume (51). In addition to the previous studies, EAT was indicated to significantly and independently predict both acute coronary syndrome as well as myocardial ischemia in individuals without known CAD (157, 279, 280).

Mahabadi et al. measured EAT volume in approximately 4000 participants of the Heinz Nixdorf Recall study cohort, authors examined the connection between epicardial fat depots and the incidence of coronary events over a follow-up of approximately 10 years. The incidence of coronary events continuously increased with the EAT volume, even after adjustments for cardiovascular risk factors (281). One more research with participants from the Framingham Heart Study cohort demonstrated a strong association between the size of EAT and the incidence of MACE, whereas visceral abdominal adipose tissue was associated with the incidence of stroke (90). It should be pointed out that paracardial thoracic adipose tissue did not relate to cardiovascular diseases or MACE (51, 90, 157). This further strengthens the hypothesis of a possible impact of epicardial fat depots on coronary arteries.

Finally, patients with the stable CAD who eventually died from cardiac death during long term follow-up, showed significantly lower BSA-indexed EAT mass. Reduced BSA-indexed EAT mass below 22 g/m^2 was associated with substantially higher rate of death (76).

2.6.5 Conflicting studies and results

Although the majority of published studies showed promising diagnostic importance of epicardial fat depots, incidental investigations pointed out no significant value of non-invasive EAT measurements in prediction of patients with CAD. All in this subsection mentioned studies were observational and prone to biases which include population selection, ascertainment of findings and unbalanced use of predictors in regression modeling. Moreover, ethnic related discrepancies in study cohorts and outcomes could have impacted the reported results as well. Additional well controlled populations with corresponding adjustments for confounders are needed to clarify those issues.

The strongest conflicting material, which contradicted the association between epicardial fat depots and CAD, was published by Tanami et al. in 2015. Authors analyzed CT and SPECT images of 380 patients with suspected or diagnosed CAD. The study reported no connection between the size of EAT volume and the presence or severity of CAD as well as myocardial perfusion abnormalities. It is worth pointing out that approximately 30% of the study population represented high-risk population for cardiovascular diseases (282). Van Meijeren et al. compared BSA-indexed EAT volume between patients with stable CAD, individuals who suffered from MACE and healthy controls. BSA-indexed EAT volume was similar within all groups of subjects. A possible reason for unusual study results could be the broad definition of CAD which included patients with both early and late stages of disease. In addition, authors studied a small sample of patients which did not permit an employment of complex statistical analysis methods (283).

Otaki et al. indexed EAT volume measurements to BSA in 106 subjects without coronary calcifications at a baseline. Over the course of 3-5 years, monitored individuals developed coronary calcium on CT images. Authors did not find a connection between the development of coronary calcifications and the rise of EAT volume. However, an unusual estimation method of EAT was used in this study – authors did not measure EAT areas around the whole heart, but only around the cranial part of it. Moreover, confounders were not removed from the final analysis, the sample size was rather not representative as well (284). Romijin et al. examined CT images of 122 patients with suspected CAD and indicated that EAT volume showed no significant diagnostic importance beyond cardiovascular risk factors and CCS (285). Gorter et al. included 128 subjects with CAD in the study population; authors reported a missing connection between EAT thickness and volume, measured on CT images, and the severity of coronary stenosis or CCS. However, after adjusting the results to BMI, patients with BMI<27 kg/m^2 demonstrated a significant association of EAT measurements with the CAD severity (156).

Bastarrika et al. presented a significantly greater EAT volume in individuals with coronary artery stenosis (155±59 cm^3) in comparison to those with healthy coronary vessels (121±82 cm^3). Authors compared epicardial fat volume values, acquired from automated CT volumetry. On the other hand, EAT thickness measurements between the two groups were not significantly different. Insignificant results could be explained due to a very small study population – only 45 individuals (166). Panda et al. compared volumes of both epicardial and paracardial fat in 54 patients with present or absent CAD. Measurements were performed on CT coronary angiogram. Authors did not find significant epicardial or paracardial fat differences in respect to CAD. In contrast, EAT significantly and positively correlated with CCS (286). Another small study by Muthalaly et al. assessed 38 patients with suspected CAD. Authors investigated the connection between the size of EAT volume and the presence of perfusion defects on myocardial CT perfusion images. No significant results were reported in this study (EAT volume of 84 cm^3 with myocardial perfusion defects vs. 81 cm^3 without) (287). Finally, Chaowalit et al. demonstrated no correlation between EAT thickness and the presence or severity of CAD. Poor reproducibility of two-dimensional guided M-mode echocardiography could determine discrepant results (288).

2.7 Distribution and changes of epicardial adipose tissue in other important pathological conditions

2.7.1 Obesity, diabetes and metabolic syndrome

In general, hyperplasia of fat cells, endothelial cell activation and fibrosis are important pathophysiological processes which characterize inflamed adipose tissue in obese individuals (289). Moreover, in case of obesity adipose tissue expresses significantly more immune cells (macrophages, mast cells, lymphocytes), which act as a source of chronic systemic inflammation (290, 291). As a result, adipose tissue is brought to a state of impaired adipokine balance as well as increased production of pro-inflammatory cytokines together with FFA (292). The association between epicardial fat depots and the obesity has been described (146, 293). Moreover, EAT strongly correlated with the intraabdominal visceral fat (135, 145).

Obese adolescents with metabolic syndrome showed higher EAT thickness measurements; epicardial fat positively correlated with the concentration of fasting plasma glucose, triglycerides, uric acid in blood and some parameters of cardiac dysfunction – for instance, with left ventricular mass (294). In addition, a link between the increased EAT and non-alcoholic fatty liver disease was observed among obese adolescents (295). Overall, excess of EAT in obese children has demonstrated a clear association with cardiometabolic variables.

As a result, EAT could be considered an attractive target for interventions that might lower cardiac adiposity in early life (294, 295).

Obesity is a major element of the metabolic syndrome. Metabolic syndrome is attributed to a combination of several cardiovascular risk factors that exist together at the same time (insulin resistance, dyslipidemia, hypertension, visceral adiposity) (296). Increasing number of published studies have shown toxic effects of lipid excess, accompanying metabolic syndrome, which eventually lead to cardiac fibrosis, apoptosis of the heart cells and insufficiency of cardiac function (297-300).

Many research papers have demonstrated significantly greater amounts of EAT in patients with metabolic syndrome (73, 136, 142, 145, 146, 249, 293, 301-303). Important pathophysiological processes which define metabolic syndrome, such as inflammation, insulin sensitivity disorder, visceral adiposity and arterial hypertension, have shown strong association with increased EAT (78, 81, 206, 303-305). According to the study by Iacobellis et al., echocardiographic EAT thickness measurements over 7.5 mm and 9.5 mm are considered to be strong predictors of metabolic syndrome in European women and men, respectively (146).

Patients with type 2 diabetes exhibit higher amounts of glycation end products. These molecules damage endothelium and cause disclosure of the subendothelial collagen tissue (201). As a result, platelets can easily attach to the injured endothelium and cause local thrombosis. In addition, hyperglycemia promotes the inflammatory state of small arterial vessels, causes microcirculatory obstructions and impairs the blood supply of cardiomyocytes. Diabetes and impaired glucose tolerance have both been closely linked to cardiac lipotoxicity (190, 306).

EAT mass and thickness have been revealed to be significantly increased in patients with impaired glucose tolerance (307). Furthermore, the inflammatory burden of epicardial fat depots proved to be higher in prediabetic patients than in healthy individuals (308). EAT thickness demonstrated inverse correlation with the insulin sensitivity (138). A 9.5 mm cut-off value of EAT thickness over the RVFW predicted increased insulin resistance (146). Patients with type 2 diabetes often developed expansion of EAT mass to over 400 g, occasionally reaching 800 g (190). This exorbitant degree of EAT expansion has always caused an evident mechanical load. As a result, the peripheral vascular resistance has increased, whereas both cardiac output and ejection fraction have dropped (67).

As an illustration, Versteylen et al. investigated the size of EAT volume, glycemic state and CAD status in 410 patients. Authors found an independent association between the size of EAT and the presence of type 2 diabetes as well as with the impaired fasting glucose. However, EAT volume was not an independent predictor of CAD in this population. Furthermore, EAT volume was not associated with a specific type of coronary plaque (309).

2.7.2 Atrial fibrillation

AF is the most common type of cardiac arrhythmia. AF contributes greatly to the morbidity and mortality from congestive heart failure and cerebrovascular events (201).

Uneven atrial and ventricular distribution of epicardial fat depots could suggest the participation of EAT in the pathogenesis of AF (310). Indeed, EAT thickness was significantly positively associated with the right atrial and ventricular size in obese patients with AF (311). Moreover, greater EAT volume was connected to AF even after adjustments for traditional cardiovascular risk factors (281). Other visceral adipose tissue depots and paracardial fat were not significantly related to the presence of AF (200).

Several pathophysiological pathways of a possible EAT role in the development of AF have been observed. First of all, numerous pro-inflammatory cytokines, secreted by epicardial fat, promoted fibrosis in atrial myocardium (312). Secondly, atrial EAT was found to be rich of

ganglionated plexuses which have commonly been recognized to initiate and sustain AF (310). Finally, invasion of fat cells within an atrial myocardium have caused an electrical stimulation of conduction delays as well as a heterogeneous voltage. These pathological states are well known to be predisposing conditions of AF (312).

2.7.3 Heart failure

Individuals with severe heart failure showed decreased epicardial fat depots, measured on CMR images (313). EAT gradually decreased with the progressively reduced left ventricle function in patients with congestive heart failure (54, 314). Particularly, a reduction of EAT depots was independent from the underlying cause of cardiomyopathy (313).

Several authors in previous studies addressed the connection between the increasing size of EAT and the rise of the ventricular mass as a compensatory mechanism of the left ventricle remodeling in response to volume overload. Furthermore, left ventricle hypertrophy developed proportionally to the EAT expansion, measured by transthoracic echocardiography. The association was not related to the overall adiposity of subjects (101, 315). Possible pathogenesis of this connection included an overload of the heart muscle as well as insulin resistance, caused by the excess of EAT (140, 316); EAT induced myocardial steatosis as a result of greater intracellular lipid content (67); local and systemic effects of the pro-inflammatory cytokines, secreted by EAT (42).

Flüchter et al. revealed both lower EAT thickness over the RVFW and lower EAT volume in heart failure patients compared to healthy controls with similar BSA, BMI and age. Authors noted that during the progress of heart failure EAT did not only diminish but also redistributed around the heart muscle (168). Doesch et al. showed similar results in their study – patients with congestive heart failure displayed reduced EAT volume (317). In addition, reduced BSA-indexed EAT mass was a significant predictor of cardiac death in patients with heart failure (optimal cut-off value of 22 g/m^2) (313). Finally, one postmortem study by Schejbal showed comparable results. Human hearts with the signs of heart failure displayed significantly less EAT than healthy hearts (198).

Increased EAT accumulation is considered to be linked to the ejection fraction in heart failure patients (140, 318). Khawaja et al. evaluated 381 patients; authors noticed that on CT images measured EAT volume decreased persistently in patients with moderate (ejection fraction 35-55%) or severe (ejection fraction <35%) ventricular dysfunction in comparison to individuals with no history of heart failure (314). In contrast, heart failure patients with preserved ejection fraction showed significantly higher EAT depots than healthy controls (319).

The decrease of epicardial fat depots in heart failure patients suggests that the regulatory role of EAT in homeostasis diminishes, since a dysfunctional myocardium develops anatomic alterations and atypical metabolic needs (314). Progressive advanced heart diseases result in decline of EAT perfusion, as EAT derives its blood supply from coronary arteries (76). As a result, the protective influence of EAT on coronary vessels, heart muscle and cardiac autonomic nerves weakens. Eventually, EAT shrinks (93, 102). In addition, EAT reduction in patients with heart failure is considered to exceed a global fat decrease as a result of disease related wasting (313). Finally, a decline of EAT leads to fat accumulation in cardiomyocytes, which is shown to be an important trigger of cardiac fibrosis, dysfunction and apoptosis of the cardiac myocytes (299, 320).

2.7.4 Coronavirus disease 2019

Only data of a small number of studies with limited sample sizes are presently available about the association of epicardial fat depots and the coronavirus disease 2019 (COVID-19). Evidence presented both increased EAT volume and density as independent predictors of adverse and fatal COVID-19 courses (321). In another example, Slipczuk et al. showed the EAT volume above 98 cm^3 to be a strong and independent predictor for in-hospital mortality from COVID-19 after adjustments for age, BMI, diabetes, arterial hypertension and hyperlipidemia (322). Finally, large EAT depots were closely associated with cardiovascular complications in patients with COVID-19 (323).

2.8 Epicardial adipose tissue as a potential novel therapeutic target in cardiovascular diseases

Non-invasive assessment of epicardial fat depots is considered to be a reliable indicator of the cardiovascular risk and the total amount of visceral adipose tissue (102). EAT can be stimulated to resume its cardioprotective brown fat functions in patients with cardiovascular diseases (96). In addition, diseased pro-inflammatory epicardial fat can be therapeutically targeted as the understanding of its involvement in the pathogenesis of cardiovascular diseases increases. Potential treatment strategies include pharmacotherapy, lifestyle changes and bariatric surgery (324).

2.8.1 Pharmacotherapy

Statins and anti-diabetic drugs proved to reduce the size of EAT depots.

Hydroxymethylglutaryl-CoA reductase inhibitors are also known as statins. Statin medication group restricts the biosynthesis of cholesterol and increases the expression of low-density lipoprotein receptors (325). Some other functions of statins include an inhibition of cell adhesion in pathogenesis of atherosclerosis as well as a restriction of macrophage growth. In addition, statins suppress the production of metalloproteinases. Therefore, this drug group is categorized as vascular plaque stabilizers (326). Statins do not only reduce the size of epicardial fat depots but also suppress the pro-inflammatory metabolic EAT activity as a result of pleiotropic characteristics of this medication group (327).

Park et al. analyzed data of 145 subjects – approximately half of them daily consumed 20 milligrams (mg) of atorvastatin, others took 10 mg of simvastatin combined with 10 mg of ezetimibe. EAT thickness was regularly measured over a period of two years with transthoracic echocardiography. All individuals showed a significant decline of the cholesterol concentration in blood as well as of the measured EAT amount. However, atorvastatin was revealed to cause a significantly greater decrease of the EAT thickness in comparison to simvastatin (328).

Alexopoulos et al. in another study assessed 420 hyperlipidemic postmenopausal women who received either atorvastatin or pravastatin therapy for one year. A significant EAT size reduction was achieved only in atorvastatin group. Moreover, an intensive statin therapy showed more effective results than a moderate intensity treatment (329). In the similar way, Raggi et al. evaluated the effect of atorvastatin and pravastatin in 420 postmenopausal women. EAT volume together with the fat attenuation in the area of RCA were measured on CT images. Both atorvastatin and pravastatin effectively reduced EAT volume as well as the attenuation of pericoronary adipose tissue (330).

Parisi et al. revealed a direct independent relationship between the decrease of EAT and the statin therapy in patients with aortic stenosis. Furthermore, authors additionally analyzed EAT biopsies, collected during cardiac surgery. The inflammatory EAT status within statin group was significantly lower than in non-statin group (331).

Anti-diabetic drugs have shown a strong potential in reducing EAT depots in addition to the glycemic control. Metformin is the most frequently prescribed gold standard anti-diabetic drug worldwide. Metformin therapy significantly increases insulin sensitivity in visceral adipose tissue (308). It seems to stimulate both fat oxidation and thermogenesis, but the exact mechanism of its relationship with EAT is not fully understood (332). As an illustration, 3 months lasting metformin monotherapy decreased EAT thickness by 10% (333).

Thiazolidinediones are another group of anti-diabetic medications. Thiazolidinediones simultaneously inhibit the secretion of pro-inflammatory cytokines (IL-6, TNF-α, resistin, etc.) from different visceral adipose tissue depots. Most of EAT produced inflammatory markers were reduced in diabetes type 2 patients, treated with pioglitazone (334-336). A 24-week comparison study of the impact of both pioglitazone and metformin treatment in patients with diabetes type 2, was performed. Interestingly, an increase of both paracardial and epicardial fat volume in pioglitazone group was observed, regardless of the cardiac diastolic function improvement, presumably as a result of the inflammatory suppression of epicardial fat depots (337).

Sodium-glucose transport protein 2 (SGLT2) inhibitors are anti-diabetic drugs which block a glucose reabsorption in proximal kidney tubules, resulting in glucosuria (338). Lipolysis, ketogenesis and FFA oxidation are promoted as a result of a reduced glucose concentration in plasma, leading to the reduction of body weight due to a visceral fat burn (339). This medication group has effectively reduced visceral adipose tissue depots and EAT among diabetes type 2 patients with or without obesity (340-342). In addition to this, inflammatory qualities of EAT were significantly improved (340). As an example, Sato et al. reported a notable decrease of EAT volume and TNF-α plasma level in patients with both diabetes type 2 and CAD, treated with dapagliflozin for 6 months (342). Comparable findings were observed after the treatment with empagliflozin (343).

Incretin based anti-diabetic drugs (Glucagon-Like Peptide-1 (GLP-1) receptor agonists and Dipeptidyl Peptidase 4 (DPP-4) inhibitors) reduce blood glucose concentration by restoring insulin level, suppressing glucagon production and stimulating the release of incretin (126). In addition, this medication group has significantly reduced the body weight and the size of visceral and EAT depots as a result of an increased FFA oxidation (344, 345). Incretin based drugs have at the same time induced a browning process of adipose cells and a thermogenesis (346). Interestingly, this medication group does not lower inflammatory properties of a dysfunctional adipose tissue (347). Furthermore, incretin based anti-diabetic drugs may sometimes stimulate cardiac inflammatory conditions, resulting in myocardial fibrosis (348). It is worth mentioning that visceral adipose tissue cells express GLP-1 receptors, whereas subcutaneous fat cells do not (349). Lima-Martinez et al. evaluated the effect of sitagliptin on echocardiographically measured EAT thickness over a 24-week period in patients with diabetes type 2. After the therapy a significant reduction of epicardial fat depots was observed (350). Similar decreasing effect of liraglutide, semaglutide and dulaglutide on EAT was described in studies, conducted by Iacobellis et al. (351, 352).

Insulin restoring treatment showed a significant relationship with the decrease of epicardial fat measurements. As an example, results of the study by Elisha et al. illustrated a significant reduction of EAT thickness in diabetes type 2 patients, treated with either detemir or glargine for 6 months (353).

Several anti-inflammatory medications have demonstrated the ability of EAT modulation – colchicine, canakinumab, evolocumab, alirocumab, methotrexate and others. However, possible mechanisms of the impact as well as the effect range and are yet to be understood (126, 354).

2.8.2 Lifestyle changes and bariatric surgery

Both resistance and endurance training have reduced EAT depots (355-357). As an illustration, Christensen et al. demonstrated a decrease of EAT volume up to 32% after the 12-week continuing endurance and resistance training program (355). Moreover, Konwerski et al. studied the connection of intense aerobic physical training with EAT volume in ultramarathon amateur athletes. Epicardial fat volume proved to be significantly lower in athletes compared to non-athletes (358). The meta-analysis by Saco-Ledo et al. confirmed a positive effect of endurance training as a way of EAT reduction (359).

Low calorie diet is another way to decrease epicardial fat depots (360, 361). Kim et al. evaluated obese middle-aged individuals which were exposed to a hypocaloric diet (reduction up to 27% of the daily caloric intake) and an aerobic exercise program for an interval of 12 weeks. Authors reported a mean decrease of EAT volume by 17% by the end of the study (362). Furthermore, reduction of EAT thickness proved to be more significant than a decrease of BMI or waist circumference. Aerobic exercise program additionally resulted in corrected systolic blood pressure and increased insulin sensitivity (363). Iacobellis et al. showed that a decrease in EAT thickness, rather than waist circumference, improved cardiac diastolic function after a significant weight loss, caused by a 6 month very low calorie (900 kcal/day) diet program in critically obese Caucasians. Of note, EAT depots decreased significantly quicker in comparison to other fat depots (364).

A substantial weight loss in patients with severe obesity after a bariatric surgery has been followed by a reduction of epicardial fat depots (365-368). As an example, Willens et al. demonstrated a significant decrease of EAT thickness measurements in extremely obese patients after bariatric surgery and an average weight loss of 40±14 kg (369). Other authors reported a reduction of epicardial fat depots by 31% two years after bariatric surgery procedures (367).

A meta-analysis by Rabkin and Campbell clearly identified epicardial fat as a modifiable risk factor, associated with CAD. Dietary interventions with a consequent weight loss correlated with the linear reduction of EAT. Exercise programs were less connected to a decrease of epicardial fat depots, often due to the lack of a consequent reduction in total body weight. Therefore, it can be speculated that weight loss might be essential for a drop in EAT mass. Although the most spectacular weight loss can be achieved after bariatric surgery procedures, the decrease of EAT in this group was similar to that of the diet group. One potential explanation could be the existence of a certain limit of epicardial fat size, below which an additional reduction could not be achieved (370).

3 Materials and methods

3.1 Study design and population

This retrospective case-control study involved adult individuals who received CMR scan in the past due to different medical conditions. The data was gathered in Gemeinschaftsklinikum Mittelrhein gGmbH, Academic Educational Hospital of the Johannes Gutenberg University of Mainz.

Between January 2017 and January 2022, 760 consecutive adult patients underwent CMR imaging in our institution. Some of the study subjects had to be removed from the final analysis. 55 patients were withdrawn due to the absence of necessary CMR sequences because of different reasons: investigation without contrast media, scan interruption as a result of abundant extrasystoles or claustrophobia, substantial artefact burden in CMR images. 30 patients were excluded due to the significant pericardial effusion, which made the quantification of EAT impossible. 14 patients with coronary artery bypass or stent were removed from the analysis to avoid potential confounding. 4 patients were withdrawn because of the absence of medical records. 24 patients underwent CMR imaging several times over the course of 5 years. In this instance, only the initial CMR scan was examined. In 3 cases the initial CMR scan was not generated between January 2017 and January 2022 – these individuals were excluded. Finally, 630 study subjects entered the final analysis.

Because of the retrospective nature of our study, the approval of a local ethic committee was not required. Gathered data was anonymized to prevent the identification of patients and to comply with the European Union's new General Data Protection Regulation.

3.2 Cardiac magnetic resonance imaging protocol

All imaging studies were performed using two systems – either 1.0-Tesla whole-body magnetic resonance imaging (MRI) system (Panorama HFO™, Philips Healthcare, Best, The Netherlands) or 3.0-Tesla whole-body MRI system (Achieva™, Philips Healthcare, Best, The Netherlands). In cardiac imaging, a Body/Spine XL coil was used for the 1.0-Tesla system; a SENSE Torso/Cardiac coil for the 3.0-Tesla system. CMR images were acquired during repeated end-expiratory breathholds. Cardiac synchronization was achieved with a four-electrode vector electrocardiogram, image acquisitions were triggered during the R-wave.

First of all, sagittal, coronal and axial scout images were obtained for further planning of the cardiac long- and short-axis views. After that, electrocardiogram-gated images were achieved using a SSFP algorithm – 2D multiphase (cine) B-SSFP sequence, acquired in three short axial slices (basal, mid-ventricular and apical) of the left and right ventricle (time to echo/time of repetition – 2.6/5.2 milliseconds (ms), flip angle – 70°, slice thickness – 8 mm, interslice gap – 20 mm for 1.0-Tesla system; time to echo/time of repetition – 1.6/3.1 ms, flip angle – 40°, slice thickness – 8 mm, interslice gap – 20 mm for 3.0-Tesla system). Using the same algorithm, transversal long-axis four-chamber images were acquired. Imaging parameters were as follows: time to echo/time of repetition – 2.5/5.0 ms, flip angle – 70°, slice thickness – 8 mm for 1.0-Tesla system; time to echo/time of repetition – 1.5/3.1 ms, flip angle – 40°, slice thickness – 8 mm for 3.0-Tesla system.

Approximately 10-15 minutes after the injection of a gadolinium-based contrast agent Dotarem (Guerbet, Raleigh, NC, USA), late gadolinium enhancement imaging was performed using the inversion recovery prepared T1 weighted gradient echo sequence. Overall, six to fifteen short-axis views, covering the whole left and right ventricle in same orientations, applied for cine

short-axis images, were obtained. Additional four- and two-chamber long-axis images were acquired. Imaging parameters were as follows: time to echo/time of repetition – 1.5/4.1 ms, flip angle – 15°, slice thickness – 10 mm, interslice gap – 5 mm for 1.0-Tesla system; time to echo/time of repetition – 1.8/3.7 ms, flip angle – 15°, slice thickness – 10 mm, interslice gap – 5 mm for 3.0-Tesla system.

3.3 Measurements of epicardial adipose tissue depots

Although 3.0 Tesla MRI scanners provide better resolution, field strength does not have a significant impact on the assessment of cardiac volume or mass. Values, obtained on lower field strength scanners, can be applied to scans obtained on 3.0 Tesla scanners. Moreover, MRI is considered to be the gold standard modality for visualization of adipose tissue and total body fat, which allows uncomplicated analysis of EAT on both 3.0 and 1.0 Tesla MRI scanners (6, 22, 48, 371-373).

Overall, 351 (55.7%) individuals were examined with 1.0 Tesla scanner, 279 (44.3%) – with 3.0 Tesla scanner.

CMR scan images were assessed off-line using the Digital Imaging and Communications in Medicine (DICOM) viewer “Carestream Picture Archiving and Communication System (PACS)” software (Carestream Inc. New York, USA).

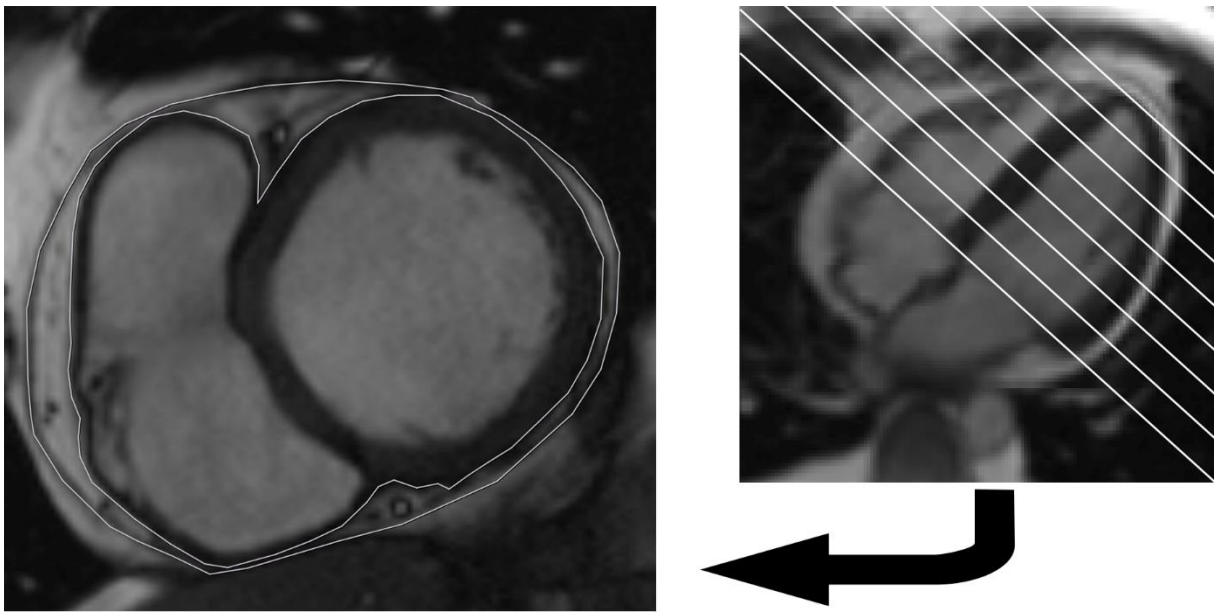

Figure 5. Calculation of epicardial adipose tissue volume by using modified Simpson rule with integration over the image slices.

EAT was cranially confined by the origin of the pulmonary trunk, caudally by the diaphragmal base of the heart. EAT volume was calculated by using modified Simpson rule with integration over the image slices (45). EAT volume was measured on both 2D multiphase (cine) B-SSFP sequence (further in text SSFP EAT volume) and inversion recovery prepared T1 weighted gradient echo sequence (further in text T1IR EAT volume). Late gadolinium imaging allowed more precise measurements of EAT volume as a result of smaller interslice gaps. Outlines of EAT (between the heart muscle and pericardium) on the entire left and right ventricles were manually defined using an area measurement tool on CMR short-axis images during the left

ventricle end-diastolic phase. The sum of EAT areas, subtended by the manual tracings, was multiplied by the sum of both slice thickness (8 mm) and interslice gap (20 mm) on B-SSFP sequence. The sum of EAT areas from late gadolinium enhancement images was multiplied by the difference between slice thickness (10 mm) and interslice gap (5 mm) as a result of overlapped slice interval settings. The final result was defined as an EAT volume (Figure 5).

EAT thickness was measured manually using a distance measurement tool on 2D multiphase (cine) B-SSFP sequence short-axis and long-axis images during the left ventricle end-diastolic phase. Altogether there were 11 EAT thickness measurements conducted: three measurements over the RVFW, three over the LVFW, single measurement in the superior interventricular groove (SIVG), inferior interventricular groove (IIVG), AIVG, RAVG and LAVG. Specifically, measurements over the RVFW and LVFW were performed at the 25%, 50% and 75% location from the wall, perpendicular to the surface of the heart (Figure 6).

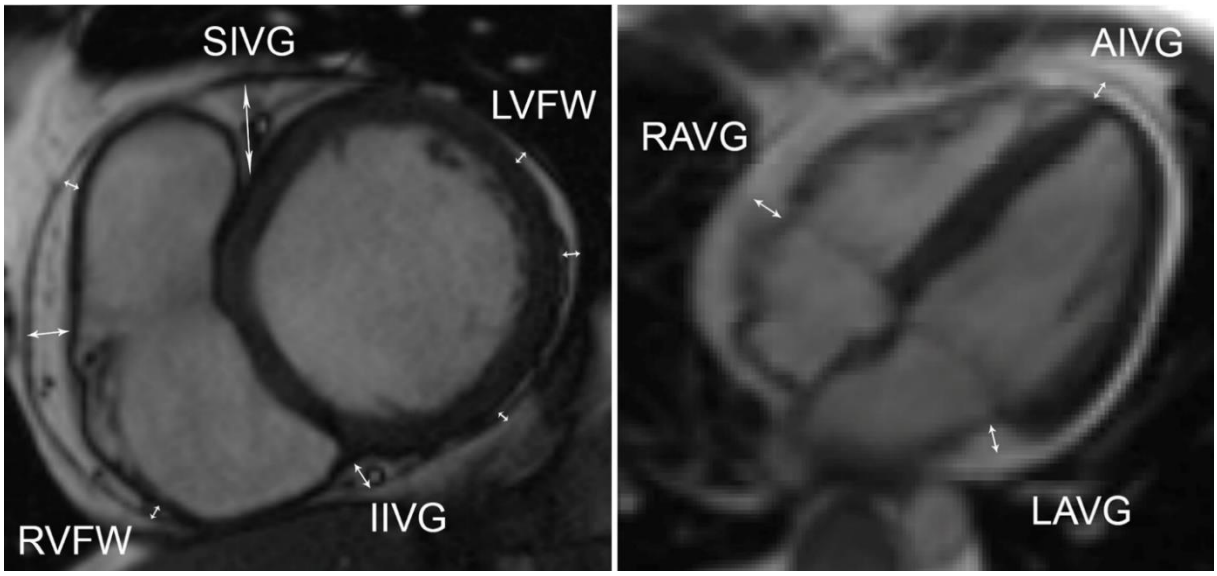

Figure 6. Measurements of epicardial adipose tissue thickness. Abbreviations: AIVG – anterior interventricular groove, IIVG – inferior interventricular groove, LAVG – left atrioventricular groove, LVFW – left ventricular free wall, RAVG – right atrioventricular groove, RVFW – right ventricular free wall, SIVG – superior interventricular groove.

In the final analysis, separate EAT thickness measurements as well as mean values of EAT thickness were used as follows: overall mean thickness from measurements in 11 locations, mean thickness of groove measurements (5 locations), mean thickness of measurements over the ventricular FW (6 locations), mean thickness of measurements over the RVFW (3 locations) and mean thickness of measurements over the LVFW (3 locations).

3.4 Assessment of coronary artery disease severity

According to health records, patients were assigned to either CAD or non-CAD group. The diagnosis of CAD was determined by health care professionals according to the European Society of Cardiology (ESC) guidelines on chronic coronary syndromes (374, 375) as well as the 3rd and 4th universal definition of myocardial infarction (376, 377). It should be noted that patients with the coronary procedure related myocardial infarction were not included in the final analysis to avoid possible confounding.

All CAD patients received a coronary angiography procedure either in our or in an external institution. Overall, patients with the angiographic evidence of ≥1 stenosis of ≥50% in diameter in a major coronary artery (RCA, LAD or LCX) were assigned to the CAD group. CAD group additionally included patients who suffered from acute myocardial infarction as a result of the atherothrombotic CAD (type 1 myocardial infarction) (377). Patients without a coronary stenosis or with ≥1 stenosis of <50% in a major coronary artery were assigned to the non-CAD group. The severity of CAD was assessed with two grading scales – the Canadian Cardiovascular Society grading of angina pectoris and the Gensini Score.

3.4.1 Canadian Cardiovascular Society grading of angina pectoris

The Canadian Cardiovascular Society grading system for angina pectoris is a clinical classification, used by cardiologists to estimate the extent of severity of a chest pain or pressure, caused by insufficient blood flow to the myocardium (378). The system consists of four grades. Aggravation rate of angina pectoris corresponds with the increase of grades (Table 5).

Grade	Description
Grade I	Ordinary physical activity does not cause angina, such as walking and climbing stairs. Angina with strenuous or rapid or prolonged exertion at work or recreation.
Grade II	Slight limitation of ordinary activity. Walking or climbing stairs rapidly, walking uphill, walking or stair climbing after meals, or in cold, or in wind, or under emotional stress, or only during the few hours after awakening. Walking more than two blocks on the level and climbing more than one flight of ordinary stairs at a normal pace and in normal conditions.
Grade III	Marked limitation of ordinary physical activity. Walking one or two blocks on the level and climbing one flight of stairs in normal conditions and at normal pace.
Grade IV	Inability to carry on any physical activity without discomfort, anginal syndrome may be present at rest.

Table 5. Canadian Cardiovascular Society grading of angina pectoris.

CAD patients in our study were assigned to the corresponding grade of the Canadian Cardiovascular Society grading system for angina pectoris by cardiologists during their stay in a hospital.

3.4.2 Gensini Score

The Gensini score is a commonly used angiographic grading system for calculating the severity of CAD (379-381). The Gensini score takes into account 3 variables for each coronary lesion - severity score, region multiplying factor and collateral adjustment factor. The severity score for each lesion may rank from 1 to 32, based on the degree of stenosis. The multiplying factor is applied to each coronary lesion according to its location. The extent of multiplying factor relies on the importance of the area which is supplied by a specific coronary segment. A step-by-step algorithm for the Gensini score calculation can be found in Table 6.

Coronary arteries of CAD patients, who received coronary angiography procedure, were evaluated – Gensini score for each CAD patient was calculated.

Step 1. Severity score calculation for each coronary lesion and adjustment for total occlusion or receiving collaterals			
Degree of stenosis (%)	**Receiving collaterals**	**Adjustment for collaterals**	**Severity score**
1-25	-	0	1
26-50	-	0	2
51-75	-	0	4
76-90	-	0	8
91-99	no	0	16
99	yes	-8	8
100	no	0	32
100	yes, and normal source vessel	-16	32-16=16
100	yes, and 25% stenosis source vessel	-12	32-12=20
100	yes, and 50% stenosis source vessel	-8	32-8=24
100	yes, and 75% stenosis source vessel	-4	32-4=28
100	yes, and 90% stenosis source vessel	-2	32-2=30
100	yes, and 99% stenosis source vessel	-1	32-1=31
Step 2. A multiplying factor is applied to each coronary lesion based upon its location			
Coronary segment		**Right dominance**	**Left dominance**
Proximal segment of right coronary artery		1	1
Middle segment of right coronary artery		1	1
Distal segment of right coronary artery		1	1
Posterior descending artery		1	1
Posterolateral artery		0.5	0.5
Left main coronary arery		5	5
Proximal segment of left anterior descending artery		2.5	2.5
Middle segment of left anterior descending artery		1.5	1.5
Distal segment of left anterior descending artery		1	1
1st diagonal artery		1	1
2nd diagonal artery		0.5	0.5
Proximal segment of left circumflex artery		2.5	3.5
Middle segment of left circumflex artery		1	2
Distal segment of left circumflex artery		1	2
Obtuse marginal artery		1	1
Step 3. Sum of all coronary lesion severity scores			

Table 6. A step-by-step algorithm for the Gensini score calculation.

3.5 Other variables

The age and gender of patients were registered according to their health records. An additional binary variable of age ≥ 50 years was built as a risk factor for CAD (382). The height and weight of patients were recorded from the MRI safety screening questionnaire. These two variables were used to calculate BMI according to the formula: weight (kg) / (height (m) ^{2}). Subjects with BMI≥30 kg/m^2 were defined as obese (383). In addition to this, BSA was calculated by a variation of the DuBois and DuBois formula: BSA (m^2) = (weight (kg)$^{0.425}$ × height (cm)$^{0.725}$) × 0.007184 (384, 385). Finally, interventricular septum length (ISL) was manually measured using a distance measurement tool on CMR 2D multiphase (cine) B-SSFP long-axis images during the left ventricle end-diastolic phase.

3.6 Statistical analysis

All statistical tests were undertaken using SPSS 22.0 for Windows (SPSS, Inc, Chicago, Illinois). Significance level $\alpha=0.05$ was chosen for the statistical analysis. A normality of the variable distribution was not tested according to the central limit theorem and as a result of the large sample size (N>30). Measures of central tendency were presented as follows – mean ± standard deviation. Categorical variables were displayed as frequencies or percentages. A T-test was used for the comparison of variable means. Frequencies between the studied groups were compared using the chi-squared criterion. All tests were two-tailed.

A binary logistic regression analysis was conducted for the identification of possible CAD predictors. Overall three models were built with the most commonly reported EAT measurements – EAT volume (both SSFP and T1IR) as well as average EAT thickness over the RVFW. For the purpose of model stabilization, EAT measurements were transformed into categorical variables. Moreover, previously established and in this study examined CAD risk factors were used as additional predictors – age≥50 years, male gender, BMI≥30 kg/m^2 (obese patients) (382). Odds ratios and confidence intervals were calculated for each variable in the model. Hosmer–Lemeshow goodness of fit test was applied.

All EAT thickness measurements and EAT volume were indexed by BMI, BSA and ISL. Receiver operating characteristic (ROC) curve analysis was performed in order to identify the most suitable EAT measurement as well as reference values for the prediction of CAD. AUC was assessed to determine the accuracy of both indexed and non-indexed EAT measurements. In addition, ROC analysis showed whether indexation of EAT measurements provided benefit in identification of CAD patients. Finally, sensitivity and specificity were calculated for cut-off values of EAT measurements with the highest AUC value.

Analysis of variance (ANOVA) was performed in order to evaluate the connection between most feasible EAT measurements in regard to the Canadian Cardiovascular Society grading system for angina pectoris. Pearson correlation coefficient was applied for the estimation of a possible association between most effective EAT measurements and the Gensini score.

4 Results

Overall, 630 study subjects entered the final analysis.

4.1 Descriptive analysis

The mean age of individuals in our study was 54±16 years. Of 630 subjects studied, 405 (64.3%) were males. The mean BMI was 26.38±4.35 kg/m^2, the mean BSA was 1.95±0.21 m^2. Overall, 273 (43.3%) individuals were diagnosed with CAD. According to the Canadian Cardiovascular Society grading system for angina pectoris, CAD patients aligned as follows: grade I – 51 (18.7%), grade II – 100 (36.6%), grade III – 76 (27.8%), grade IV – 46 (16.8%). Of 273 CAD patients, 208 (76.2%) received coronary angiography. The mean Gensini score among these patients was 42.1±33.2 points.

The mean SSFP EAT volume was 97.45±38.02 cm^3 in the whole studied population. The mean T1IR EAT volume was 103.34±37.16. The overall mean value of the average EAT thickness in all locations was 7.1±2.2 mm. Other mean values of both indexed and non-indexed EAT measurements can be found in Table 7. Finally, the mean ISL was 89.05±9.84 mm.

EAT Measurements	Non-indexed (cm^3 or mm)	BMI-indexed (cm^3/(kg/m^2) or mm/(kg/m^2))	BSA-indexed (cm^3/m^2 or mm/m^2)	ISL-indexed (cm^3/mm or mm/mm)
EAT Volume				
SSFP	97.45±38.02	3.68±1.29	49.65±17.85	1.10±0.44
T1IR	103.34±37.16	3.92±1.27	52.59±16.95	1.16±0.41
EAT Thickness				
RVFW1	6.0±3.3	0.23±0.12	3.09±1.68	0.07±0.04
RVFW2	6.3±3.4	0.24±0.12	3.22±1.70	0.07±0.04
RVFW3	7.7±4.3	0.29±0.16	3.91±2.16	0.09±0.05
LVFW1	2.6±1.8	0.10±0.07	1.35±0.95	0.03±0.02
LVFW2	3.0±2.3	0.11±0.08	1.51±1.14	0.03±0.03
LVFW3	2.8±2.0	0.10±0.07	1.42±0.98	0.03±0.02
RAVG	12.6±4.7	0.48±0.17	6.44±2.32	0.14±0.06
AIVG	8.9±4.3	0.34±0.16	4.54±2.07	0.10±0.05
LAVG	10.6±3.6	0.40±0.14	5.43±1.80	0.12±0.04
IIVG	6.1±2.4	0.24±0.10	3.18±1.30	0.07±0.03
SIVG	11.3±3.9	0.43±0.14	5.82±1.93	0.13±0.05
Average RVFW	6.7±3.2	0.25±0.12	3.41±1.60	0.08±0.04
Average LVFW	2.8±1.8	0.11±0.06	1.43±0.90	0.03±0.02
Average FW	4.7±2.2	0.18±0.08	2.42±1.08	0.05±0.02
Average groove	9.9±2.8	0.38±0.10	5.08±1.35	0.11±0.03
Average all locations	7.1±2.2	0.27±0.08	3.63±1.09	0.08±0.03

Table 7. Non-indexed and indexed mean values of epicardial fat measurements of individuals included in the final analysis. Abbreviations: AIVG – anterior interventricular groove, BMI – body mass index, BSA – body surface area, cm – centimeter, EAT – epicardial adipose tissue, FW – free wall, IIVG – inferior interventricular groove, ISL - interventricular septum length, kg – kilogram, LAVG – left atrioventricular groove, LVFW – left ventricular free wall, m – meter, mm – millimeter, RAVG – right atrioventricular groove, RVFW – right ventricular free wall, SIVG – superior interventricular groove, SSFP - steady state free precession, T1IR – T1 inversion recovery.

4.2 Differences in subjects with and without coronary artery disease

Despite the efforts to create groups of patients as similar as possible in terms of CAD risk factors, they did have some differences. First of all, CAD patients were older – 64±10 vs. 47±16 years, p<0.001. Furthermore, male patients were significantly more common in CAD group – 220 (80.6%) vs. 185 (51.8%), p<0.001. Finally, CAD group showed significantly higher BMI in comparison to non-CAD patients – 27.58±4.26 vs. 25.46±4.19 kg/m^2, p<0.001. BSA and ISL did not significantly differ between the two groups.

All executed EAT measurements were significantly higher in CAD group in comparison to non-CAD patients, p<0.001 (Table 8).

Non-indexed EAT Measurements	CAD group (N=273)	Non-CAD Group (N=357)
SSFP volume (cm^3)	123.44±35.68	77.58±25.82
T1IR volume (cm^3)	128.46±34.96	84.13±25.52
RVFW1 thickness (mm)	7.6±3.7	4.8±2.4
RVFW2 thickness (mm)	8.0±3.5	5.0±2.6
RVFW3 thickness (mm)	9.8±4.7	6.0±3.1
LVFW1 thickness (mm)	3.3±2.1	2.1±1.4
LVFW2 thickness (mm)	3.9±2.7	2.3±1.6
LVFW3 thickness (mm)	3.4±2.2	2.3±1.5
RAVG thickness (mm)	14.8±4.4	10.9±4.1
AIVG thickness (mm)	10.8±4.7	7.5±3.2
LAVG thickness (mm)	12.5±3.4	9.1±3.0
IIVG thickness (mm)	6.8±2.7	5.6±2.1
SIVG thickness (mm)	12.9±3.8	10.1±3.4
Average RVFW thickness (mm)	8.5±3.3	5.3±2.2
Average LVFW thickness (mm)	3.5±2.0	2.2±1.3
Average FW thickness (mm)	6.0±2.2	3.7±1.5
Average groove thickness (mm)	11.6±2.5	8.6±2.2
Average all locations thickness (mm)	8.5±2.0	6.0±1.6

Table 8. Non-indexed epicardial fat measurements in subjects with and without coronary artery disease. Abbreviations: AIVG – anterior interventricular groove, CAD – coronary artery disease, cm – centimeter, EAT– epicardial adipose tissue, FW – free wall, IIVG – inferior interventricular groove, LAVG – left atrioventricular groove, LVFW – left ventricular free wall, mm – millimeter, RAVG – right atrioventricular groove, RVFW – right ventricular free wall, SIVG – superior interventricular groove, SSFP - steady state free precession, T1IR – T1 inversion recovery

Although the two groups showed differences in terms of CAD risk factors, the relatively large number of patients involved in this study allowed us to perform more complex methods of statistical analysis. A multivariate binary logistic regression was conducted to assess further the association of EAT measurements in regard to CAD. Overall, 3 models were constructed. The most commonly in literature reported EAT measurements were used as predictors – SSFP EAT volume, T1IR EAT volume, average EAT thickness over the RVFW. For the purpose of model stabilization, EAT measurements were transformed into categorical variables. According to the systematic review by Bertaso et al., EAT volume over 125 cm^3, as well as EAT thickness over 5 mm should be considered abnormal (45). Moreover, previously established and in this study examined CAD risk factors were used as additional predictors – age ≥ 50 years, male gender, BMI ≥ 30 kg/m^2 (obese patients) (382). All three logistic regression models are displayed in Table 9.

Model 1. Prediction of CAD with SSFP EAT volume among other predictors		
Risk factor	**Odds Ratio (95% CI)**	**p value**
Male gender	3.355 (2.176-5.172)	<0.001
Age ≥ 50 years	12.138 (7.107-20.731)	<0.001
BMI ≥ 30 kg/m^2 (obese patients)	1.769 (1.044-2.999)	0.034
SSFP EAT volume ≥ 125 cm^3	5.983 (3.426-10.449)	<0.001
Model 2. Prediction of CAD with T1IR EAT volume among other predictors		
Risk factor	**Odds Ratio (95% CI)**	**p value**
Male gender	2.647 (1.702-4.119)	<0.001
Age ≥ 50 years	12.912 (7.483-22.280)	<0.001
BMI ≥ 30 kg/m^2 (obese patients)	1.487 (0.866-2.554)	0.150
T1IR EAT volume ≥ 125 cm^3	6.817 (4.012-11.584)	<0.001
Model 3. Prediction of CAD with average RVFW EAT thickness among other predictors		
Risk factor	**Odds Ratio (95% CI)**	**p value**
Male gender	3.872 (2.501-5.997)	<0.001
Age ≥ 50 years	10.988 (6.403-18.855)	<0.001
BMI ≥ 30 kg/m^2 (obese patients)	1.821 (1.090-3.041)	0.022
Average RVFW EAT thickness ≥ 5 mm	5.609 (3.454-9.107)	<0.001

Table 9. Multivariate binary logistic regression models for the prediction of coronary artery disease. Abbreviations: BMI – body mass index, CAD – coronary artery disease, CI – confidence interval, cm – centimeter, EAT– epicardial adipose tissue, kg – kilogram, mm – millimeter, RVFW – right ventricular free wall, SSFP - steady state free precession, T1IR – T1 inversion recovery

Hosmer–Lemeshow goodness of fit test was p=0.889 for the first, p=0.635 for the second, p=0.661 for the third model, indicating a good logistic regression model fit. Results of the multivariate binary logistic regression analysis showed that both EAT volume and thickness over the RVFW acted as an independent predictor of CAD among other established CAD risk factors. Moreover, EAT measurements demonstrated higher odds ratios than obesity or male gender. In the predictive model with T1IR EAT volume, obesity became an insignificant predictor of CAD – meaning that epicardial fat depots, as another accepted indicator of visceral adiposity, outperformed obesity in identification of CAD patients. Overall, EAT measurements seem to be a reliable marker of CAD risk evaluation.

During the next step, non-indexed EAT measurements were indexed by BMI, BSA and ISL. BMI-indexed EAT measurements were in all cases significantly higher in CAD group in comparison to non-CAD patients, p<0.001 (Table 10).

BMI-indexed EAT Measurements	CAD group (N=273)	Non-CAD Group (N=357)
SSFP volume (cm^3/(kg/m^2))	4.51±1.26	3.05±0.88
T1IR volume (cm^3/(kg/m^2))	4.71±1.26	3.32±0.89
RVFW1 thickness (mm/(kg/m^2))	0.28±0.14	0.19±0.09
RVFW2 thickness (mm/(kg/m^2))	0.29±0.13	0.20±0.10
RVFW3 thickness (mm/(kg/m^2))	0.36±0.18	0.24±0.12
LVFW1 thickness (mm/(kg/m^2))	0.12±0.08	0.08±0.06
LVFW2 thickness (mm/(kg/m^2))	0.14±0.10	0.09±0.06
LVFW3 thickness (mm/(kg/m^2))	0.13±0.08	0.09±0.06
RAVG thickness (mm/(kg/m^2))	0.54±0.17	0.43±0.16
AIVG thickness (mm/(kg/m^2))	0.40±0.18	0.29±0.12
LAVG thickness (mm/(kg/m^2))	0.46±0.13	0.36±0.12
IIVG thickness (mm/(kg/m^2))	0.25±0.11	0.23±0.09
SIVG thickness (mm/(kg/m^2))	0.47±0.15	0.40±0.13
Average RVFW thickness (mm/(kg/m^2))	0.31±0.13	0.21±0.08
Average LVFW thickness (mm/(kg/m^2))	0.13±0.07	0.09±0.05

BMI-indexed EAT Measurements	CAD group (N=273)	Non-CAD Group (N=357)
Average FW thickness (mm/(kg/m^2))	0.22±0.08	0.15±0.05
Average groove thickness (mm/(kg/m^2))	0.43±0.10	0.34±0.08
Average all locations thickness (mm/(kg/m^2))	0.31±0.08	0.24±0.06

Table 10. Epicardial fat measurements indexed by body mass index in subjects with and without coronary artery disease. Abbreviations: AIVG – anterior interventricular groove, BMI – body mass index, CAD – coronary artery disease, cm – centimeter, EAT– epicardial adipose tissue, FW – free wall, IIVG – inferior interventricular groove, kg – kilogram, LAVG – left atrioventricular groove, LVFW – left ventricular free wall, m – meter, mm – millimeter, RAVG – right atrioventricular groove, RVFW – right ventricular free wall, SIVG – superior interventricular groove, SSFP - steady state free precession, T1IR – T1 inversion recovery

Similarly, BSA-indexed EAT measurements were in all cases significantly increased in CAD group, p<0.001 (Table 11).

BSA-indexed EAT Measurements	CAD group (N=273)	Non-CAD Group (N=357)
SSFP volume (cm^3/m^2)	61.91±16.92	40.27±11.85
T1IR volume (cm^3/m^2)	64.33±16.08	43.60±11.10
RVFW1 thickness (mm/m^2)	3.86±1.87	2.51±1.24
RVFW2 thickness (mm/m^2)	4.04±1.81	2.60±1.30
RVFW3 thickness (mm/m^2)	4.94±2.36	3.13±1.59
LVFW1 thickness (mm/m^2)	1.65±1.06	1.12±0.77
LVFW2 thickness (mm/m^2)	1.94±1.36	1.19±0.80
LVFW3 thickness (mm/m^2)	1.72±1.12	1.19±0.78
RAVG thickness (mm/m^2)	7.43±2.20	5.69±2.12
AIVG thickness (mm/m^2)	5.41±2.29	3.88±1.58
LAVG thickness (mm/m^2)	6.32±1.75	4.76±1.53
IIVG thickness (mm/m^2)	3.45±1.46	2.97±1.13
SIVG thickness (mm/m^2)	6.49±1.95	5.31±1.76
Average RVFW thickness (mm/m^2)	4.28±1.72	2.74±1.12
Average LVFW thickness (mm/m^2)	1.77±1.02	1.16±0.70
Average FW thickness (mm/m^2)	3.02±1.14	1.95±0.76
Average groove thickness (mm/m^2)	5.82±1.27	4.52±1.12
Average all locations thickness (mm/m^2)	4.29±1.05	3.12±0.81

Table 11. Epicardial fat measurements indexed by body surface area in subjects with and without coronary artery disease. Abbreviations: AIVG – anterior interventricular groove, BSA – body surface area, CAD – coronary artery disease, cm – centimeter, EAT– epicardial adipose tissue, FW – free wall, IIVG – inferior interventricular groove, LAVG – left atrioventricular groove, LVFW – left ventricular free wall, m – meter, mm – millimeter, RAVG – right atrioventricular groove, RVFW – right ventricular free wall, SIVG – superior interventricular groove, SSFP - steady state free precession, T1IR – T1 inversion recovery

Finally, ISL-indexed EAT measurements were also in all cases significantly increased in CAD group, p<0.001 (Table 12).

ISL-indexed EAT Measurements	CAD group (N=273)	Non-CAD Group (N=357)
SSFP volume (cm^3/mm)	1.39±0.44	0.89±0.31
T1IR volume (cm^3/mm)	1.43±0.40	0.96±0.28
RVFW1 thickness (mm/mm)	0.09±0.04	0.06±0.03
RVFW2 thickness (mm/mm)	0.09±0.04	0.06±0.03
RVFW3 thickness (mm/mm)	0.11±0.05	0.07±0.04

ISL-indexed EAT Measurements	CAD group (N=273)	Non-CAD Group (N=357)
LVFW1 thickness (mm/mm)	0.04±0.02	0.02±0.02
LVFW2 thickness (mm/mm)	0.04±0.03	0.03±0.02
LVFW3 thickness (mm/mm)	0.04±0.03	0.03±0.02
RAVG thickness (mm/mm)	0.17±0.05	0.12±0.05
AIVG thickness (mm/mm)	0.12±0.06	0.09±0.04
LAVG thickness (mm/mm)	0.14±0.04	0.10±0.04
IIVG thickness (mm/mm)	0.08±0.03	0.06±0.03
SIVG thickness (mm/mm)	0.15±0.05	0.12±0.04
Average RVFW thickness (mm/mm)	0.10±0.04	0.06±0.03
Average LVFW thickness (mm/mm)	0.04±0.02	0.03±0.02
Average FW thickness (mm/mm)	0.07±0.03	0.04±0.02
Average groove thickness (mm/mm)	0.13±0.03	0.10±0.03
Average all locations thickness (mm/mm)	0.10±0.03	0.07±0.02

Table 12. Epicardial fat measurements indexed by interventricular septum length in subjects with and without coronary artery disease. Abbreviations: AIVG – anterior interventricular groove, CAD – coronary artery disease, cm – centimeter, EAT– epicardial adipose tissue, FW – free wall, IIVG – inferior interventricular groove, ISL – interventricular septum length, LAVG – left atrioventricular groove, LVFW – left ventricular free wall, mm – millimeter, RAVG – right atrioventricular groove, RVFW – right ventricular free wall, SIVG – superior interventricular groove, SSFP - steady state free precession, T1IR – T1 inversion recovery

All in all, indexation of EAT measurements did not influence the difference between two groups. Indexed EAT measurements remained in all cases significantly higher in CAD patients in comparison to healthy controls.

4.3 Receiver operating characteristic curve analysis

Receiver operating characteristic curve (ROC) analysis was performed to identify the most suitable EAT measurements (indexed or non-indexed) for identification of CAD patients. The area under the curve (AUC) was assessed to determine the accuracy of both indexed and non-indexed EAT measurements. The results of ROC analysis of non-indexed EAT measurements are displayed in Table 13.

Non-indexed EAT Measurements	Area Under the Curve (AUC)
SSFP volume (cm^3)	0.881
T1IR volume (cm^3)	0.866
RVFW1 thickness (mm)	0.755
RVFW2 thickness (mm)	0.771
RVFW3 thickness (mm)	0.766
LVFW1 thickness (mm)	0.682
LVFW2 thickness (mm)	0.688
LVFW3 thickness (mm)	0.665
RAVG thickness (mm)	0.744
AIVG thickness (mm)	0.729
LAVG thickness (mm)	0.779
IIVG thickness (mm)	0.627
SIVG thickness (mm)	0.711
Average RVFW thickness (mm)	0.808
Average LVFW thickness (mm)	0.708

Non-indexed EAT Measurements	Area Under the Curve (AUC)
Average FW thickness (mm)	0.821
Average groove thickness (mm)	0.816
Average all locations thickness (mm)	0.848

Table 13. Results of the receiver operating characteristic curve analysis of non-indexed epicardial adipose tissue measurements. The top 5 EAT measurements with the highest AUC values are highlighted with the green color. Abbreviations: AIVG – anterior interventricular groove, AUC – area under the curve, cm – centimeter, EAT– epicardial adipose tissue, FW – free wall, IIVG – inferior interventricular groove, LAVG – left atrioventricular groove, LVFW – left ventricular free wall, mm – millimeter, RAVG – right atrioventricular groove, RVFW – right ventricular free wall, SIVG – superior interventricular groove, SSFP - steady state free precession, T1IR – T1 inversion recovery

ROC analysis of non-indexed EAT measurements identified 5 variables with the highest AUC values – SSFP and T1IR EAT volume, average EAT thickness over the FW and in the areas of grooves, average EAT thickness in all locations (Figure 7).

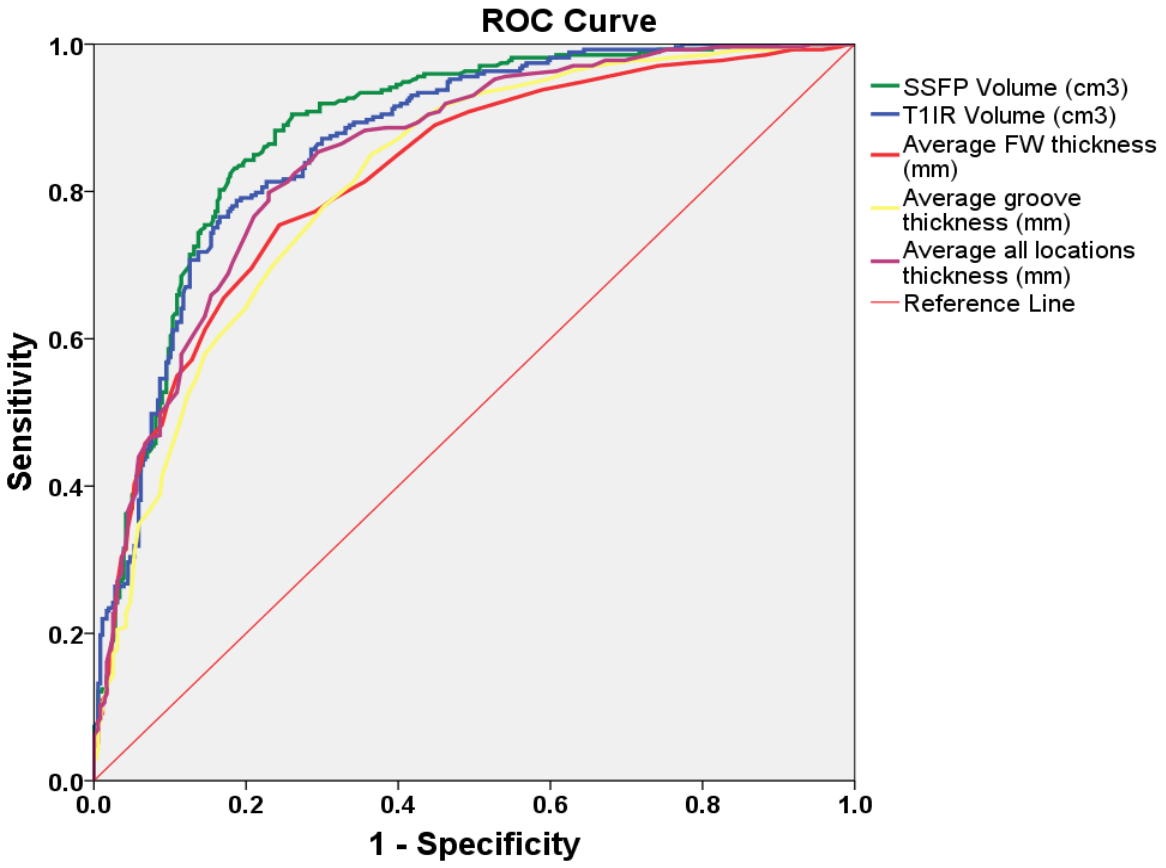

Figure 7. Receiver operating characteristic curve containing 5 non-indexed measurements of epicardial adipose tissue with the highest area under the curve values. Abbreviations: cm – centimeter, FW – free wall, mm – millimeter, ROC – receiver operating characteristic, SSFP - steady state free precession, T1IR – T1 inversion recovery

All in Figure 7 presented non-indexed EAT measurements with the highest AUC values demonstrated AUC>0.8, which indicated a very good level of discrimination between individuals with and without CAD. SSFP EAT volume showed the AUC of 0.881, which is

considered a near-excellent level of classification. LAVG EAT thickness was revealed to be an isolated EAT thickness measurement with the highest AUC value (0.779).

Results of the ROC analysis of BMI-indexed EAT measurements are displayed in Table 14.

BMI-indexed EAT Measurements	Area Under the Curve (AUC)
SSFP volume ($cm^3/(kg/m^2)$)	0.856
T1IR volume ($cm^3/(kg/m^2)$)	0.833
RVFW1 thickness ($mm/(kg/m^2)$)	0.718
RVFW2 thickness ($mm/(kg/m^2)$)	0.738
RVFW3 thickness ($mm/(kg/m^2)$)	0.734
LVFW1 thickness ($mm/(kg/m^2)$)	0.647
LVFW2 thickness ($mm/(kg/m^2)$)	0.651
LVFW3 thickness ($mm/(kg/m^2)$)	0.626
RAVG thickness ($mm/(kg/m^2)$)	0.691
AIVG thickness ($mm/(kg/m^2)$)	0.681
LAVG thickness ($mm/(kg/m^2)$)	0.719
IIVG thickness ($mm/(kg/m^2)$)	0.564
SIVG thickness ($mm/(kg/m^2)$)	0.644
Average RVFW thickness ($mm/(kg/m^2)$)	0.769
Average LVFW thickness ($mm/(kg/m^2)$)	0.670
Average FW thickness ($mm/(kg/m^2)$)	0.785
Average groove thickness ($mm/(kg/m^2)$)	0.739
Average all locations thickness ($mm/(kg/m^2)$)	0.795

Table 14. Results of the receiver operating characteristic curve analysis of body mass index indexed epicardial adipose tissue measurements. Abbreviations: AIVG – anterior interventricular groove, AUC – area under the curve, BMI – body mass index, cm – centimeter, EAT– epicardial adipose tissue, FW – free wall, IIVG – inferior interventricular groove, kg – kilogram, LAVG – left atrioventricular groove, LVFW – left ventricular free wall, m – meter, mm – millimeter, RAVG – right atrioventricular groove, RVFW – right ventricular free wall, SIVG – superior interventricular groove, SSFP - steady state free precession, T1IR – T1 inversion recovery

All BMI-indexed EAT measurements showed lower AUC values in comparison to non-indexed counterparts. As a result, indexation of epicardial fat size with BMI turned out to be not useful in identification of CAD patients.

Results of ROC analysis of BSA-indexed EAT measurements are displayed in Table 15.

BSA-indexed EAT Measurements	Area Under the Curve (AUC)
SSFP volume (cm^3/m^2)	0.880
T1IR volume (cm^3/m^2)	0.875
RVFW1 thickness (mm/m^2)	0.738
RVFW2 thickness (mm/m^2)	0.756
RVFW3 thickness (mm/m^2)	0.752
LVFW1 thickness (mm/m^2)	0.656
LVFW2 thickness (mm/m^2)	0.663
LVFW3 thickness (mm/m^2)	0.637
RAVG thickness (mm/m^2)	0.723
AIVG thickness (mm/m^2)	0.709
LAVG thickness (mm/m^2)	0.752
IIVG thickness (mm/m^2)	0.593
SIVG thickness (mm/m^2)	0.678

BSA-indexed EAT Measurements	Area Under the Curve (AUC)
Average RVFW thickness (mm/m^2)	0.791
Average LVFW thickness (mm/m^2)	0.683
Average FW thickness (mm/m^2)	0.802
Average groove thickness (mm/m^2)	0.784
Average all locations thickness (mm/m^2)	0.823

Table 15. Results of the receiver operating characteristic curve analysis of body surface area indexed epicardial adipose tissue measurements. Only a slight improvement of the AUC value in case of BSA-indexed T1IR EAT volume measurement was observed (highlighted green) in comparison to the non-indexed counterpart. Abbreviations: AIVG – anterior interventricular groove, AUC – area under the curve, BSA – body surface area, cm – centimeter, EAT– epicardial adipose tissue, FW – free wall, IIVG – inferior interventricular groove, LAVG – left atrioventricular groove, LVFW – left ventricular free wall, m – meter, mm – millimeter, RAVG – right atrioventricular groove, RVFW – right ventricular free wall, SIVG – superior interventricular groove, SSFP - steady state free precession, T1IR – T1 inversion recovery

Only a slight improvement of the AUC value in case of BSA-indexed T1IR EAT volume measurement was observed (from 0.866 to 0.875) in comparison to the non-indexed counterpart. All other BSA-indexed EAT measurements showed lower AUC values in comparison to non-indexed equivalents.

Results of the ROC analysis of ISL-indexed EAT measurements are displayed in Table 16.

ISL-indexed EAT Measurements	Area Under the Curve (AUC)
SSFP volume (cm^3/mm)	0.856
T1IR volume (cm^3/mm)	0.864
RVFW1 thickness (mm/mm)	0.738
RVFW2 thickness (mm/mm)	0.754
RVFW3 thickness (mm/mm)	0.754
LVFW1 thickness (mm/mm)	0.669
LVFW2 thickness (mm/mm)	0.675
LVFW3 thickness (mm/mm)	0.648
RAVG thickness (mm/mm)	0.720
AIVG thickness (mm/mm)	0.711
LAVG thickness (mm/mm)	0.753
IIVG thickness (mm/mm)	0.603
SIVG thickness (mm/mm)	0.675
Average RVFW thickness (mm/mm)	0.785
Average LVFW thickness (mm/mm)	0.689
Average FW thickness (mm/mm)	0.798
Average groove thickness (mm/mm)	0.771
Average all locations thickness (mm/mm)	0.809

Table 16. Results of the receiver operating characteristic curve analysis of interventricular septum length indexed epicardial adipose tissue measurements. Abbreviations: AIVG – anterior interventricular groove, AUC – area under the curve, EAT– epicardial adipose tissue, FW – free wall, IIVG – inferior interventricular groove, ISL – interventricular septum length, LAVG – left atrioventricular groove, LVFW – left ventricular free wall, mm – millimeter, RAVG – right atrioventricular groove, RVFW – right ventricular free wall, SIVG – superior interventricular groove, SSFP - steady state free precession, T1IR – T1 inversion recovery

All ISL-indexed EAT measurements showed lower AUC values in comparison to non-indexed counterparts. As a result, the indexation of epicardial fat size with ISL turned out to be not useful in identification of CAD patients.

All in all, nearly all measurements with the highest AUC values were non-indexed. Only the BSA-indexed T1IR EAT volume showed a slight improvement in AUC value in comparison to non-indexed equivalent (from 0.866 to 0.875).

The next ROC curve depicts five EAT measurements with the highest AUC values – non-indexed SSFP EAT volume, BSA-indexed T1IR EAT volume, non-indexed average EAT thickness over the FW, non-indexed average EAT thickness in the groove areas, non-indexed average EAT thickness in all locations (Figure 8). The most commonly reported EAT measurement in literature – non-indexed average EAT thickness over the RVFW – is included in the ROC curve as well. The isolated EAT thickness measurement with the highest AUC value – non-indexed LAVG thickness – is also represented in the ROC curve.

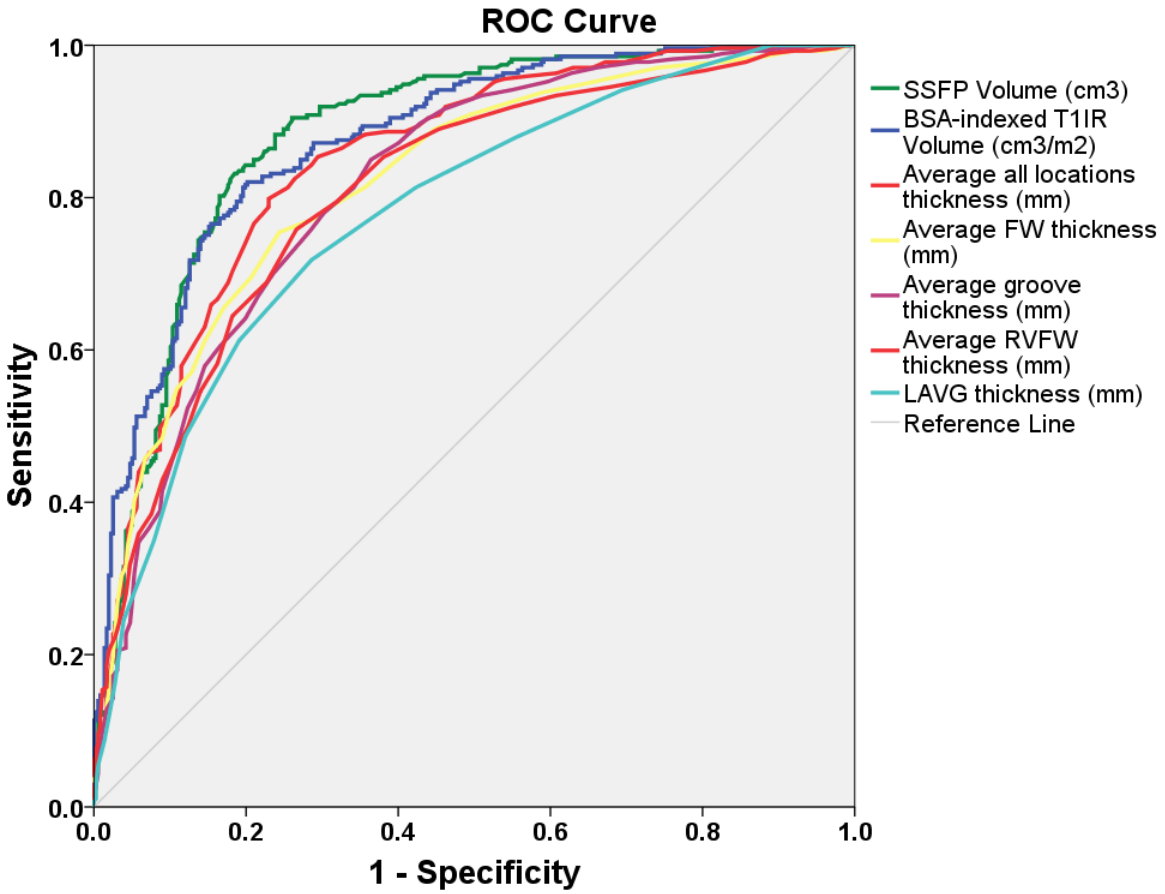

Figure 8. Receiver operating characteristic curve containing measurements of epicardial adipose tissue with the highest area under the curve values. Abbreviations: BSA – body surface area, cm – centimeter, FW – free wall, LAVG – left atrioventricular groove, m – meter, mm – millimeter, RVFW – right ventricular free wall, ROC – receiver operating characteristic, SSFP - steady state free precession, T1IR – T1 inversion recovery

Reference cut-off values of EAT measurements, showed in Figure 8, were established for identification of CAD patients. Corresponding sensitivity and specificity values were calculated. The results are displayed in Table 17. BSA-, BMI- and ISL-indexed SSFP volumes were included in the table as well.

EAT Measurements	AUC	Cut-off Value	Sensitivity	Specificity
SSFP volume	0.881	93.62 cm^3	84%	80%
BSA-indexed SSFP volume	0.880	48.59 cm^3/m^2	82%	80%
BSA-indexed T1IR volume	0.875	51.63 cm^3/m^2	82%	80%
BMI-indexed SSFP volume	0.856	3.60 $cm^3/(kg/m^2)$	78%	78%
ISL-indexed SSFP volume	0.856	1.07 cm^3/mm	77%	77%
Average all locations thickness	0.848	7.0 mm	79%	77%
Average FW thickness	0.821	4.6 mm	76%	76%
Average groove thickness	0.816	9.9 mm	73%	74%
Average RVFW thickness	0.808	6.2 mm	76%	73%
LAVG thickness	0.779	10.5 mm	72%	71%

Table 17. Reference cut-off values of epicardial adipose tissue measurements with the highest area under the curve values. Abbreviations: AUC – area under the curve, BMI – body mass index, BSA – body surface area, cm – centimeter, EAT – epicardial adipose tissue, FW – free wall, ISL – interventricular septum length, kg – kilogram, LAVG – left atrioventricular groove, m – meter, mm – millimeter, RVFW – right ventricular free wall, SSFP - steady state free precession, T1IR – T1 inversion recovery

As an example, CAD was correctly identified in patients with the EAT SSFP volume above 93.62 cm^3 (sensitivity of 84% and specificity of 80%). An average EAT thickness in all locations over 7 mm correctly characterized CAD patients with the sensitivity of 79% and specificity of 77%.

4.4 Epicardial adipose tissue measurements in context of coronary artery disease severity

The severity of CAD in this study was assessed with two different grading scales – Canadian Cardiovascular Society grading of angina pectoris and Gensini Score. Canadian Cardiovascular Society grading of angina pectoris consists of four grades. Aggravation rate of angina pectoris corresponds with the increase of grade from I to IV. ANOVA was performed to evaluate the connection between the most feasible EAT measurements (non-indexed SSFP volume and non-indexed average all location thickness) in regard to the CAD severity.

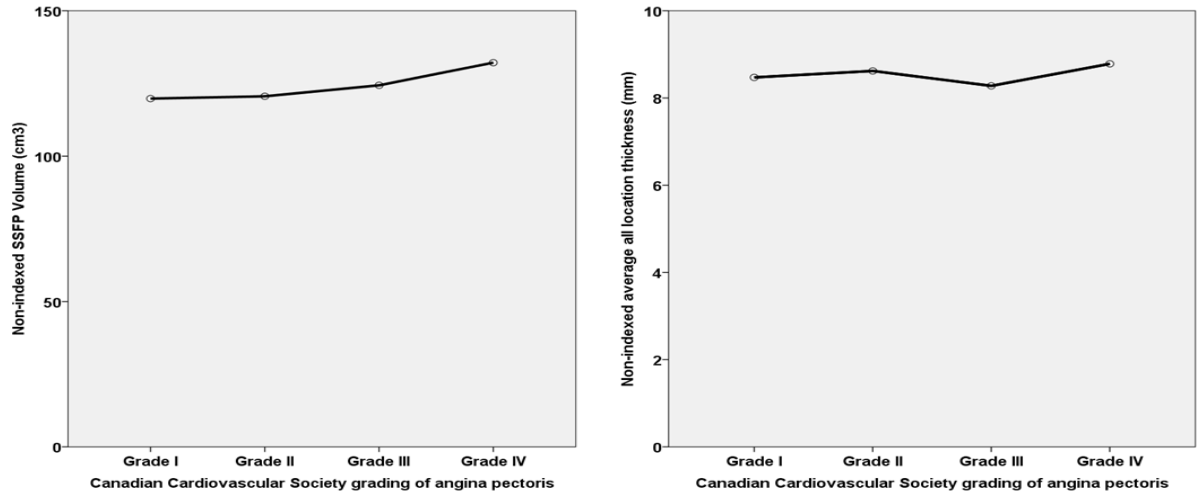

Figure 9. Analysis of variance of the most feasible measurements of epicardial adipose tissue in context of the Canadian Cardiovascular Society grading of angina pectoris. Abbreviations: cm – centimeter, mm – millimeter, SSFP - steady state free precession

The first means plot in Figure 9 shows a rising EAT volume trend with the exacerbation of angina pectoris symptoms (Grade I – 119.8±27.74 cm^3, Grade II – 120.59±36.59 cm^3, Grade III – 124.37±33.18 cm^3, Grade IV – 132.16±44.14 cm^3). However, the difference between the groups did not show any statistical significance.

The second means plot in Figure 9 demonstrates a sideways average all locations EAT thickness trend with the exacerbation of angina pectoris symptoms (Grade I – 8.5±1.6 mm, Grade II – 8.6±2.2 mm, Grade III – 8.3±1.9 mm, Grade IV – 8.8±2.2 mm). No significant difference was observed between the groups as well.

Gensini score is a commonly used angiographic grading system for calculating the severity of CAD (379-381). Gensini score considers 3 variables for each coronary lesion– severity score, region multiplying factor and collateral adjustment factor. Coronary arteries of CAD patients, who received coronary angiography, were evaluated – Gensini score for each patient was calculated. Pearson correlation coefficient was applied for the estimation of a possible association between most effective EAT measurements (non-indexed SSFP volume and non-indexed average all location thickness) and the calculated Gensini score.

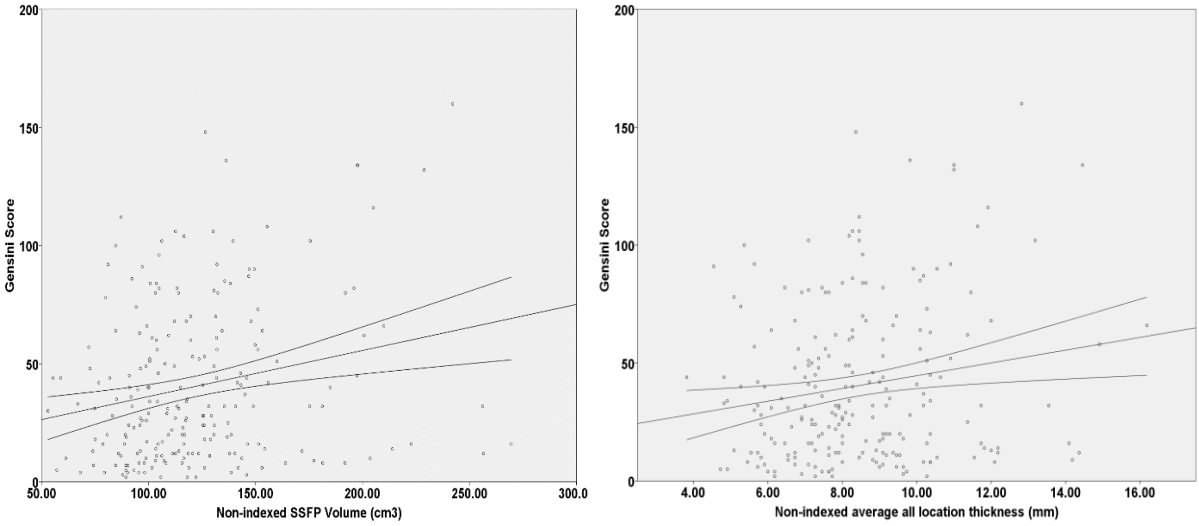

Figure 10. Scatter plots of correlations between most feasible measurements of epicardial adipose tissue and Gensini Score. Abbreviations: cm – centimeter, mm – millimeter, SSFP - steady state free precession

The first scatter plot in Figure 10 demonstrates a weak correlation between non-indexed EAT volume measurements and Gensini score (r=0.222, p=0.001). In a similar way, the second scatter plot in Figure 10 shows only a very weak correlation between non-indexed overall average EAT thickness measurements and Gensini score (r=0.174, p=0.01).

All in all, although with a very good ability to identify CAD patients, EAT measurements failed to show any considerable capacity to assess the severity of CAD.

5 Discussion

5.1 Main important results of this study

This study revealed some important results. First of all, EAT proved to independently predict CAD along with other established CAD risk factors – age, male gender and obesity. Interestingly, EAT measurements predicted CAD more efficiently than male gender or obesity in the logistic regression analysis.

Indexation of EAT measurements did not provide a significant benefit in identification of CAD patients. Nevertheless, non-indexed EAT measurements showed an outstanding performance in prediction of CAD. Non-indexed SSFP EAT volume demonstrated the best efficiency in classification of subjects with CAD. Non-indexed average all location EAT thickness showed a comparable classification power. The most commonly reported EAT measurement in literature – non-indexed average EAT thickness over the RVFW – displayed a good ability to distinguish between patients with CAD and healthy controls.

CAD was correctly identified in subjects with the EAT SSFP volume above 93.62 cm^3 with sensitivity of 84% and specificity of 80%. The non-indexed average all location EAT thickness above 7 mm correctly characterized CAD patients with sensitivity of 79% and specificity of 77%. Finally, the non-indexed average EAT thickness over the RVFW above 6.2 mm properly distinguished individuals with CAD with sensitivity of 76% and specificity of 73%.

Although with a very good ability to identify CAD patients, EAT measurements failed to show any potential to determine the severity of CAD (assessed with the Canadian Cardiovascular Society grading of angina pectoris and Gensini score).

5.2 Published epicardial adipose tissue measurements for coronary artery disease risk stratification

5.2.1 Non-indexed epicardial adipose tissue thickness measurements

Systematic evaluation and quantification of EAT in clinical praxis could significantly improve the risk estimation in asymptomatic patients with no history of CAD (51). It is important to identify the upper threshold, above which EAT measurement would be considered abnormal for cardiovascular risk stratification.

Overall, normal EAT thickness is reported to be 5-7 mm over the RVFW and 10-14 mm in the atrioventricular and interventricular grooves (71, 197). Flüchter et al. quantified EAT thickness over the RVFW in CMR images – values appeared to be similar to those, measured during 200 autopsies in Caucasian individuals without heart failure (mean thickness – 4±1 mm) (168, 198). Furthermore, a mean echocardiographic EAT thickness of 5±2 mm was reported in 356 asymptomatic individuals by Nelson et al. (72).

Iacobellis et al. reported the high-risk threshold median value of echocardiographic EAT thickness measurements of 7 mm for a sample of obese and overweight patients (146). Despite varying results, the systematic review by Bertaso et al. suggested that EAT thickness over 5 mm should serve as a cut-off value for increased epicardial fat depots in low-risk populations with a suspicion of CAD (45). The meta-analysis, conducted by Xu et al. and involving 2872 subjects, revealed that CAD patients had significantly thicker EAT than healthy controls (61).

The main important EAT thickness findings of this study and the summary of results in other related publications are listed in Table 18. It is important to point out that listed authors did not aim to compare different EAT measurement techniques. Only occasional studies, published to this day, compared to a limited extent individual EAT measurement approaches in regard to CAD. These investigations are discussed in section 5.2.4 of this work. Conflicting and controversial results and possible causes were already examined in section 2.6.5 of this study.

Although CMR modality has been viewed as a gold standard for evaluation of adipose tissue, it was to this day rarely employed in quantification of EAT in CAD patients (54, 68-70, 74-77). Possible reasons could be high cost and limited access to this modality, long scan duration, complex assessment of CMR images and reduced patient tolerance in comparison to other imaging modalities (CT or transthoracic echocardiography). The majority of published CMR studies examined small samples of patients which did not permit the employment of complex statistical analysis methods. Unusual approaches of data collection and presentation made it difficult to compare results of our study and several other published CMR works. For example, Doesch et al. calculated the mass of EAT from volume measurements and indexed it to BSA. Unfortunately, authors did not operate with initial EAT volume measurements in the statistical analysis (54, 76). In other instances, patients were divided into two groups – high and low EAT depots – and then compared with one another. As a result, ROC analysis could not be performed (74, 75, 77). Nevertheless, three comparable CMR studies are mentioned in this discussion (68-70). Altogether, the majority of published works applied either transthoracic echocardiography or CT when quantifying epicardial fat depots.

Authors	Measurement modality (EAT measurements)	CAD characteristics	Number of subjects	EAT thickness measurements and important results	ROC analysis solely with EAT
This study	CMR (indexed and non-indexed thickness and volume)	≥1 stenosis of ≥50% in a major coronary artery based on coronary angiography images	630	Average all locations: CAD: 8.5±2.0 mm, non-CAD: 6.0±1.6 mm (p<0.001); Average RVFW: CAD: 8.5±3.3 mm, non-CAD: 5.3±2.2 mm (p<0.001); Average LVFW: CAD: 3.5±2.0 mm, non-CAD: 2.2±1.3 mm (p<0.001); Mean groove thickness: CAD: 11.6±2.5 mm, non-CAD: 8.6±2.2 mm (p<0.001); RAVG: CAD: 14.8±4.4 mm, non-CAD: 10.9±4.1 mm (p<0.001); AIVG: CAD: 10.8±4.7 mm, non-CAD: 7.5±3.2 mm (p<0.001); LAVG: CAD: 12.5±3.4 mm, non-CAD: 9.1±3.0 mm (p<0.001); SIVG: CAD: 12.9±3.8 mm, non-CAD: 10.1±3.4 mm (p<0.001); IIVG: CAD: 6.8±2.7 mm, non-CAD: 5.6±2.1 mm (p<0.001); EAT thickness – independent predictor of CAD along with male gender, age and obesity; weak EAT thickness correlation with Gensini score: r=0.174, p=0.01	Average all locations thickness: cut-off value – 7 mm, AUC=0.848, sensitivity – 79%, specificity – 77%; Average RVFW thickness: cut-off value – 6.2 mm, AUC=0.808, sensitivity – 76%, specificity – 73%; Average groove thickness: cut-off value – 9.9 mm, AUC=0.816, sensitivity – 73%, specificity – 74%; AIVG EAT thickness: AUC – 0.729;

Authors	Measurement modality (EAT measurements)	CAD characteristics	Number of subjects	EAT thickness measurements and important results	ROC analysis solely with EAT
Jeong et al. (137)	Echocardiography (end-diastolic RVFW thickness)	≥1 stenosis of ≥50% in a major coronary artery based on coronary angiography images	203	Difference in Gensini score (p=0.006) between patients with EAT thickness above and below 7.6 mm	Not performed
Ahn et al. (136)	Echocardiography (end-diastolic RVFW thickness)	≥1 stenosis of ≥50% in a major coronary artery based on coronary angiography images	527	4.0 mm (multi-vessel CAD) vs. 3.5 mm (single –vessel CAD) vs. 1.5 mm (non-CAD) (p<0.05); Cut-off value – 3.0 mm	Not performed
Eroglu et al. (142)	Echocardiography (end-diastolic RVFW thickness)	≥1 stenosis of ≥20% in a major coronary artery based on coronary angiography images	150	CAD: 6.9±1.5 mm, non-CAD: 4.4±0.8 mm (p<0.001); EAT correlation with Gensini score: r=0.600, p<0.001	Cut-off value – 5.2 mm, AUC=0.914, sensitivity – 85%, specificity – 81%
Parsaee et al. (386)	Echocardiography (end-diastolic RVFW thickness)	≥1 stenosis of ≥50% in a major coronary artery based on coronary angiography images	62	CAD: 4.2±1.4 mm, non-CAD: 2.6±1.2 mm (p<0.001); EAT – independent predictor of CAD along with statin therapy, higher waist circumference and higher BMI	Cut-off value – 2.95 mm, AUC=0.810, sensitivity – 83%, specificity – 75%
Kamal et al. (387)	Echocardiography (end-diastolic RVFW thickness)	Documented CAD based on coronary angiography images	150	CAD: 7.4±1.3 mm, non-CAD: 4.1±0.8 mm (p<0.001)	Cut-off value – 5.5 mm, AUC=0.992, sensitivity – 98%, specificity – 100%
Tekin et al. (388)	Echocardiography (end-diastolic RVFW thickness)	≥1 stenosis of ≥50% in a major coronary artery based on coronary angiography images	97	CAD: 6 mm, non-CAD: 4.6 mm (p<0.001); EAT – independent predictor of obstructive CAD	Cut-off value – 5.5 mm, AUC=0.832, sensitivity – 67%, specificity – 71%
Meenakshi et al. (389)	Echocardiography (end-systolic RVFW thickness)	≥1 points in Gensini score	110	CAD: 6.9±1.9 mm, non-CAD: 4.4±1.2 mm (p<0.001); Strong EAT correlation with Gensini score: r=0.704, p=0.001	Not performed
Erkan et al. (390)	Echocardiography (end-systolic RVFW thickness)	≥1 points in Gensini score	183	Critical CAD: 7.5±1.9 mm, non-critical CAD: 5.2±1.5 mm, non-CAD: 4.3±0.9 mm (p<0.01); strong EAT correlation with Gensini score: r=0.82, p<0.001; EAT – independent predictor of critical CAD along with diabetes	Cut-off value – 5.75 mm, AUC=0.875, sensitivity – 77%, specificity – 83%
Ghaderi et al. (391)	Echocardiography (end-systolic RVFW thickness)	≥1 stenosis of ≥50% in a major coronary artery based on coronary angiography images	100	CAD: 6.9±3.0 mm, non-CAD: 3.6±1.2 mm (p<0.0001); strong EAT correlation with Gensini score: r=0.765, p<0.0001	Cut-off value – 4.25 mm, AUC=0.82, sensitivity – 79%, specificity – 68%

Authors	Measurement modality (EAT measurements)	CAD characteristics	Number of subjects	EAT thickness measurements and important results	ROC analysis solely with EAT
Shemirani et al. (392)	Echocardiography (end-systolic RVFW thickness)	≥1 stenosis of ≥75% in a major coronary artery based on coronary angiography images	292	CAD: 5.4±1.9 mm, non-CAD: 4.4±1.8 mm (p<0.001); weak EAT correlation with Califf score: r=0.3, p<0.001	Not performed
Yanez-Rivera et al. (393)	Echocardiography (end-systolic RVFW thickness)	≥1 stenosis of ≥50% in a major coronary artery based on coronary angiography images	153	CAD: 5.4±1.8 mm, non-CAD: 4.0±1.7 mm (p<0.001); EAT – independent predictor of obstructive CAD along with male gender, higher waist-hip ratio, smoking	Not performed
Mustelier et al. (139)	Echocardiography (end-systolic RVFW thickness)	≥1 stenosis of ≥50% in a major coronary artery based on coronary angiography images	250	CAD: 6.6±2.8 mm, non-CAD: 4.7±2.3 mm (p<0.001)	Cut-off value – 5.2 mm, AUC=0.712, sensitivity – 65%, specificity – 62%
Iacobellis et al. (394)	Echocardiography (end-systolic RVFW thickness)	Severe CAD (three-vessel disease) with need of coronary bypass intervention	40	CAD: 12.9±2.7 mm, non-CAD: 8.4±2.5 mm (p<0.01); moderate EAT correlation with degree of coronary stenosis (r=0.68, p<0.01)	Not performed
Tachibana et al. (64)	Echocardiography (end-systolic RVFW thickness)	High-risk plaque based on CT angiography images	406	Weak EAT correlation with number of stenotic coronary vessels (r=0.14, p=0.003); EAT – independent predictor of high-risk coronary plaques along with higher CCS, number of coronary arteries with stenosis and renal insufficiency	Cut-off value – 5.6 mm, AUC=0.600, sensitivity – 82%, specificity – 62%
Shambu et al. (395)	Echocardiography (end-systolic RVFW thickness)	≥1 stenosis of ≥50% in left main artery or ≥70% in another major coronary artery based on coronary angiography images	503	CAD: 5.5±1.2 mm, non-CAD: 3.3±1.2 mm (p<0.001); strong EAT correlation with Gensini score: r=0.906, p<0.001	Cut-off value – 4.75 mm, AUC=0.831, sensitivity – 87%, specificity – 63%
Hirata et al. (49)	Echocardiography (end-systolic RVFW and AIVG thickness)	≥1 stenosis of ≥75% in a major coronary artery based on coronary angiography images	311	AIVG: CAD: 8.3±3.0 mm, non-CAD: 6.3±2.5 mm (p<0.001); RVFW: CAD: 5.0±2.1 mm, non-CAD: 4.4±2.3 mm (p<0.001)	AIVG thickness: cut-off value – 7.1 mm, AUC=0.704, sensitivity – 66%, specificity – 66%; RVFW thickness: cut-off value – 4.2 mm, AUC=0.615, sensitivity and specificity not reported
Aydin et al. (242)	CT (AIVG, RAVG, LAVG thickness)	Presence of at least one coronary artery plaque based on CT angiography images	150	AIVG: CAD: 9.0±2.4 mm, non-CAD: 7.3±2.1 mm (p<0.001); RAVG: CAD: 18.4±3.4 mm, non-CAD: 16.6±3.3 mm (p=0.002); LAVG: CAD: 11.7±3.9 mm, non-CAD: 10.5±2.9 mm (p=0.038)	Not performed

Authors	Measurement modality (EAT measurements)	CAD characteristics	Number of subjects	EAT thickness measurements and important results	ROC analysis solely with EAT
Maimaituxun et al. (396)	CT (AIVG, RAVG, LAVG thickness, non-indexed volume, BSA-indexed EAT volume)	≥1 stenosis of >50% in a major coronary artery based on CT angiography images	197	AIVG: CAD: 6.9±2.2 mm, non-CAD: 5.5±2.2 mm (p<0.001); RAVG: CAD: 16.5±4.8 mm, non-CAD: 15.5±4.7 mm (p=0.160); LAVG: CAD: 10.3±3.6 mm, non-CAD: 9.8±3.4 mm (p=0.297); weak AIVG EAT correlation with Gensini score: r=0.263, p<0.001, other EAT measurements did not correlate with Gensini score; EAT – independent predictor of CAD along with a higher age or Framingham risk score	AIVG thickness cut-off value – 5.7 mm, AUC – 0.686, sensitivity – 72%, specificity – 57%
Gac et al. (397)	CT (SIVG, IIVG, LAVG, RVFW thickness)	CCS >0	80	SIVG: CAD: 7.9±2.6 mm, non-CAD: 7.2±3.2 mm (p>0.05); IIVG: CAD: 6.7±2.9 mm, non-CAD: 5.4±1.8 mm (p<0.05); LAVG: CAD: 2.6±1.3 mm, non-CAD: 3.0±0.8 mm (p>0.05); RVFW: CAD: 10.0±3.1 mm, non-CAD: 7.6±2.2 mm (p<0.05); weak correlation between CCS and EAT (r≤0.3)	RVFW thickness: cut-off value – 8.8 mm, AUC=0.706, sensitivity – 79%, specificity – 60%
Bachar et al. (398)	CT (RVFW thickness)	≥1 stenosis of ≥50% in a major coronary artery based on CT angiography images	190	CAD: 3.5±1.6 mm, non-CAD: 1.9±1.3 mm (p<0.001); EAT – independent predictor of CAD along with diabetes and hypertension	Cut-off value – 2.4 mm, AUC – not reported, sensitivity – 80%, specificity – 73%
Demircelik et al. (243)	CT (RVFW thickness, the mean of groove thickness)	≥1 stenosis of ≥50% in a major coronary artery or obstruction of a left main artery based on CT angiography images	131	Mean groove thickness: CAD: 16.3±2.1 mm, non-CAD: 10.9±1.7 mm (p<0.001); RVFW: CAD: 7.1±2.7 mm, non-CAD: 3.2±1.1 mm (p<0.001)	Mean groove thickness: cut-off value – 13.8 mm, AUC=0.714, sensitivity – 72%, specificity – 68%; RVFW thickness: cut-off value – 6.8 mm, AUC=0.715, sensitivity – 74%, specificity – 69%
Alnaggar et al. (399)	CT (RVFW thickness, the mean of groove thickness)	≥1 stenosis of ≥50% in a major coronary artery based on CT angiography images	70	Mean groove thickness: CAD: 14.0±2.4 mm, non-CAD: 10.8±1.7 mm (p<0.001); RVFW: CAD: 8.5±3.1 mm, non-CAD: 6.2±1.2 mm (p<0.001); no significant correlation between EAT and Gensini score	Mean groove thickness: cut-off value – 12.6 mm, AUC=0.767, sensitivity – 72%, specificity – 62%; RVFW thickness: cut-off value – 7.2 mm, AUC=0.645, sensitivity – 64%, specificity – 64%

Authors	Measurement modality (EAT measurements)	CAD characteristics	Number of subjects	EAT thickness measurements and important results	ROC analysis solely with EAT
Picard et al. (57)	CT (RVFW thickness, LVFW thickness)	≥1 stenosis of ≥50% in a major coronary artery based on CT angiography images	970	RVFW: CAD: 5.6±3.1 mm, non-CAD: 4.8±2.7 mm (p=0.0004); LVFW: CAD: 2.7±2.4 mm, non-CAD: 2.1±2.1 mm (p=0.0001); EAT – independent predictor of CAD along with male gender, higher age, dyslipidemia and hypertension; LVFW thickness ≥2.8 mm (but not RVFW thickness) predicted CAD after adjusting for CAD risk factors	LVFW thickness: cut-off value – 2.8 mm, AUC=0.580, sensitivity – 46%, specificity – 67%; RVFW thickness: cut-off value – 5.3 mm, AUC – not reported, sensitivity – 45%, specificity – 68%
Kim et al. (68)	CMR (LAVG thickness)	≥1 stenosis of ≥50% in a major coronary artery based on CMR angiography images	100	CAD: 13.0±2.6 mm, non-CAD: 11.5±2.1 mm (p=0.01); EAT – independent predictor of CAD after adjustment for traditional cardiovascular risk factors	Not performed

Table 18. Overview of comparable studies with data about thickness of epicardial adipose tissue and its connection to coronary artery disease. Abbreviations: AIVG – anterior interventricular groove, AUC – area under the curve, BMI – body mass index, BSA – body surface area, CAD – coronary artery disease, CCS – coronary calcium score, CMR – cardiac magnetic resonance, CT – computed tomography, EAT – epicardial adipose tissue, IIVG – inferior interventricular groove, LAVG – left atrioventricular groove, LVFW – left ventricular free wall, mm – millimeter, RAVG – right atrioventricular groove, RVFW – right ventricular free wall, ROC – receiver operating characteristic, SIVG – superior interventricular groove

All in Table 18 mentioned studies, which employed transthoracic echocardiography, showed significantly higher EAT thickness measurements in CAD patients (49, 64, 136, 139, 142, 386-395). The results are consistent with those of our study – all EAT thickness measurements, performed on CMR images, were significantly higher in subjects with CAD. It is important to stress that transthoracic echocardiography allows only EAT thickness measurements, mainly over the RVFW (135). Of note, Hirata et al. offered a novel approach of visualizing EAT thickness in the area of AIVG with a linear probe. Authors validated echocardiographic EAT-AIVG thickness results with the EAT volume, measured on CT images in 71 patients (r=0.714) (49).

One important debatable issue concerns the time of the cardiac cycle which should be used for echocardiographic measurements of EAT thickness. Some authors assessed EAT thickness during a systole to prevent possible compression of epicardial fat during a diastole (49, 64, 139, 389-395). Others performed EAT measurements in a diastole to coincide with other imaging modalities such as CT or CMR (136, 137, 142, 386-388). Indeed, because of the prospective ECG-gating during the cardiac CT scan, images can only be evaluated during a diastole. On the other hand, epicardial fat depots can be estimated both in a systole and a diastole on CMR images. We performed EAT measurements during a diastole to be able to compare our results with those of other studies, which employed cross-sectional imaging techniques.

Although authors, who employed CT for estimation of EAT thickness, showed in general similar results to ultrasound studies, there were some differences (57, 242, 243, 396-399). Gac. et al. assessed the association between EAT thickness measurements and CCS in 80 patients, referred to CT angiography. Although RVFW and IIVG thickness measurements were significantly larger in patients with CAD (10.0±3.1 vs. 7.6±2.2 mm and 6.7±2.9 vs.5.4±1.8 mm, respectively), SIVG and LAVG EAT thickness showed no considerable difference between both groups (397). Even though this study is one of the few to assess EAT thickness in the

areas of SIVG and IIVG, CCS>0 does not accurately represent CAD patients. Furthermore, small study population is another factor that could explain discrepancies in published results.

Maimaituxun et al. retrospectively compared EAT thickness measurements on CT images between individuals with significant coronary stenosis and healthy controls. Only AIVG EAT thickness was significantly larger in CAD patients (6.9±2.2 mm vs. 5.5±2.2 mm), RAVG and LAVG EAT thickness showed no considerable difference between the two groups (396). Absence of significant EAT thickness differences in the areas of RAVG and LAVG could be accredited to Asian population. The study of Maimaituxun et al. consisted solely of Japanese individuals who in general exhibit smaller visceral adipose tissue depots in comparison to Caucasians (78).

EAT thickness was numerous times confirmed to be an independent predictor of CAD among both transthoracic echocardiography and CT studies. Other independent predictors included higher age; male gender; increased BMI, waist circumference and waist-hip ratio; smoking status; diabetes; hypertension; dyslipidemia; renal insufficiency; higher CCS, Framingham risk score and a number of coronary arteries with a significant stenosis; statin therapy (57, 64, 386, 388, 390, 393, 396, 398). Our results corresponded with those of other studies. The multivariate binary logistic regression analysis showed that EAT thickness over the RVFW acted as an independent predictor of CAD among other independent predictors such as age ≥50 years, male gender and obesity.

Interestingly, most of ultrasound studies reported a strong correlation of EAT thickness measurements with the severity of CAD, measured with Gensini score (137, 142, 389-391, 395). In contrast, EAT thickness measurements in our study showed only a weak correlation with Gensini score. Similar results displayed several studies which employed cross-sectional imaging techniques to assess EAT thickness (396, 399).

Several authors evaluated other markers of the CAD severity than Gensini score. Shemirani et al. positively correlated EAT thickness measurements with the angiographic Califf scoring system of CAD severity, although the connection was revealed to be weak (r=0.3) (392). Gac et al. in the same way reported only a weak correlation between EAT thickness and CCS (r≤0.3) (397). In the study by Mustelier et al., EAT thickness did not significantly differ between patients with multi-vessel vs. two-vessel vs. single-vessel disease (139). Similarly, studies by Tachibana et al. and Bachar et al. revealed no relevant association between EAT thickness measurements and the number of stenotic coronary vessels (64, 398). On the other hand, Ahn et al. demonstrated that patients with multi-vessel disease expressed significantly thicker EAT in comparison to patients with one-vessel disease (4.0 mm vs. 3.5 mm) (136). Moreover, EAT thickness correlated with the degree of coronary stenosis (r=0.68) in the study by Iacobellis et al. (394).

Of note, our study is the first one to examine the association between EAT measurements and the Canadian Cardiovascular Society grading of angina pectoris. Similar to Gensini score, Canadian Cardiovascular Society grading of angina pectoris showed no relevant connection with EAT thickness measurements.

All in all, the association between EAT thickness measurements and the severity of CAD remains unclear. Discrepant published results could be explained by differences in population groups, in particular age-specific variance of the studied groups. Age is proven to play one of the most important roles in spread of both coronary atherosclerosis and CAD (374). Furthermore, the definition of CAD varied from study to study. As a result, many of the listed publications included patients with severe CAD and accompanying chronic heart failure. Individuals with the heart failure repeatedly showed decreased epicardial fat depots, assessed with cross-sectional imaging methods (313). The postmortem research showed consistent results – human hearts with signs of heart failure displayed significantly less EAT than healthy hearts (198). Thus, cases with the severe heart failure could play a significant confounding role in the analysis of correlation between EAT depots and the severity of CAD. Further studies with strictly controlled group samples are required to verify the possible connection between these two variables.

Jeong et al. proposed a border value of echocardiographic end-diastolic RVFW EAT thickness of 7.6 mm in 203 CAD patients, submitted to coronary angiography (137). Ahn et al. in the similar way suggested a RVFW EAT thickness cut-off value of 3 mm for CAD prediction in 527 patients, who received coronary angiography because of the chest pain (136). Although authors of both studies proposed a possible threshold value of EAT thickness over the RVFW in identification of CAD patients, absence of ROC analysis questions the reliability of suggested cut-off values.

Some of in Table 18 listed authors, who employed transthoracic echocardiography in quantification of EAT thickness, performed ROC analysis. AUC of EAT thickness measurements over the RVFW varied from 0.600 to 0.992 (49, 64, 139, 142, 386-388, 390, 391, 395). Interestingly, EAT measurements, performed during a diastole, showed higher AUC values in comparison to systolic EAT measurements (0.810-0.992 vs. 0.600-0.875). Of note, diastolic EAT measurements are comparable with those carried out on CT images. We have performed EAT measurements during a diastole as well. AUC of the mean EAT thickness over the RVFW in our study (0.808) was consistent with published results which indicated a very good EAT ability to predict CAD.

Hirata et al. carried out systolic echocardiographic EAT thickness measurements in the area of AIVG as a novel approach to quantify EAT depots. A linear probe was used for the examination (7.5 MHz, spatial resolution – 0.1 mm). The high-frequency linear probe allowed more precise EAT thickness measurements. This method related to the EAT volume, measured on CT images, beyond of the echocardiographic EAT thickness measurements over the RVFW. ROC analysis showed that EAT thickness in the AIVG area predicted CAD more effectively than EAT measurements over the RVFW (AUC – 0.704 vs. 0.615) (49). This seems reasonable since LAD courses directly through the AIVG area. ROC analysis in our study revealed partially different results – EAT thickness over the RVFW predicted CAD more efficiently than in the area of AIVG (AUC – 0.771 vs. 0.729). However, the average EAT thickness measurements in the area of atrio- and interventricular grooves in our study predicted CAD slightly better than the average EAT thickness measurements over the RVFW (AUC – 0.816 vs. 0.808), which indicated consistent results with those of Hirata et al.

Some authors, who evaluated epicardial fat thickness in different localizations on CT images, performed ROC analysis in prediction of patients with CAD (57, 243, 396, 397, 399). Maimaituxun et al. predicted CAD by applying AIVG thickness measurement with the AUC of 0.686 (vs. 0.729 in our study) (396). Gac. et al. assessed the association between EAT thickness measurements and CCS in 80 patients referred to CT angiography. ROC analysis revealed the AUC value of 0.706 (vs. 0.808 in our study) in case of the EAT thickness over the RVFW for the presence of coronary sclerosis (397). Demircelik et al. divided 131 patients into 3 groups – no atherosclerosis, non-obstructive atherosclerosis and obstructive CAD. Scientists measured EAT thickness over the RVFW as well as in the areas of RAVG, LAVG and AIVG (average pericoronary EAT). Authors reported similar AUC values of pericoronary (0.714 vs. 0.816 in our study) and RVFW (0.715 vs. 0.808 in our study) EAT thickness for the obstructive CAD risk prediction (243). Another study with the similar design was conducted on 70 subjects by Alnaggar et al. AUC of the pericoronary EAT demonstrated higher values (0.767 vs. 0.816 in our study) than over the RVFW (0.645 vs. 0.808 in our study), which was consistent with the results of our study (399). Finally, Picard et al. measured EAT thickness over both RVFW and LVFW in 970 subjects of the EVASCAN cohort (EVAluation of CT SCANer). AUC of EAT thickness over the LVFW was 0.58 (vs. 0.708 in our study), AUC value of EAT thickness over RVFW was not reported (57).

It is important to point out that cut-off values in the ROC analysis are chosen individually from the general pool according to the calculated combination of sensitivity and specificity. Some border values may have high sensitivity, other – high specificity. Basically, cut-off values are selected according to the study objectives (high sensitivity or high specificity) and are not comparable across the studies. In our work we have chosen balanced cut-off values of EAT measurements with similar sensitivity and specificity in identification of patients with a

significant CAD. All cut-off values of EAT thickness in the studies, summarized in this discussion, are listed in Table 18.

Finally, one comparable CMR study was conducted by Kim et al. Authors evaluated EAT thickness in the area of LAVG on CMR images in asymptomatic type 2 diabetic patients with a suspicion of CAD. CAD patients showed significantly larger EAT depots (13.0±2.6 mm vs. 11.5±2.1 mm). Furthermore, EAT thickness was revealed to be an independent indicator of a significant coronary stenosis after adjusting for age, gender, BMI, Hemoglobin A1C, low-density lipoprotein, systolic blood pressure and the history of smoking. ROC analysis in this study was not performed (68).

5.2.2 Volumetric assessment of epicardial adipose tissue

Volumetric assessment of EAT is only possible with cross-sectional imaging modalities (CT or CMR) (48). EAT volume of healthy 3312 individuals from the Framingham Heart Study, measured on CT images, was identified as high with 139 cm^3 for men and 119 cm^3 for women (200). Other authors evaluated EAT volume in the same cohort and reported high measurement values of 110±41 cm^3 in women and 137±53 cm^3 in men (30). Overall, Bertaso et al. in their systematic review suggested that EAT volume over 125 cm^3 could be considered abnormal in low-risk populations (45).

Studies, listed in Table 19, contain information about EAT volume measurements in patients with CAD with different coronary plaque characteristics. Most authors assessed EAT volume on CT images. It is important to mention that the main aim of these studies was not to compare different EAT quantification techniques. Nevertheless, the results obtained from different cohorts allowed us to match them to the results obtained in our study. The main non-indexed EAT volume measurements of this study and the results of other publications are shortly listed in Table 19.

Authors	Measurement modality (EAT properties)	CAD characteristics	Number of subjects	EAT volume measurements and other important results	ROC analysis exclusively with EAT
This study	CMR (indexed and non-indexed thickness and volume)	≥1 stenosis of ≥50% in a major coronary artery	630	SSFP volume: CAD: 123.44±35.68 cm^3, non-CAD: 77.58±25.82 cm^3 ($p<0.001$); T1IR volume: CAD: 128.46±34.96 cm^3, non-CAD: 84.13±25.52 cm^3 ($p<0.001$); EAT volume – independent predictor of CAD along with male gender, higher age and obesity; weak EAT volume correlation with Gensini score: r=0.222, p=0.001	SSFP volume: cut-off value – 93.62 cm^3, AUC=0.881, sensitivity – 84%, specificity – 80%;
Djaberi et al. (252)	CT (volume)	≥1 stenosis of ≥50% in a major coronary artery or obstruction of left main artery based on CT angiography images	190	CAD: 99±40 cm^3, non-CAD: 63±31 cm^3 ($p<0.001$); Multi-vessel vs. single-vessel disease: no significant EAT difference; EAT – independent predictor of CAD along with higher age, hypertension, hypercholesterolemia and increased BMI	Cut-off value – 77 cm^3, AUC – not reported, sensitivity – 72%, specificity – 70%

Authors	Measurement modality (EAT properties)	CAD characteristics	Number of subjects	EAT volume measurements and other important results	ROC analysis exclusively with EAT
Refaat et al. (400)	CT (volume)	Presence of coronary lesions based on CT angiography images	75	CAD: 94.67±17.74 cm^3, non-CAD: 60.08±26.25 cm^3 ($p<0.05$); EAT – independent predictor of CAD	Cut-off value – 60.39 cm^3, AUC – 0.813, sensitivity – not reported, specificity – not reported
Goeller et al. (245)	CT (volume and density)	MACE	456	CAD: 135.0 (111.4-158.6) cm^3, non-CAD: 79.3 (75.4-83.2) cm^3 ($p<0.001$); EAT ≥125 cm^3 – independent predictor of CAD along with increased CCS and lower EAT density	Not performed
Sarin et al. (249)	CT (volume)	≥1 stenosis of >50% in a major coronary artery based on CT angiography images	151	Higher prevalence of CAD in patients with EAT volume >100 cm^3 (28% vs. 18%, p=0.007)	Not performed
Abazid et al. (171)	CT (volume and density)	CCS >0	609	CAD: 74±27 cm^3, non-CAD: 62±26 cm^3 ($p<0.0001$); Significant EAT volume expansion together with increase of CCS; EAT >100 cm^3 – independent predictor of CAD along with male gender, higher age and lower EAT density	Not performed
Yerramasu et al. (50)	CT (volume)	CCS >0	333	CAD: 85.8 cm^3, non-CAD: 69.3 cm^3 ($p<0.001$); EAT – independent predictor of CAD along with higher age, male gender, Caucasian ethnicity, higher systolic blood pressure, higher osteoprotegerin level in serum	Not performed
Mahabadi et al. (250)	CT (volume)	CCS progression over 5 years	3367	Significant CCS progression: 101.4±47.1 cm^3, insignificant CCS progression: 84.4±43.4 cm^3; Strong independent association between EAT volume and CCS progression, especially in young and lean individuals	Not performed
Alexopoulos et al. (78)	CT (volume)	≥1 stenosis in a major coronary artery based on CT angiography images	214	Severe CAD: 100±52 cm^3, moderate CAD: 100±44 cm^3, mild CAD: 87±41 cm^3, non-CAD: 62±33 cm^3 ($p<0.001$)	Not performed
Okada et al. (264)	CT (volume)	Presence of ≥1 coronary plaque based on CT angiography images	140	Obstructive CAD in multiple vessels: 105.7±7.3 cm^3, obstructive CAD in single vessel: 94.8±6.8 cm^3, non-obstructive CAD: 91.0±8.8 cm^3, non-CAD: 85.0±4.2 cm^3 ($p<0.05$); No connection between EAT and CCS	Cut-off value – 85.8 cm^3, AUC – 0.576, sensitivity – 64%, specificity – 51%
Iwasaki et al. (269)	CT (volume)	Presence of ≥1 coronary plaque based on CT angiography images	197	Severe CAD: 146.4±63.9 cm^3, moderate CAD: 105.2±41.1 cm^3, mild CAD: 92.4±34.8 cm^3, non-CAD: 97±36.9 cm^3 ($p<0.0068$)	Not performed

Authors	Measurement modality (EAT properties)	CAD characteristics	Number of subjects	EAT volume measurements and other important results	ROC analysis exclusively with EAT
Khurana et al. (401)	CT (volume)	Presence of ≥1 coronary plaque based on CT angiography images	950	Obstructive CAD: 82.87±32.32 cm^3, non-obstructive CAD: 68.67±29.18 cm^3, non-CAD: 56.73±27.63 cm^3 ($p<0.001$); EAT – independent predictor of CAD along with family history of CAD, increased CCS	Cut-off value – 67.69 cm^3, AUC – 0.709, sensitivity – 65%, specificity – 66%
Konishi et al. (262)	CT (volume)	Presence of ≥1 coronary plaque based on CT angiography images	171	CAD: 201±71 cm^3, non-CAD: 144±45 cm^3 ($p<0.001$); EAT – independent predictor of CAD along with higher age and increased hemoglobin A1c	Cut-off value – 180 cm^3, AUC – 0.709, sensitivity – 60%, specificity – 81%
Kim et al. (273)	CT (volume)	≥1 stenosis of >20% in a major coronary artery based on coronary angiography images	209	CAD: 125.36±47.64 cm^3, non-CAD: 102.4±41.87 cm^3 ($p<0.001$); EAT – independent predictor of CAD after adjustment for age, gender, smoking, alcohol and BMI;	Not performed
Bettencourt et al. (253)	CT (thickness and volume)	Presence of ≥1 coronary plaque based on CT angiography images	215	CAD: 94±35 cm^3, non-CAD: 83±31 cm^3 ($p=0.017$); EAT – independent predictor of CAD after adjustment for age, gender, abdominal visceral fat	Not performed
Ito et al. (260)	CT (volume)	≥1 stenosis of >50% in a major coronary artery based on CT angiography images	1308	CAD: 124.3±43.2 cm^3, non-CAD: 95.1±40.3 cm^3 ($p<0.01$); EAT – independent predictor of CAD after adjustment for age, male gender, diabetes and CAD symptoms	Cut-off value – 126.8 cm^3, AUC – 0.69, sensitivity – 50%, specificity – 81%
Schlett et al. (270)	CT (volume)	Presence of ≥1 coronary plaque based on CT angiography images	358	CAD: 111.7 (84.5-145.2) cm^3, non-CAD: 74.8 (58.2-111.7) cm^3 ($p<0.0001$); EAT – independent predictor of CAD after adjustment for age, gender, hypertension, diabetes, hyperlipidemia and BMI	Cut-off value – 144.88 cm^3, AUC – 0.756, sensitivity – 62%, specificity – 83%
Shehata et al. (402)	CT (volume)	≥1 stenosis of >70% in a major coronary artery based on CT angiography images	90	CAD: 327.94±90.17 cm^3, non-CAD: 125.14±56.88 cm^3 ($p<0.001$)	Cut-off value – 148.7 cm^3, AUC – not reported, sensitivity – 70%, specificity – 80%
Taha et al. (403)	CT (volume)	Presence of ≥1 coronary stenosis based on CT angiography images	120	CAD: 160.9±42.43 cm^3, non-CAD: 107.5±36.24 cm^3 ($p<0.001$); strong EAT correlation with the number of affected coronary vessels: $r=0.782$, $p<0.001$; EAT – independent predictor of CAD along with higher age, male gender and increased CCS	Cut-off value – 124 cm^3, AUC – 0.833, sensitivity – 79%, specificity – 73%
Bo et al. (275)	CT (volume)	Presence of ≥1 coronary plaque based on CT angiography and conventional coronarography images	208	CAD: 192.57±30.32 cm^3, non-CAD: 138.56±23.18 cm^3 ($p<0.01$); EAT – independent predictor of CAD after adjustment for age, male gender, hypertension, diabetes, smoking, family history of CAD, BMI, waist circumference and hyperlipidemia; weak EAT correlation with Gensini score: $r=0.285$, $p<0.001$	Not performed

Authors	Measurement modality (EAT properties)	CAD characteristics	Number of subjects	EAT volume measurements and other important results	ROC analysis exclusively with EAT
Rajani et al. (58)	CT (volume)	Presence of ≥1 coronary plaque based on CT angiography images	402	CAD: 108±53 cm^3, non-CAD: 89±41 cm^3 ($p<0.001$); EAT – independent predictor of severe coronary stenosis along with higher age, diabetes and smoking	Not performed
Mahabadi et al. (281)	CT (volume and pericoronary fat area)	Incident coronary event	4093	CAD: 121 cm^3, non-CAD: 95 cm^3 ($p<0.001$); EAT – independent predictor of CAD after adjustment for traditional cardiovascular risk factors and CCS	Not performed
Cheng et al. (51)	CT (volume)	MACE	232	CAD: 102±49 cm^3, non-CAD: 85±38 cm^3 ($p=0.007$); EAT – independent predictor of CAD after adjustment for BMI, CCS and Framingham risk score	Not performed
Hell et al. (173)	CT (volume and density)	Inducible ischemia in SPECT	213	CAD: 96±49 cm^3, non-CAD: 82±37 cm^3 ($p=0.041$); EAT – independent predictor of CAD after adjustment for age, CAD symptoms and traditional risk factors	Not performed
Harada et al. (280)	CT (volume)	MACE	170	CAD: 117±47 cm^3, non-CAD: 95±33 cm^3 ($p=0.01$); EAT – independent predictor of CAD along with the low level of high-density lipoprotein in blood	Cut-off value – 100.3 cm^3, AUC – 0.685, sensitivity – 75%, specificity – 57%
Janik et al. (52)	PET-CT (volume)	Presence of perfusion defects in myocardium	97	CAD: 134.0±39.2 cm^3, non-CAD: 96.9±43.3 cm^3 ($p<0.0001$); EAT – independent predictor of CAD after adjustment for CCS, age, gender and BMI	Cut-off value – 100.8 cm^3, AUC – 0.762, sensitivity – 87%, specificity – 60%
Tamarappoo et al. (157)	CT (volume)	Inducible ischemia in SPECT	219	CAD: 99±43 cm^3, non-CAD: 80±32 cm^3 ($p=0.0003$); EAT >125 cm^3 – independent predictor of CAD along with increased CCS and increased total thoracic fat volume	Not performed
Petrini et al. (70)	CMR (volume and mass)	History of coronary occlusion and ischemic scar based on CMR images	150	CAD: 30 (16-54) cm^3, non-CAD: 18 (12-26) cm^3 ($p<0.001$)	Not performed

Table 19. Overview of comparable studies with data about non-indexed volume of epicardial adipose tissue and its connection to coronary artery disease. Abbreviations: AUC – area under the curve, BMI – body mass index, CAD – coronary artery disease, CCS – coronary calcium score, cm^3 – cubic centimeter, CMR – cardiac magnetic resonance, CT – computed tomography, EAT – epicardial adipose tissue, MACE – major adverse cardiac event, PET – positron emission tomography, ROC – receiver operating characteristic, SPECT – single-photon emission computed tomography, SSFP - steady state free precession, T1IR – T1 inversion recovery

All in Table 19 mentioned studies, which employed cross-sectional imaging modalities, showed significantly higher EAT volume measurements in CAD patients (50-52, 58, 70, 78, 157, 171, 173, 245, 249, 250, 252, 253, 260, 262, 264, 269, 270, 273, 275, 280, 281, 391, 400-403). The results are consistent with those of our study – EAT volume measurements, performed on CMR images, were significantly higher in subjects with CAD. Because of the prospective ECG-

gating during cardiac CT scan, images could only be evaluated during a diastole. We performed EAT measurements in the same way on CMR images during a diastole to be able to compare our results with those of other studies.

EAT volume was numerous times confirmed to be an independent predictor of CAD. Other independent predictors included age, male gender, Caucasian ethnicity, increased BMI, higher amounts of abdominal visceral fat, higher waist circumference, higher amounts of total thoracic fat volume, smoking status, alcohol consumption, diabetes, hypertension, dyslipidemia, higher osteoprotegerin level in serum, higher hemoglobin A1c in blood, increased CCS, family history of CAD, CAD symptoms, increased Framingham risk score and lower EAT density (50-52, 58, 157, 171, 173, 245, 252, 253, 260, 262, 270, 273, 275, 280, 281, 400, 401, 403). Our results corresponded with those of other studies. Multivariate binary logistic regression analysis identified EAT thickness over the RVFW as an independent predictor of CAD among other independent predictors (age ≥50 years, male gender and obesity).

Similar to EAT thickness measurements, EAT volume showed inconsistent findings with the respect to CAD severity, measured with Gensini score. First of all, 209 subjects with suspected CAD underwent both cardiac CT and coronary angiography in a retrospective study by Kim et al. Patients were divided into tertiles according to the EAT volume. EAT volume significantly and linearly increased with the severity of CAD – mean Gensini scores for each EAT tertile were 5.477±14.84, 7.887±15.72, and 12.507±20.59, respectively, p=0.018 (273). Bo et al. correlated CT measurements of EAT volume with the severity of coronary lesions in subjects with CAD. EAT volume poorly correlated with Gensini score (r=0.285) (275). Comparable to the results in the research by Bo et al., EAT volume measurements in our study showed only a weak correlation with Gensini score.

Several authors evaluated other markers of CAD severity than Gensini score. First of all, EAT was assessed in regard to CCS. Djaberi et al. performed volumetric quantification of EAT in subjects with suspected CAD, referred to CT. EAT volume correlated poorly with CCS (r=0.33). Furthermore, EAT volume did not significantly differ among patients with different numbers of diseased coronary vessels (252). Goeller et al. randomly selected and evaluated 456 asymptomatic patients from the EISNER cohort. EAT volume did not differ between the groups with significant coronary calcifications (patient groups with CCS <100, 100-399, ≥400) (245). In contrast, Abazid et al. presented a significant increase of EAT volume with higher CCS score (patient groups with CCS=0 – 62 cm^3, CCS 1-100 – 71 cm^3, CCS ≥101 – 80 cm^3, p<0.05). However, this study included a population with the high prevalence of arterial hypertension and diabetes, which could serve as confounding factors (171). Mahabadi et al. similarly assessed the association of CCS and EAT volume over a period of 5 years in the Heinz Nixdorf Recall population. Authors reported a significantly higher EAT volume in those subjects who showed relevant CCS progression over time (101.4±47.1 cm^3 vs. 84.4±43.4 cm^3). The results were stronger in younger and leaner individuals (250). Yerramasu et al. similarly measured an increased EAT volume in patients with the positive CCS (85.8 cm^3 vs. 69.3 cm^3 in healthy controls). Three years after the initial CT scan, a second CT examination was performed. For an every EAT volume increase of 10 cm^3 during the control CT, CCS rose up by 12% (50). Finally, Bettencourt et al. determined that an increase of EAT volume by 10 cm^3 corresponded with the rise of CCS by 14.7% (253).

Some authors assessed a connection between EAT and the severity of CAD in patients with different coronary plaque characteristics. In a study by Alexopoulos et al., EAT volume significantly increased in subjects with large non-calcified plaques (plaque burden ≥40%) compared to patients with absent or calcified plaques (99±36 cm^3 vs. 62±33 cm^3 or 63±22 cm^3, respectively). Furthermore, EAT volume steadily increased with the extent of coronary stenosis (Severe CAD: 100±52 cm^3, moderate CAD: 100±44 cm^3, mild CAD: 87±41 cm^3, non-CAD: 62±33 cm^3) (78). In another study, Okada et al. measured EAT volume in 140 non-obese patients with chest pain. EAT volume steadily increased with the escalation of CAD (85±4.2 cm^3 in healthy patients, 91±8.8 cm^3 with non-obstructive plaques, 94.8±6.8 cm^3 with obstructive plaques in one vessel, 105.7±7.3 cm^3 with obstructive plaques in multiple vessels). Moreover, EAT volume rose in proportion to the number of coronaries with obstructive plaques.

Patients with non-calcified or mixed coronary plaques had significantly larger EAT depots compared to subjects with absent or calcified plaques (264). Iwasaki et al. conducted a comparable study with 197 patients who received CT angiography. Study results showed a significant rise of EAT volume with the increase of coronary stenosis degree (92.4±34.8 cm^3 among patients with mild non-obstructive CAD, 105.2±41.1 cm^3 with moderate CAD and 146.4±63.9 cm^3 with severe CAD) (269). Khurana et al. compared EAT volume between 950 consecutive Indian patients free of CAD, with or without significant coronary stenosis (>50%). EAT volume significantly and steadily increased according to the CAD severity (57.63±27.63 cm^3 in CAD free patients, 68.67±29.18 cm^3 in patients with insignificant coronary stenosis, 82.87±32.32 cm^3 in patients with significant coronary stenosis) (401).

Several studies did not report a significant connection between EAT depots and the severity of CAD in patients with different coronary plaque characteristics. In a study by Ito et al., EAT volume was compared between symptomatic CAD patients with either obstructive (124.3±43.2 cm^3) or vulnerable (133±40.2 cm^3) coronary plaques and healthy controls (95.1±40.3 cm^3). No significant EAT volume difference was identified between CAD patients with obstructive or vulnerable coronary plaques (260). Rajani et al. examined EAT volume in individuals with suspected CAD and compared EAT values between different types of coronary plaque. EAT volume showed no significant difference between patients with calcified coronary plaques (112±55 cm^3), with partially calcified plaques (110±57 cm^3) or non-calcified plaques (115±44 cm^3) (58).

Our study is the first one to examine the association between EAT volume measurements and the Canadian Cardiovascular Society grading of angina pectoris. Similar to Gensini score, Canadian Cardiovascular Society grading of angina pectoris showed no relevant association with EAT volume measurements.

All in all, the association between EAT volume measurements and the severity of CAD remains unclear. Similar to EAT thickness measurements, discrepancy of the published results could be explained by differences in population groups, in particular age-specific variance of the studied groups. Furthermore, the definition of CAD varied from study to study. Patients with severe CAD and accompanying chronic heart failure were sometimes included in the study population. Individuals with chronic heart failure repeatedly showed decreased epicardial fat depots, assessed with cross-sectional imaging methods and during postmortem research (198, 313). Thus, cases with the severe heart failure could play a significant confounding role in the analysis of correlation between EAT depots and the severity of CAD. Further studies with strictly controlled group samples are required to verify the possible connection between these two variables.

Regression analysis in a study by Goeller et al. pointed out the EAT volume ≥125 cm^3 along with the lower EAT density and increased CCS as independent MACE predictors (245). Tamarappoo et al. selected 219 patients with intermediate pre-test probability for CAD from the EISNER registry who received both CT and SPECT within 6 months. Both EAT volume and myocardial perfusion were assessed. Authors offered a possible EAT volume cut-off value of 125 cm^3 for prediction of perfusion defects in the heart muscle (157). In one more study from the EISNER registry with 2751 patients, Cheng et al. determined the upper EAT volume cut-off value of 125 cm^3 for identification of patients who suffered from MACE (51). Schlett et al. reported the EAT volume value of 74.07 cm^3, below which high-risk coronary plaques in CAD patients could be completely excluded (270). Sarin et al., Abazid et al. and Iwasaki et al. in their studies selected the high-risk EAT volume limit of 100 cm^3 for identification of CAD patients with either coronary stenosis or CCS >0 (171, 249, 269). Although authors of mentioned studies proposed possible cut-off values of EAT volume for identification of CAD patients, absence of ROC analysis questions the reliability of suggested values.

Some of the studies, listed in Table 19, included ROC analysis. AUC of EAT volume measurements varied from 0.576 to 0.833 (52, 260, 262, 264, 270, 280, 400, 401, 403). AUC of the EAT volume in our study (0.881) was consistent with published results, which indicated a very good ability of EAT volume measurements to predict CAD. Our study offered an EAT

volume cut-off value of 93.62 cm^3 for prediction of a significant coronary stenosis in patients with CAD.

Finally, one comparable CMR study was conducted by Petrini et al. Authors performed CMR on 150 individuals because of different reasons. Positive CAD was assessed on conventional coronary angiography (coronary occlusion) as well as on CMR images (evidence of myocardial scar) in 50 patients. EAT volume was revealed to be higher in subjects with CAD in comparison to healthy controls (30 (16-54) cm^3 vs. 18 (12-26) cm^3) (70). Wide discrepancy of volumetric EAT measurements between the study by Petrini et al. and this work could be attributed to the different estimation approach of epicardial fat depots. Petrini et al. considered only segmented EAT areas on the right side of the heart prior to the calculation of EAT volume. Whereas we estimated EAT areas on both sides of the heart.

5.2.3 Indexed epicardial adipose tissue measurements

The effect of anthropometric EAT variability is assumed to play an important role in identifying individuals with increased cardiovascular risk (78). Generally, EAT volume was to this day rarely indexed in clinical studies. EAT thickness was on the other hand never indexed to this day. As a consequence, there were no studies published on the topic of possible advantages of indexed EAT thickness measurements in comparison to non-indexed counterparts in identification of individuals with CAD. Furthermore, no studies indexed EAT with anthropometric heart measurements such as interventricular septum length (ISL).

Besides different non-indexed EAT depots measurements, some authors derived EAT volume, indexed to BSA or BMI. Most of the published literature, related to the indexation of EAT measurements, did not compare the performance of indexed vs. non-indexed EAT values. Nevertheless, the results obtained from different cohorts allowed us to match them to the results obtained in this study. Bertaso et al. in their systematic review suggested that the BSA-indexed EAT volume over 68 cm^3/m^2 should be considered abnormal in low-risk populations (45). The main important indexed EAT findings of this study and the summary of results in other related publications are listed in Table 20.

Authors	Measurement modality (EAT properties)	CAD characteristics	Number of subjects	Non-indexed and indexed EAT volume measurements and other important results	ROC analysis exclusively with EAT
This study	CMR (indexed and non-indexed thickness and volume)	≥1 stenosis of ≥50% in a major coronary artery	630	BMI-indexed SSFP volume: CAD: 4.51±1.26 $cm^3/(kg/m^2)$, non-CAD: 3.05±0.88 $cm^3/(kg/m^2)$ ($p<0.001$); BSA-indexed SSFP volume: CAD: 61.91±16.92 cm^3/m^2, non-CAD: 40.27±11.85 cm^3/m^2 ($p<0.001$); ISL-indexed SSFP volume: CAD: 1.39±1.26 cm^3/mm, non-CAD: 0.89±0.31 cm^3/mm ($p<0.001$)	BMI-indexed SSFP volume: cut-off value – 3.60 $cm^3/(kg/m^2)$, AUC=0.856, sensitivity – 78%, specificity – 78%; BSA-indexed SSFP volume: cut-off value – 48.59 cm^3/m^2, AUC=0.880, sensitivity – 82%, specificity – 80%; ISL-indexed SSFP volume: cut-off value – 1.07 cm^3/mm, AUC=0.856, sensitivity – 77%, specificity – 77%;

Authors	Measurement modality (EAT properties)	CAD characteristics	Number of subjects	Non-indexed and indexed EAT volume measurements and other important results	ROC analysis exclusively with EAT
Nakanishi et al. (257)	CT (BSA-indexed and non-indexed volume)	Significant progression of CCS (follow-up CT scan) 3-5 years after the initial CT scan	162	Non-indexed EAT volume: CAD: 102±38 cm^3, non-CAD: 90±35 cm^3 (p=0.03); BSA-indexed EAT volume: CAD: 50±16 cm^3/m^2, non-CAD: 46±15 cm^3/m^2 (p=0.03); higher increase of BSA-indexed EAT volume in CAD group during the follow-up CT scan: 14±23% vs. 7±21%, p=0.04; BSA-indexed EAT volume – independent predictor of a CCS progression along with hypertension	Not performed
Merelo-Nicolas et al. (404)	CT (BSA-indexed and non-indexed volume)	Presence of cardiovascular events	179	Non-indexed EAT volume: CAD: 121.64±40.44 cm^3, non-CAD: 100.10±43.44 cm^3 (p=0.007); BSA-indexed EAT volume: CAD: 63.79±19.22 cm^3/m^2, non-CAD: 53.78±20.93 cm^3/m^2 (p=0.009); BSA-indexed EAT volume – independent predictor of CAD along with higher age, male gender; BSA-indexed EAT volume >52.51 cm^3/m^2 as an indicator of a higher risk of cardiovascular events	Not performed
Hwang et al. (240)	CT (BSA-indexed and non-indexed volume)	Presence of non-calcified plaques (follow-up CT scan) 5 years after the initial CT scan	122	Non-indexed EAT volume: CAD: 146.00±55.96 cm^3, non-CAD: 110.95±45.80 cm^3 (p=0.013); BSA-indexed EAT volume: CAD: 79.93±30.30 cm^3/m^2, non-CAD: 62.52±24.72 cm^3/m^2 (p=0.007); BSA-indexed EAT volume – independent predictor of CAD along with hypertension and diabetes	Not performed
Lu et al. (59)	CT (BSA-indexed and non-indexed volume)	Presence of high-risk coronary plaques based on CT angiography images	467	Non-indexed EAT volume: CAD: 123 (93.4-155.8) cm^3, non-CAD: 97.9 (68.2-126.5) cm^3 (p<0.001); BSA-indexed EAT volume: CAD: 59.2 (45.2-75.2) cm^3/m^2, non-CAD: 49.2 (35.2-64.9) cm^3/m^2 (p<0.001); BSA-indexed EAT volume – independent predictor of CAD along with higher age, male gender, increased CCS and presence of a significant (≥50%) coronary stenosis	BSA-indexed EAT volume cut-off value – 62.3 cm^3/m^2, AUC – not reported, sensitivity – 49%, specificity – 73%

Authors	Measurement modality (EAT properties)	CAD characteristics	Number of subjects	Non-indexed and indexed EAT volume measurements and other important results	ROC analysis exclusively with EAT
Maimaituxun et al. (396)	CT (AIVG, RAVG, LAVG thickness, non-indexed volume, BSA-indexed EAT volume)	≥1 stenosis of >50% in a major coronary artery based on CT angiography images	197	Non-indexed EAT volume: CAD: 124±57 cm^3, non-CAD: 104±45 cm^3 (p=0.006); BSA-indexed EAT volume: CAD: 75±32 cm^3/m^2, non-CAD: 63±25 cm^3/m^2 (p=0.004); BSA-indexed EAT volume not correlated with Gensini score; BSA-indexed EAT volume – independent predictor of CAD along with increased Framingham risk score	BSA-indexed EAT volume cut-off value – 90 cm^3/m^2, AUC – not reported, sensitivity – 33%, specificity – 88%
Saad et al. (79)	CT (BSA-indexed, BMI-indexed and non-indexed volume)	≥1 stenosis of >50% in a major coronary artery based on CT angiography images	170	Non-indexed EAT volume: CAD: 113 (92.0-138.0) cm^3, non-CAD: 81 (59.4-124.0) cm^3 (p=0.004); BSA-indexed EAT volume: CAD: 61.8 (48.1-75.4) cm^3/m^2, non-CAD: 45.6 (35.3-66.9) cm^3/m^2 (p=0.011); BMI-indexed EAT volume: CAD: 3.8 (3.0-4.6) $cm^3/(kg/m^2)$, non-CAD: 2.7 (1.9-3.9) $cm^3/(kg/m^2)$ (p=0.014)	Non-indexed EAT volume cut-off value – 80.3 cm^3, AUC – 0.620, sensitivity – 92%, specificity – 35%; BSA-indexed EAT volume cut-off value – 41.7 cm^3/m^2, AUC – 0.610, sensitivity – 94%, specificity – 32%; BMI-indexed EAT volume cut-off value – 2.4 $cm^3/(kg/m^2)$, AUC – 0.600, sensitivity – 93%, specificity – 31%
Ueno et al. (239)	CT (BSA-indexed volume)	Presence of total coronary occlusions based on conventional coronarography images	71	BSA-indexed EAT volume: CAD: 57.6±13.4 cm^3/m^2, non-CAD: 43.9±13.6 cm^3/m^2 (p=0.003); BSA-indexed EAT volume not correlated with Gensini score; BSA-indexed EAT volume – independent predictor of CAD along with overweight (BMI ≥25 kg/m^2)	Not performed
Shmilovich et al. (80)	CT (BSA-indexed volume)	MACE	226	BSA-indexed EAT volume: CAD: 42.7 (31.3-67.9) cm^3/m^2, non-CAD: 39.2 (28.5-52.3) cm^3/m^2 (p=0.045); BSA-indexed EAT volume – independent predictor of CAD after adjusting for CCS and Framingham risk score	Not performed
Nakazato et al. (271)	CT (BSA-indexed volume)	Presence of both perfusion defects in myocardium based on PET/CT images and ≥1 stenosis of >50% in a major coronary artery based on conventional coronarography images	92	BSA-indexed EAT volume: CAD: 64.6±20.6 cm^3/m^2, non-CAD: 49.7±14.2 cm^3/m^2 (p=0.0002); BSA-indexed EAT volume – independent predictor of CAD after adjusting for age, gender, cardiovascular risk factors, chest pain and CCS	BSA-indexed EAT volume cut-off value – 68.1 cm^3/m^2, AUC – not reported, sensitivity – 40%, specificity – 90%

Authors	Measurement modality (EAT properties)	CAD characteristics	Number of subjects	Non-indexed and indexed EAT volume measurements and other important results	ROC analysis exclusively with EAT
Homsi et al. (69)	CMR (BSA-indexed volume)	Presence of myocardial infarction	65	BSA-indexed EAT volume: CAD: 94.14±43.16 cm^3/m^2, non-CAD: 52.98±19.81 cm^3/m^2 ($p<0.001$); No association between EAT and the number of CAD affected vessels	Not performed

Table 20. Overview of comparable studies with data about indexed volume of epicardial adipose tissue and its connection to coronary artery disease. Abbreviations: AIVG – anterior interventricular groove AUC – area under the curve, BMI – body mass index, BSA – body surface area, CAD – coronary artery disease, CCS – coronary calcium score, cm^3 – cubic centimeter, CMR – cardiac magnetic resonance, CT – computed tomography, EAT – epicardial adipose tissue, ISL – interventricular septum length, kg – kilogram, LAVG – left atrioventricular groove, m^2 – square meter, mm – millimeter, MACE – major adverse cardiac event, PET – positron emission tomography, RAVG – right atrioventricular groove, ROC – receiver operating characteristic, SPECT – single-photon emission computed tomography, SSFP - steady state free precession

All in Table 20 mentioned studies showed significantly higher indexed EAT volume measurements in CAD patients (59, 69, 79, 80, 239, 240, 257, 271, 396, 404). The results are consistent with those of our study – all indexed EAT measurements, performed on CMR images, were significantly higher in subjects with CAD.

Indexed EAT measurements were numerous times confirmed to be an independent predictor of CAD. Other independent predictors included higher age, male gender, overweight (BMI ≥25 kg/m^2), hypertension, diabetes, chest pain, increased CCS, significant coronary stenosis (≥50%), increased Framingham risk score (59, 80, 239, 240, 257, 271, 396, 404). Interestingly, indexed EAT measurements did not represent the severity of CAD, measured with the Gensini score (239, 396). However, increase of BSA-indexed EAT volume over 15% was associated with the considerable increase of CCS (257).

Merelo-Nicolas et al. calculated BSA-indexed EAT volume in 179 symptomatic individuals with the suspicion of CAD. Some patients developed cardiovascular events. During the follow up of approximately 5.5 years, BSA-indexed EAT volume >52.51 cm^3/m^2 served as a risk indicator of cardiovascular events (404). Another study from the EISNER registry by Shmilovich et al. reported the upper limit of BSA-indexed EAT volume of 68 cm^3/m^2 in prediction of MACE, after adjusting for CCS and Framingham risk score. Unfortunately, authors did not assess the prediction ability of EAT measurements alone, but rather of the CCS, EAT and Framingham risk score combination (80). Although authors of both studies proposed a possible cut-off value of BSA-indexed EAT volume in identification of severe CAD patients, absence of ROC analysis questions the reliability of suggested values.

Some of authors, listed in Table 20, performed ROC analysis with indexed EAT volume measurements. Unfortunately, only one study published AUC values of indexed epicardial fat measurements. Saad et al. revealed that BSA-indexed EAT volume over 41.7 cm^3/m^2 could significantly predict a relevant coronary stenosis in CAD patients (AUC – 0.610, sensitivity – 94%, specificity – 32%). Furthermore, authors reported the BMI-indexed EAT volume cut-off value of 2.4 $cm^3/(kg/m^2)$ in prediction of a significant coronary stenosis (AUC – 0.600, sensitivity – 93%, specificity – 31%) (79). Our study results showed higher AUC values for BSA-indexed EAT volume measurement – 0.880 as well as for BMI-indexed EAT volume measurement – 0.856. A discrepancy of the results in both studies could be attributed to the selection bias factor – Saad et al. picked only those patients with the clinical suspicion of CAD. Whereas we included all individuals (except for those meeting the exclusion criteria) who received a CMR scan during the period of 5 years.

Three studies performed the ROC analysis without publishing an AUC value of indexed BSA-indexed EAT volume measurements. Lu et al. compared the distribution of EAT in subjects

with and without high-risk coronary plaques. Authors measured EAT volume on CT images and then indexed it to BSA. BSA-indexed EAT volume over 62 cm^3/m^2 significantly predicted high-risk plaques in CAD patients (AUC – not reported, sensitivity – 49%, specificity – 73%) (59). Maimaituxun et al. estimated EAT volume on CT images in 197 patients with suspected CAD. BSA-indexed EAT volume of over 90 cm^3/m^2 predicted CAD with sensitivity of 33% and specificity of 88% (AUC was not reported) (396). Finally, Nakazato et al. evaluated 92 consecutive patients who received non-contrast cardiac CT, PET/CT and conventional coronary angiography within a period of 6 months. Authors established a threshold BSA-indexed EAT volume value of 68.1 cm^3/m^2 in prediction of both myocardial ischemia and obstructive coronary stenosis (AUC not reported, sensitivity 40%, specificity 90%) (271).

Finally, one comparable CMR study was conducted by Homsi et al. Authors assessed 55 hypertensive and 10 healthy men; EAT volume was quantified and indexed to BSA. Some hypertensive men suffered from myocardial infarction. BSA-indexed EAT volume was significantly higher in myocardial infarction group in comparison to healthy controls (94.14±43.16 cm^3/m^2 vs. 52.98±19.81 cm^3/m^2). No association was found between EAT measurements and the number of affected coronary arteries in CAD patients. ROC analysis was not performed (69).

5.2.4 Comparison of epicardial adipose tissue measurement techniques

Only occasional published studies matched reproducibility of different EAT measurements. At all times, comparison involved only certain two or three EAT measurement techniques and, therefore, could not be sufficient. These comparable research works are mentioned in the subsection below. On the other hand, our study is the first one to compare all most commonly reported ways of quantifying epicardial fat depots in regard to CAD. Our comparison involved both non-indexed and indexed EAT measurements. Furthermore, this study is the first one to index EAT thickness measurements. Finally, for the first time we indexed the size of epicardial fat depots with anthropometric heart measurements such as ISL.

Hirata et al. echocardiographically estimated EAT thickness in the AIVG area, which predicted CAD better than measurements over the RVFW (AUC – 0.704 vs. 0.615) (49). ROC analysis in our study revealed partially different results – EAT thickness over the RVFW predicted CAD slightly better than in the area of AIVG (AUC – 0.771 vs. 0.729). Most importantly, the average EAT thickness measurements in the area of atrio- and interventricular grooves in our study predicted CAD slightly better than the average EAT thickness measurements over the RVFW (AUC – 0.816 vs. 0.808), which is consistent with the results of Hirata et al.

Demircelik et al. divided 131 patients into 3 groups – no atherosclerosis, non-obstructive atherosclerosis and obstructive CAD. Scientists measured EAT thickness over the RVFW as well as in the areas of RAVG, LAVG and AIVG (average pericoronary EAT). Authors reported comparable AUC values of pericoronary (0.714 vs. 0.816 in our study) and RVFW (0.715 vs. 0.808 in our study) EAT thickness for the risk prediction of obstructive CAD (243). Another research with the similar design was conducted with 70 subjects by Alnaggar et al. AUC of the pericoronary EAT demonstrated higher values (0.767 vs. 0.816 in our study) than over the RVFW (0.645 vs. 0.808 in our study) (399). Our work demonstrated similar results.

A meta-analysis by Wu et al. sought to study the possible connection between location specific EAT thickness measurements and an obstructive CAD. Authors compared EAT thickness measurements over the RVFW and in the area of LAVG with respect to CAD. RVFW thickness proved to be less reliable than LAVG EAT thickness measurements. In addition to this, authors observed the extreme between-study heterogeneity in echocardiography-based studies in comparison to either CT or CMR based investigations. The main reason of this discrepancy was considered to be the poor reproducibility of echocardiographic EAT measurements in comparison to those, performed on CT or CMR images (405).

Saad et al. compared a predictive power of non-indexed, BSA- and BMI-indexed EAT volume measurements for the presence of a significant coronary artery stenosis in 170 CAD patients. Authors revealed AUC values of non-indexed (0.620 vs. 0.881 in our study), BSA-indexed (0.610 vs. 0.880 in our study), BMI-indexed (0.600 vs. 0.856 in our study) epicardial fat volume measurements (79). Although our work showed generally higher AUC values in prediction of a significant coronary artery stenosis, non-indexed EAT volume measurement remained the most powerful predictor of CAD, which is consistent with the results of Saad et al. Indexation of EAT measurements in our work as well as in the study of Saad et al. did not bring a significant advantage in identification of patients with CAD in comparison to non-indexed EAT measurements.

All in all, non-indexed SSFP EAT volume demonstrated the best efficiency in classification of subjects with CAD in our study (AUC=0.881). Non-indexed average all location EAT thickness showed comparable, yet somewhat lower classification power (AUC=0.848). Since none of the published studies compared the prediction power between EAT volume and thickness measurements, our work is the first one to report these results.

5.3 Limitations and strengths of the study

This research is not without several limitations. First of all, this study was performed retrospectively in a group of patients, referred to CMR based on clinical signs. As a result, the study population included no asymptomatic patients who would represent a standard control group. The control group in our study consisted of individuals who received CMR because of other reasons, however, with no suspicion of CAD. In addition, the population of this study was heterogeneous – it was derived from a single center which would suggest a possible sampling bias. Larger multicenter studies are required to confirm the results of our study.

Secondly, the quantification of EAT in our work was conducted only by one certified radiologist. As a result, an interobserver variability of performed EAT measurements could not be assessed. Fortunately, high reproducibility of EAT measurements on the images of cross-sectional imaging techniques does not alter the reliability of EAT quantification, performed in our study. Nevertheless, more data from different readers in other study cohorts are necessary to further validate the performance of EAT measurements in identification of CAD patients.

Thirdly, the information concerning CAD risk factors was not thorough in medical records, which limited our ability to construct more reliable logistic regression models. Furthermore, medications were not considered in statistical analysis of our data, which may be regarded as a possible confounder. A significant coronary stenosis was defined as a ≥50% narrowing of the artery lumen in our study – the most commonly known angiographic definition of a significant CAD. However, this CAD definition does not account for the existence of instable coronary plaques, which often lead to MACE. CAD has been discussed as a complex disease with perplexed pathophysiology and various clinical manifestations. Despite the evident independent association between EAT and CAD in our study, we did not perform a causal analysis of this connection.

Our work demonstrated several strengths. First of all, this study is the first one to extensively compare all most commonly reported ways of quantifying epicardial fat depots in regard to CAD. Our comparison involved both non-indexed and indexed EAT thickness and volume measurements. We used to this day the best available radiological modality for quantification of epicardial fat depots – CMR. Although two systems were employed in terms of image acquisition, it did not affect reliability of EAT measurements. Secondly, our research can be defined as the largest single center CMR study about the association between EAT and CAD. Between January 2017 and January 2022, overall 760 consecutive adult patients underwent CMR imaging in our institution. 630 study subjects entered the final analysis. Thirdly, our study is the first one to index EAT thickness measurements. This study is the first one to compare

the predictive power of EAT volume and thickness measurements in terms of a significant coronary stenosis. Furthermore, for the first time we indexed the size of epicardial fat depots with anthropometric heart measurements such as ISL. Finally, our study is the first one to examine the association between EAT measurements and the severity of CAD, measured with the Canadian Cardiovascular Society grading of angina pectoris.

5.4 Future perspectives

The pathophysiology and clinical appliance of epicardial fat depots allow to define EAT as a novel measurable and modifiable cardiovascular risk factor.

Diagnosis and management of coronary atherosclerotic plaques before the development of a significant coronary stenosis or MACE is crucial to stop or even to reverse the progression of CAD. EAT, as a visceral adipose tissue, is strongly associated with the presence of both asymptomatic and clinical evident CAD. As a result, epicardial fat depots have the potential to become a strong radiological predictive marker for the identification of CAD patients. Imaging techniques, as quantification tools of EAT, may be implemented as a screening method for an effective prediction of the CAD risk. Furthermore, EAT can help with the high-risk patient selection for coronary angiography, most importantly, of individuals without clinical signs of angina pectoris.

Besides quantification of coronary artery calcium, native cardiac CT scan provides sufficient quality images to perform accurate EAT thickness and volume measurements. A combination of CCS and EAT size has the potential to improve patient cardiovascular risk stratification. Future studies are required to validate pretest probability model, adding EAT measurements to CCS for identification of patients with CAD. Although CMR is comparable to CT in assessing epicardial fat depots, CMR lacks possible physical damage associated with ionizing radiation. Overall, both CT and CMR enable a reliable and reproducible quantification of EAT. In addition, EAT thickness measurements over the RVFW or in the area of AIVG can be simply added to the regular transthoracic echocardiographic examination as a low-cost screening method for prediction of CAD. Altogether, quantification of EAT shows promise to be integrated into the workflow of cardiac imaging as an additional marker of cardiovascular risk.

Even though cut-off values of EAT measurements in context of CAD only begin to emerge in literature, there are only occasional studies which considered normalization of EAT size. Only isolated works compared the performance of non-indexed vs. indexed EAT volume measurements in prediction of CAD. None of these studies differentiated EAT amounts by gender. Calculation of gender-specific EAT cut-off values is necessary in future larger longitudinal cohort studies. Furthermore, it is crucial to establish the value of gender-specific EAT measurements as a prognostic factor of CAD. Finally, ethnic EAT differences should also be clarified in future works.

Recently, a new innovative qualitative method of pericoronary EAT analysis has been presented – fat attenuation index. This measurement can detect local inflammation around the coronary vessel, which is not represented with the markers of systemic inflammation. Future research is necessary to address the differences of fat attenuation index in stable CAD patients and in individuals after MACE. Furthermore, a complementary use of fat attenuation index and other functional imaging methods (for example 18F-FDG-PET–CT) could additionally help to assess the inflammatory activity within epicardial fat depot.

Artificial intelligence refers to the application of algorithmic operations to certain assignments that are commonly performed by a human. Machine learning models are employed as a combination of clinical results and specific information, deduced by artificial intelligence. Deep learning generates assumptions from the input data through artificial neural networks. Although volumetric estimation of epicardial fat depots, using cross-sectional imaging, is a burdensome process, automated quantification methods have emerged recently. Artificial intelligence and

radiomic analysis could be implemented into praxis to improve the assessment of both EAT quantity and quality. With the use of a convolutional neural network approach, the quantification time of EAT volume could be significantly reduced.

Finally, EAT has an opportunity to become a treatment target in case of systemic atherosclerosis. Several successful weight loss interventions (bariatric surgery or aerobic exercise programs) and pharmacological treatments, targeting epicardial fat depots, have been developed. Healthy lifestyle as well as treatment strategy with traditional or novel lipid lowering or antidiabetic medications demonstrated promising results. Further research is crucial to determine the best possible treatment approach of EAT reduction with the aim of applying it in larger populations with cardiovascular diseases. The potential to restore the epicardial fat to its protective properties once again is an intriguing concept.

5.5 Conclusions

EAT proved to independently predict CAD along with other established CAD risk factors – age, male gender and obesity. EAT measurements predicted CAD more efficiently than male gender or obesity.

Non-indexed EAT measurements showed an outstanding performance in identification of CAD patients. Indexation of EAT measurements did not provide a significant benefit in prediction of CAD. Non-indexed SSFP EAT volume demonstrated the best efficiency in classification of subjects with CAD. Non-indexed average all location EAT thickness showed a comparable classification power. The most commonly reported EAT measurement in literature – non-indexed average EAT thickness over the RVFW – displayed a good ability to distinguish between patients with CAD and healthy controls. Overall, both non-indexed EAT volume and thickness showed a promising potential as an additional marker of identification of patients with CAD.

CAD was correctly identified in subjects with non-indexed SSFP EAT volume above 93.62 cm^3 with the sensitivity of 84% and specificity of 80%. The non-indexed average all location EAT thickness above 7 mm correctly characterized CAD patients with sensitivity of 79% and specificity of 77%. The non-indexed average EAT thickness over the RVFW above 6.2 mm properly distinguished individuals with CAD with sensitivity of 76% and specificity of 73%.

Although with a very good ability to identify CAD patients, EAT measurements failed to show any potential to determine the severity of CAD (assessed with the Canadian Cardiovascular Society grading of angina pectoris and the Gensini score). A possible reason could be the opposing effect of accompanying heart failure with the consecutive gradual reduction of epicardial fat depots.

Overall, non-indexed volumetric quantification of epicardial fat depots proved to be the most suitable EAT measurement in prediction of the presence of CAD, but not of its severity. Standardization of EAT measurements did not provide a significant benefit in identification of CAD patients.

6 Summary

Einleitung. Herz-Kreislauf-Erkrankungen sind weltweit die häufigste Todesursache. Die koronare Herzkrankheit (KHK) ist weltweit für etwa 7,4 Millionen Todesfälle pro Jahr verantwortlich. Die Suche nach neuen kardiovaskulären Risikofaktoren, die maßgeblich zur Entstehung einer KHK beitragen, dauert bis heute an.

Herz-Kreislauf-Erkrankungen werden mit übermäßiger Fettleibigkeit in Verbindung gebracht. Als epikardiales Fettgewebe (EAT) wird das viszerale Fettgewebe bezeichnet, das den Herzmuskel umgibt und direkt mit den Herzkranzgefäßen verbunden ist. EAT hat sich, neben den abdominalen Depots von viszeralem Fettgewebe, als neuer, beeinflussbarer kardiometabolischer Risikofaktor herausgestellt. Eine Vergrößerung des EAT ist mit einem erhöhten Kalziumwert in den Koronararterien, KHK, subklinischer Arteriosklerose, metabolischem Syndrom, Herzrhythmusstörungen und lipotoxischer Kardiomyopathie verbunden. Übermäßiges EAT produziert große Mengen verschiedener entzündungsfördernder Zytokine und vasoaktiver Peptide. Alle diese Substanzen begünstigen unabhängig voneinander die Bildung atheromatöser Plaques in den Herzkranzgefäßen und somit die Entwicklung einer KHK.

Die EAT-Menge kann mithilfe verschiedener radiologischer Techniken gemessen werden: Echokardiographie, Computertomographie und Kardio-Magnetresonanztomographie (Kardio-MRT). Dennoch gilt die Kardio-MRT in der Literatur als Goldstandard bei der Beurteilung der Menge an EAT. EAT wird durch Messung der Dicke an verschiedenen Stellen oder durch Messung des Volumens quantifiziert.

Da es keine in Leitlinien empfohlene Technik zur EAT-Quantifizierung gibt, unterliegt die Quantifizierung in Studien dem Ermessen und der Erfahrung der Autoren. Es besteht ein Forschungsmangel hinsichtlich des Vergleichs zwischen verschiedenen Quantifizierungsmethoden von EAT bei der Vorhersage von KHK. Es ist nicht klar, ob die an einem einzelnen Punkt gemessene EAT-Dicke mit der volumetrischen Beurteilung des epikardialen Fettes vergleichbar ist. Darüber hinaus ist die Repräsentativität kleiner Studienpopulationen in veröffentlichten Studien fraglich, um Referenzwerte der EAT-Menge bei der Vorhersage einer KHK zu bestimmen. Zum Thema EAT-Indexierung liegen noch weniger Studien vor. Der Effekt der anthropometrischen EAT-Variabilität scheint eine wichtige Rolle bei der Identifizierung von Personen mit erhöhtem kardiovaskulärem Risiko zu spielen. Neben verschiedenen nicht indexierten EAT-Depotmessungen leiteten einige Autoren EAT-Mengen ab, indexiert auf die Körperoberfläche (KOF) oder den Body-Mass-Index (BMI).

Forschungsziele. Ziel dieser Studie war es, die Vorhersagekraft verschiedener EAT-Messtechniken bei der Identifizierung von Patienten mit einer KHK zu vergleichen. Darüber hinaus sollte mit dieser Studie die Frage beantwortet werden, ob indexierte EAT-Messungen im Vergleich zu nicht indexierten Messungen bei der Vorhersage einer KHK Vorteile bringen.

Material und Methoden. An dieser retrospektiven Fall-Kontroll-Studie nahmen 760 erwachsene Personen teil, die in der Vergangenheit aufgrund verschiedener Erkrankungen eine Kardio-MRT Untersuchung erhalten hatten. Zu den Ausschlusskriterien gehörten das Fehlen der erforderlichen Sequenzen der Kardio-MRT, ein Perikarderguss, das Vorhandensein eines Koronarbypasses oder Stents, das Fehlen von Krankenakten und eine wiederholte Kardio-MRT. 630 Probanden nahmen an der endgültigen Analyse teil. Größe und Gewicht der Patienten wurden anhand des Kardio-MRT Sicherheitsscreening-Fragebogens erfasst. Diese Werte wurden zur Berechnung von BMI und KOF verwendet.

Das EAT-Volumen wurde auf Kardio-MRT Bildern unter Verwendung der modifizierten Simpson-Regel mit Integration über die Bildschnitte berechnet. Insgesamt wurden 11 EAT-Dickenmessungen durchgeführt: drei Messungen über der freien Wand des rechten Ventrikels (RVFW), drei über der freien Wand des linken Ventrikels (LVFW), eine Messung in der oberen Zwischenkammerfurche (SIVG), in der unteren Zwischenkammerfurche (IIVG), in der vorderen

Zwischenkammerfurche (AIVG), in der rechten Herzkranzfurche (RAVG) und in der linken Herzkranzfurche (LAVG). In der endgültigen Analyse wurden separate EAT-Dickenmessungen sowie Durchschnittswerte der EAT-Dicke wie folgt verwendet: Gesamtdurchschnittsdicke aus Messungen an 11 Stellen, Durchschnittsdicke der Furchenmessungen (5 Stellen), Durchschnittsdicke der Messungen an beiden freien Ventrikelwänden (6 Stellen), Durchschnittsdicke der Messungen an der RVFW (3 Stellen) und Durchschnittsdicke der Messungen an der LVFW (3 Stellen). Schließlich wurde die Länge des Ventrikelseptums (LVS) mithilfe einer Abstandsmessung auf Kardio-MRT Bildern gemessen.

Alle KHK-Patienten erhielten entweder in unserer oder einer externen Einrichtung eine Koronarangiographie. Insgesamt wurden Patienten mit dem angiografischen Nachweis von ≥1 Stenose mit ≥50% Durchmesser in einer großen Koronararterie der KHK-Gruppe zugeordnet. Zur KHK-Gruppe gehörten zusätzlich Patienten, die infolge einer atherothrombotischen KHK einen akuten Myokardinfarkt erlitten hatten. Der Schweregrad der KHK wurde anhand von zwei Bewertungsskalen beurteilt – Klassifikation von der Canadian Cardiovascular Society und Gensini-Score.

Zur Identifizierung möglicher KHK-Prädiktoren wurde eine binäre logistische Regressionsanalyse durchgeführt. Alle EAT-Dickenmessungen und das EAT-Volumen wurden auf die BMI, KOF und LVS indexiert. Es wurde eine Grenzwertoptimierungskurvenanalyse durchgeführt, um die am besten geeignete EAT-Messung sowie Referenzwerte zur Identifizierung von Patienten mit KHK zu ermitteln. Die Fläche unter der Grenzwertoptimierungskurve (AUC) wurde bewertet, um die Genauigkeit indexierter und nicht indexierter EAT-Messungen zur Vorhersage einer KHK zu bestimmen. Schließlich wurden Sensitivität und Spezifität für die Grenzwerte der EAT-Messungen mit dem höchsten AUC-Wert berechnet. Um den Zusammenhang zwischen den effizientesten EAT-Messungen im Hinblick auf den Schweregrad der KHK zu untersuchen, wurden die Varianzanalyse (ANOVA) und der Pearson-Korrelationskoeffizient angewendet.

Ergebnisse. Epikardiales Fett erwies sich als unabhängiger Prädiktor für eine KHK zusammen mit anderen bekannten KHK-Risikofaktoren – höheres Alter, männliches Geschlecht und Adipositas. Nicht indexierte EAT-Messungen zeigten eine hervorragende Leistung bei der Identifizierung von KHK-Patienten. Die Indexierung der EAT-Messungen brachte keinen signifikanten Vorteil bei der Identifizierung von KHK-Patienten. Das nicht indexierte EAT-Volumen zeigte die beste Effizienz bei der Klassifizierung von Patienten mit KHK. Eine KHK wurde bei Patienten mit einem nicht indexierten EAT-Volumen über 93,62 cm^3 mit einer Sensitivität von 84% und einer Spezifität von 80% korrekt identifiziert. Eine EAT-Gesamtdurchschnittsdicke über 7 mm charakterisierte KHK-Patienten korrekt mit einer Sensitivität von 79% und einer Spezifität von 77%. Obwohl sich EAT-Messungen sehr gut zur Identifizierung von KHK-Patienten eigneten, zeigten sie kein Potenzial zur Bestimmung des Schweregrads der KHK.

Diskussion. Die nicht-indexierte EAT-Dicke sowie das nicht-indexierte und KOF-indexierte EAT-Volumen wurden mehrfach als unabhängige Prädiktoren für KHK bestätigt. Der Zusammenhang zwischen EAT-Messungen und des Schweregrades der KHK blieb aufgrund abweichender Ergebnisse in der veröffentlichten Literatur unklar. Ein möglicher Grund hierfür könnte der gegenläufige Effekt einer begleitenden Herzinsuffizienz mit der damit einhergehenden allmählichen Reduzierung der epikardialen Fettdepots sein. Nur vereinzelt wurde in Studien die Aussagekraft von EAT-Messungen im Hinblick auf KHK verglichen, wobei immer nicht mehr als drei Messtechniken in den Vergleich einbezogen wurden. Bei den meisten Fällen war die KHK anhand der perikoronaren EAT-Dicke besser vorhersagbar als anhand der EAT-Dickenmessungen über RVFW oder LVFW. Da in keiner der veröffentlichten Studien die Vorhersagekraft zwischen EAT-Volumen- und EAT-Dickenmessung im Hinblick auf eine signifikante Koronarstenose verglichen wurde, ist unsere Arbeit die erste, die diese Ergebnisse berichtet.

Unsere Studie ist die erste, die alle am häufigsten berichteten Methoden zur Quantifizierung epikardialer Fettdepots in Bezug auf KHK umfassend vergleicht. Unsere Forschung kann als die größte Kardio-MRT Studie eines einzelnen Zentrums über den Zusammenhang zwischen

EAT und KHK definiert werden. Darüber hinaus ist unsere Studie die erste, die EAT-Dickenmessungen indexiert. Zum ersten Mal haben wir die Größe epikardialer Fettdepots mit anthropometrischen Herzmessungen wie LVS indexiert. Schließlich ist unsere Studie die erste, die den Zusammenhang zwischen EAT-Messungen und dem Schweregrad der KHK untersucht, gemessen mit der Klassifikation von der Canadian Cardiovascular Society.

Schlussfolgerungen. Die nicht-indexierte volumetrische Quantifizierung epikardialer Fettdepots erwies sich als die am besten geeignete EAT-Messung zur Vorhersage des Vorhandenseins einer KHK, jedoch nicht ihres Schweregrades. Die Standardisierung der EAT-Messungen brachte keinen nennenswerten Nutzen bei der Identifizierung von KHK-Patienten.

Introduction. Cardiovascular diseases are the main cause of death worldwide. Coronary artery disease (CAD) is responsible for approximately 7.4 million deaths per annum across the globe. The search for novel cardiovascular risk factors, which significantly contribute to CAD, continues to this day.

Cardiovascular diseases are associated with excessive adiposity. Visceral adipose tissue surrounding the heart muscle, which is directly connected to coronary arteries, is named epicardial adipose tissue (EAT). EAT has emerged as a new modifiable cardiometabolic risk factor besides abdominal depots of visceral adipose tissue. Increase in the size of EAT is associated with increased calcium score in coronary arteries, CAD, subclinical atherosclerosis, metabolic syndrome, cardiac arrhythmias, lipotoxic cardiomyopathy. Excessive EAT produces large quantities of different proinflammatory cytokines and vasoactive peptides. All those substances independently facilitate the production of atheromatous plaques in coronary vessels and thus, the progress of CAD.

The size of EAT depots may be measured using different radiological techniques: echocardiography, computed tomography and cardiac magnetic resonance (CMR). Nevertheless, recent literature has identified CMR as the golden standard in evaluation of the size of EAT. EAT depots are estimated by measuring EAT thickness on different sites and volume.

Because there is no guideline-advocated technique for EAT quantification, individual studies are subject to authors discretion and experience. There is a lack of research in terms of the comparison between different quantification methods of EAT in prediction of CAD. It is not clear whether EAT thickness measured at a single point would be comparable with the volumetric assessment of epicardial fat. Furthermore, the representation of small study populations in published studies is doubtful to determine reference values of the EAT size in prediction of CAD. Fewer studies are available on the topic of EAT indexation. The effect of anthropometric EAT variability is assumed to play an important role in identifying individuals with increased cardiovascular risk. Besides different non-indexed EAT depots measurements, some authors derived EAT amounts, indexed to body surface area (BSA) or to body mass index (BMI).

Goals of research. The aim of this study was to compare predictive powers of various EAT measurement techniques in identification of patients with CAD. Moreover, this study aimed to answer whether indexed EAT measurements bring advantage in comparison to non-indexed counterparts in prediction of CAD.

Materials and methods. This retrospective case-control study involved 760 adult individuals who received CMR scan in the past due to different medical conditions. Exclusion criteria included absence of necessary CMR sequences, pericardial effusion, presence of coronary bypass or stent, absence of medical records, repeated CMR scan. 630 study subjects entered the final analysis. Height and weight of patients were recorded from the CMR safety screening questionnaire. These variables were used to calculate BMI and BSA.

EAT volume was calculated on CMR images by using modified Simpson rule with integration over the image slices. Altogether, there were 11 EAT thickness measurements conducted: three measurements over the right ventricular free wall (RVFW), three over the left ventricular free wall (LVFW), single measurement in the superior interventricular groove (SIVG), inferior interventricular groove (IIVG), anterior interventricular groove (AIVG), right atrioventricular groove (RAVG) and left atrioventricular groove (LAVG). In the final analysis, separate EAT thickness measurements as well as mean values of EAT thickness were used as follows: overall mean thickness from measurements in 11 locations, mean thickness of groove measurements (5 locations), mean thickness of measurements over both ventricular free walls (6 locations), mean thickness of measurements over the RVFW (3 locations) and mean thickness of measurements over the LVFW (3 locations). Finally, interventricular septum length (ISL) was manually measured using a distance measurement tool on CMR images.

All CAD patients received coronary angiography either in our or in an external institution. Overall, patients with the angiographic evidence of ≥1 stenosis of ≥50% in diameter in a major coronary artery were assigned to CAD group. CAD group additionally included patients who suffered from the acute myocardial infarction as a result of the atherothrombotic CAD. The severity of CAD was assessed with two grading scales – Canadian Cardiovascular Society grading of angina pectoris and Gensini Score.

A binary logistic regression analysis was conducted for the identification of possible CAD predictors. All EAT thickness measurements and EAT volume were indexed by BMI, BSA and ISL. Receiver operating characteristic curve analysis was performed in order to identify the most suitable EAT measurement, as well as reference values for identification of patients with CAD. Area under the receiver operating characteristic curve (AUC) was assessed to determine the accuracy of indexed and non-indexed EAT measurements to predict CAD. Finally, sensitivity and specificity were calculated for cut-off EAT measurements with the highest AUC value. Analysis of variance (ANOVA) and Pearson correlation coefficient were applied to evaluate the connection between the most feasible EAT measurements in regard to the CAD severity.

Results. EAT proved to independently predict CAD along with other established CAD risk factors – higher age, male gender and obesity. Non-indexed EAT measurements showed outstanding performance in identification of CAD patients. Indexation of EAT measurements did not provide a significant benefit in identification of CAD patients. Non-indexed EAT volume demonstrated the best efficiency in classification of subjects with CAD. CAD was correctly identified in subjects with the non-indexed EAT volume above 93.62 cm^3 with sensitivity of 84% and specificity of 80%. Non-indexed average all location EAT thickness above 7 mm correctly characterized CAD patients with sensitivity of 79% and specificity of 77%. Although with a very good ability to identify CAD patients, EAT measurements failed to show any potential to determine the severity of CAD**.**

Discussion. Non-indexed EAT thickness as well as non-indexed and BSA-indexed EAT volume were numerous times confirmed to be independent predictors of CAD. The association between EAT measurements and the severity of CAD remained unclear because of discrepant results in published literature. A possible reason could be the opposing effect of accompanying heart failure with the consecutive gradual reduction of epicardial fat depots. Only occasional studies compared the predictive power of EAT measurements in regard to CAD, the comparison always involved not more than 3 measurement techniques. For the majority, pericoronary EAT thickness predicted CAD better than EAT thickness measurements over the RVFW or LVFW. Since none of the published studies compared the prediction power between EAT volume and thickness measurements in terms of a significant coronary stenosis, our work is the first one to report these results.

Our study is the first one to extensively compare all most commonly reported ways of quantifying epicardial fat depots in regard to CAD. Our research can be defined as the largest single center CMR study about the association between EAT and CAD. Moreover, our study is the first one to index EAT thickness measurements. For the first time we indexed the size of epicardial fat depots with anthropometric heart measurements such as ISL. Finally, our study is the first one to examine the association between EAT measurements and the severity of CAD, measured with the Canadian Cardiovascular Society grading of angina pectoris.

Conclusions. Non-indexed volumetric quantification of epicardial fat depots proved to be the most suitable EAT measurement in prediction of the presence of CAD, but not of its severity. Standardization of EAT measurements did not provide a significant benefit in identification of CAD patients.

7 References

(1) World Health Organization. **Cardiovascular diseases (CVDs)** Fact sheet. 2021; Accessed October, 2024. Available at: https://www.who.int/news-room/fact-sheets/detail/cardiovascular-diseases-(cvds).

(2) Mendis S, Puska P, Norrving B, World Health Organization. Global atlas on cardiovascular disease prevention and control. : World Health Organization; 2011.

(3) Eurostat. Cardiovascular diseases statistics. 2024; Accessed October, 2024. Available at: https://ec.europa.eu/eurostat/statistics-explained/index.php?title=Cardiovascular_diseases_statistics.

(4) Malakar AK, Choudhury D, Halder B, Paul P, Uddin A, Chakraborty S. A review on coronary artery disease, its risk factors, and therapeutics. J Cell Physiol 2019;234(10):16812–16823.

(5) World Health Organization. Global action plan for the prevention and control of NCDs 2013-2020. 2017; Accessed October, 2024. Available at: http://www.who.int/nmh/events/ncd_action_plan/en/.

(6) Talman AH, Psaltis PJ, Cameron JD, Meredith IT, Seneviratne SK, Wong DT. Epicardial adipose tissue: far more than a fat depot. Cardiovasc Diagn Ther 2014 Dec;4(6):416–429.

(7) Calle EE, Thun MJ, Petrelli JM, Rodriguez C, Heath Jr CW. Body-mass index and mortality in a prospective cohort of US adults. N Engl J Med 1999;341(15):1097–1105.

(8) Prospective Studies Collaboration. Body-mass index and cause-specific mortality in 900 000 adults: collaborative analyses of 57 prospective studies. The Lancet 2009;373(9669):1083–1096.

(9) Riaz H, Khan MS, Siddiqi TJ, Usman MS, Shah N, Goyal A, et al. Association between obesity and cardiovascular outcomes: a systematic review and meta-analysis of Mendelian randomization studies. JAMA network open 2018;1(7):e183788.

(10) Fuster JJ, Ouchi N, Gokce N, Walsh K. Obesity-induced changes in adipose tissue microenvironment and their impact on cardiovascular disease. Circ Res 2016;118(11):1786–1807.

(11) Mancio J, Oikonomou EK, Antoniades C. Perivascular adipose tissue and coronary atherosclerosis. Heart 2018 Oct;104(20):1654–1662.

(12) Gunawardana SC. Benefits of healthy adipose tissue in the treatment of diabetes. World J Diabetes 2014 Aug 15;5(4):420–430.

(13) Cannon B, Nedergaard J. Brown adipose tissue: function and physiological significance. Physiol Rev 2004.

(14) Roman S, Agil A, Peran M, Alvaro-Galue E, Ruiz-Ojeda FJ, Fernández-Vázquez G, et al. Brown adipose tissue and novel therapeutic approaches to treat metabolic disorders. Translational Research 2015;165(4):464–479.

(15) Lowell BB, Spiegelman BM. Towards a molecular understanding of adaptive thermogenesis. Nature 2000;404(6778):652–660.

(16) Billon N, Dani C. Developmental origins of the adipocyte lineage: new insights from genetics and genomics studies. Stem Cell Reviews and Reports 2012;8(1):55–66.

(17) Cypess AM, Lehman S, Williams G, Tal I, Rodman D, Goldfine AB, et al. Identification and importance of brown adipose tissue in adult humans. N Engl J Med 2009;360(15):1509–1517.

(18) Takx RA, Ishai A, Truong QA, MacNabb MH, Scherrer-Crosbie M, Tawakol A. Supraclavicular Brown Adipose Tissue 18F-FDG Uptake and Cardiovascular Disease. J Nucl Med 2016 Aug;57(8):1221–1225.

(19) Young P, Arch J, Ashwell M. Brown adipose tissue in the parametrial fat pad of the mouse. FEBS Lett 1984;167(1):10–14.

(20) Hyvönen MT, Spalding KL. Maintenance of white adipose tissue in man. Int J Biochem Cell Biol 2014;56:123–132.

(21) Badoud F, Perreault M, Zulyniak MA, Mutch DM. Molecular insights into the role of white adipose tissue in metabolically unhealthy normal weight and metabolically healthy obese individuals. The FASEB Journal 2015;29(3):748–758.

(22) Salazar J, Luzardo E, Mejías JC, Rojas J, Ferreira A, Rivas-Ríos JR, et al. Epicardial fat: physiological, pathological, and therapeutic implications. Cardiology research and practice 2016;2016.

(23) Sniderman AD, Bhopal R, Prabhakaran D, Sarrafzadegan N, Tchernof A. Why might South Asians be so susceptible to central obesity and its atherogenic consequences? The adipose tissue overflow hypothesis. Int J Epidemiol 2007;36(1):220–225.

(24) Okura T, Nakata Y, Yamabuki K, Tanaka K. Regional body composition changes exhibit opposing effects on coronary heart disease risk factors. Arterioscler Thromb Vasc Biol 2004;24(5):923–929.

(25) Le Jemtel TH, Samson R, Milligan G, Jaiswal A, Oparil S. Visceral adipose tissue accumulation and residual cardiovascular risk. Curr Hypertens Rep 2018;20:1–14.

(26) Mathieu P, Poirier P, Pibarot P, Lemieux I, Després J. Visceral obesity: the link among inflammation, hypertension, and cardiovascular disease. Hypertension 2009;53(4):577–584.

(27) Larsson B, Svardsudd K, Welin L, Wilhelmsen L, Bjorntorp P, Tibblin G. Abdominal adipose tissue distribution, obesity, and risk of cardiovascular disease and death: 13 year follow up of participants in the study of men born in 1913. Br Med J (Clin Res Ed) 1984 May 12;288(6428):1401–1404.

(28) Fox CS, Massaro JM, Hoffmann U, Pou KM, Maurovich-Horvat P, Liu C, et al. Abdominal visceral and subcutaneous adipose tissue compartments: association with metabolic risk factors in the Framingham Heart Study. Circulation 2007;116(1):39–48.

(29) Pou KM, Massaro JM, Hoffmann U, Vasan RS, Maurovich-Horvat P, Larson MG, et al. Visceral and subcutaneous adipose tissue volumes are cross-sectionally related to markers of inflammation and oxidative stress: the Framingham Heart Study. Circulation 2007;116(11):1234–1241.

(30) Rosito GA, Massaro JM, Hoffmann U, Ruberg FL, Mahabadi AA, Vasan RS, et al. Pericardial fat, visceral abdominal fat, cardiovascular disease risk factors, and vascular

calcification in a community-based sample: the Framingham Heart Study. Circulation 2008;117(5):605–613.

(31) Cherian S, Lopaschuk GD, Carvalho E. Cellular cross-talk between epicardial adipose tissue and myocardium in relation to the pathogenesis of cardiovascular disease. American journal of physiology-endocrinology and metabolism 2012;303(8):E937–E949.

(32) Şengül C, Özveren O. Epicardial adipose tissue: a review of physiology, pathophysiology, and clinical applications. Anadolu Kardiyol Derg 2013;13(3):261–265.

(33) Iacobellis G, Malavazos AE, Corsi MM. Epicardial fat: from the biomolecular aspects to the clinical practice. Int J Biochem Cell Biol 2011;43(12):1651–1654.

(34) Sacks HS, Fain JN. Human epicardial fat: what is new and what is missing? Clinical and Experimental Pharmacology and Physiology 2011;38(12):879–887.

(35) Ouwens DM, Sell H, Greulich S, Eckel J. The role of epicardial and perivascular adipose tissue in the pathophysiology of cardiovascular disease. J Cell Mol Med 2010;14(9):2223–2234.

(36) Gastaldelli A, Basta G. Ectopic fat and cardiovascular disease: what is the link? Nutrition, Metabolism and cardiovascular diseases 2010;20(7):481–490.

(37) Bakirci EM, Degirmenci H, Hamur H, Gunay M, Gulhan B, Aydin M, et al. New inflammatory markers for prediction of non-dipper blood pressure pattern in patients with essential hypertension: Serum YKL-40/Chitinase 3-like protein 1 levels and echocardiographic epicardial adipose tissue thickness. Clin Exp Hypertens 2015;37(6):505–510.

(38) Iacobellis G, Gao Y, Sharma AM. Do cardiac and perivascular adipose tissue play a role in atherosclerosis? Current diabetes reports 2008;8(1):20–24.

(39) Iacobellis G, Barbaro G. The double role of epicardial adipose tissue as pro-and anti-inflammatory organ. Hormone and metabolic research 2008;40(07):442–445.

(40) McLean DS, Stillman AE. Epicardial adipose tissue as a cardiovascular risk marker. Clinical Lipidology 2009;4(1):55–62.

(41) Fitzgibbons TP, Czech MP. Epicardial and perivascular adipose tissues and their influence on cardiovascular disease: basic mechanisms and clinical associations. Journal of the American Heart Association 2014;3(2):e000582.

(42) Mazurek T, Zhang L, Zalewski A, Mannion JD, Diehl JT, Arafat H, et al. Human epicardial adipose tissue is a source of inflammatory mediators. Circulation 2003;108(20):2460–2466.

(43) Hirata Y, Kurobe H, Akaike M, Chikugo F, Hori T, Bando Y, et al. Enhanced inflammation in epicardial fat in patients with coronary artery disease. International heart journal 2011;52(3):139–142.

(44) Rajsheker S, Manka D, Blomkalns AL, Chatterjee TK, Stoll LL, Weintraub NL. Crosstalk between perivascular adipose tissue and blood vessels. Current opinion in pharmacology 2010;10(2):191–196.

(45) Bertaso AG, Bertol D, Duncan BB, Foppa M. Epicardial fat: definition, measurements and systematic review of main outcomes. Arq Bras Cardiol 2013 Jul;101(1):18.

(46) Wong CX, Ganesan AN, Selvanayagam JB. Epicardial fat and atrial fibrillation: current evidence, potential mechanisms, clinical implications, and future directions. Eur Heart J 2017;38(17):1294–1302.

(47) Sengul C, Cevik C, Ozveren O, Duman D, Eroglu E, Oduncu V, et al. Epicardial fat thickness is associated with non-dipper blood pressure pattern in patients with essential hypertension. Clin Exp Hypertens 2012;34(3):165–170.

(48) Dey D, Nakazato R, Li D, Berman DS. Epicardial and thoracic fat - Noninvasive measurement and clinical implications. Cardiovasc Diagn Ther 2012 Jun;2(2):85–93.

(49) Hirata Y, Yamada H, Kusunose K, Iwase T, Nishio S, Hayashi S, et al. Clinical utility of measuring epicardial adipose tissue thickness with echocardiography using a high-frequency linear probe in patients with coronary artery disease. Journal of the American Society of Echocardiography 2015;28(10):1240–1246. e1.

(50) Yerramasu A, Dey D, Venuraju S, Anand DV, Atwal S, Corder R, et al. Increased volume of epicardial fat is an independent risk factor for accelerated progression of sub-clinical coronary atherosclerosis. Atherosclerosis 2012;220(1):223–230.

(51) Cheng VY, Dey D, Tamarappoo B, Nakazato R, Gransar H, Miranda-Peats R, et al. Pericardial fat burden on ECG-gated noncontrast CT in asymptomatic patients who subsequently experience adverse cardiovascular events. JACC: Cardiovascular Imaging 2010;3(4):352–360.

(52) Janik M, Hartlage G, Alexopoulos N, Mirzoyev Z, McLean DS, Arepalli CD, et al. Epicardial adipose tissue volume and coronary artery calcium to predict myocardial ischemia on positron emission tomography-computed tomography studies. Journal of nuclear cardiology 2010;17(5):841–847.

(53) Wong CX, Abed HS, Molaee P, Nelson AJ, Brooks AG, Sharma G, et al. Pericardial fat is associated with atrial fibrillation severity and ablation outcome. J Am Coll Cardiol 2011;57(17):1745–1751.

(54) Doesch C, Haghi D, Suselbeck T, Schoenberg SO, Borggrefe M, Papavassiliu T. Impact of functional, morphological and clinical parameters on epicardial adipose tissue in patients with coronary artery disease. Circulation Journal 2012;76(10):2426–2434.

(55) Monti M, Monti A, Murdolo G, Di Renzi P, Pirro MR, Borgognoni F, et al. Correlation between epicardial fat and cigarette smoking: CT imaging in patients with metabolic syndrome. Scandinavian Cardiovascular Journal 2014;48(5):317–322.

(56) Matloch Z, Kotulák T, Haluzík M. The role of epicardial adipose tissue in heart disease. Physiological research 2016;65(1):23.

(57) Picard FA, Gueret P, Laissy J, Champagne S, Leclercq F, Carrie D, et al. Epicardial adipose tissue thickness correlates with the presence and severity of angiographic coronary artery disease in stable patients with chest pain. PLoS One 2014;9(10):e110005.

(58) Rajani R, Shmilovich H, Nakazato R, Nakanishi R, Otaki Y, Cheng VY, et al. Relationship of epicardial fat volume to coronary plaque, severe coronary stenosis, and high-risk coronary plaque features assessed by coronary CT angiography. Journal of cardiovascular computed tomography 2013;7(2):125–132.

(59) Lu MT, Park J, Ghemigian K, Mayrhofer T, Puchner SB, Liu T, et al. Epicardial and paracardial adipose tissue volume and attenuation–Association with high-risk coronary plaque on computed tomographic angiography in the ROMICAT II trial. Atherosclerosis 2016;251:47–54.

(60) Nakanishi K, Fukuda S, Tanaka A, Otsuka K, Taguchi H, Yoshikawa J, et al. Epicardial adipose tissue accumulation is associated with renal dysfunction and coronary plaque morphology on multidetector computed tomography. Circulation Journal 2015:CJ–0477.

(61) Xu Y, Cheng X, Hong K, Huang C, Wan L. How to interpret epicardial adipose tissue as a cause of coronary artery disease: a meta-analysis. Coron Artery Dis 2012;23(4):227–233.

(62) Nerlekar N, Brown AJ, Muthalaly RG, Talman A, Hettige T, Cameron JD, et al. Association of epicardial adipose tissue and high-risk plaque characteristics: a systematic review and meta-analysis. Journal of the American Heart Association 2017;6(8):e006379.

(63) Park J, Choi S, Zheng M, Yang H, Lim H, Choi B, et al. Epicardial adipose tissue thickness is a predictor for plaque vulnerability in patients with significant coronary artery disease. Atherosclerosis 2013;226(1):134–139.

(64) Tachibana M, Miyoshi T, Osawa K, Toh N, Oe H, Nakamura K, et al. Measurement of epicardial fat thickness by transthoracic echocardiography for predicting high-risk coronary artery plaques. Heart Vessels 2016;31(11):1758–1766.

(65) Shan D, Dou G, Yang J, Wang X, Wang J, Zhang W, et al. Epicardial adipose tissue volume is associated with high risk plaque profiles in suspect CAD patients. Oxidative Medicine and Cellular Longevity 2021;2021:1–10.

(66) Ding J, Hsu F, Harris TB, Liu Y, Kritchevsky SB, Szklo M, et al. The association of pericardial fat with incident coronary heart disease: the Multi-Ethnic Study of Atherosclerosis (MESA). Am J Clin Nutr 2009;90(3):499–504.

(67) Iozzo P. Myocardial, perivascular, and epicardial fat. Diabetes Care 2011;34(Supplement_2):S371–S379.

(68) Kim HM, Kim KJ, Lee H, Yu HT, Moon JH, Kang ES, et al. Epicardial adipose tissue thickness is an indicator for coronary artery stenosis in asymptomatic type 2 diabetic patients: its assessment by cardiac magnetic resonance. Cardiovascular diabetology 2012;11:1–10.

(69) Homsi R, Sprinkart AM, Gieseke J, Yuecel S, Meier-Schroers M, Luetkens J, et al. 3D-Dixon cardiac magnetic resonance detects an increased epicardial fat volume in hypertensive men with myocardial infarction. Eur J Radiol 2016;85(5):936–942.

(70) Petrini M, Alì M, Cannaò PM, Zambelli D, Cozzi A, Codari M, et al. Epicardial adipose tissue volume in patients with coronary artery disease or non-ischaemic dilated cardiomyopathy: evaluation with cardiac magnetic resonance imaging. Clin Radiol 2019;74(1):81. e1–81. e7.

(71) Iacobellis G, Willens HJ. Echocardiographic epicardial fat: a review of research and clinical applications. Journal of the American Society of Echocardiography 2009;22(12):1311–1319.

(72) Nelson MR, Mookadam F, Thota V, Emani U, Al Harthi M, Lester SJ, et al. Epicardial fat: an additional measurement for subclinical atherosclerosis and cardiovascular risk stratification? Journal of the American Society of Echocardiography 2011;24(3):339–345.

(73) Wang T, Lee W, Shih F, Huang C, Chang Y, Chen W, et al. Relations of epicardial adipose tissue measured by multidetector computed tomography to components of the metabolic syndrome are region-specific and independent of anthropometric indexes and intraabdominal visceral fat. The Journal of Clinical Endocrinology & Metabolism 2009;94(2):662–669.

(74) Zhu J, Xie Z, Huang H, Li W, Zhuo K, Bai Z, et al. Association of Epicardial Adipose Tissue With Left Ventricular Strain and MR Myocardial Perfusion in Patients With Known Coronary Artery Disease. Journal of Magnetic Resonance Imaging 2023;58(5):1490–1498.

(75) Gohbara M, Iwahashi N, Akiyama E, Maejima N, Tsukahara K, Hibi K, et al. Association between epicardial adipose tissue volume and myocardial salvage in patients with a first ST-segment elevation myocardial infarction: an epicardial adipose tissue paradox. J Cardiol 2016;68(5):399–405.

(76) Doesch C, Jochims J, Streitner F, Kuschyk J, Akin I, Lehmann R, et al. Novel prognostic markers derived from cardiovascular magnetic resonance imaging in patients with stable chronic coronary artery disease. In Vivo 2015;29(6):737–747.

(77) Bière L, Behaghel V, Mateus V, Assunção Jr A, Gräni C, Ouerghi K, et al. Relation of quantity of subepicardial adipose tissue to infarct size in patients with ST-elevation myocardial infarction. Am J Cardiol 2017;119(12):1972–1978.

(78) Alexopoulos N, McLean DS, Janik M, Arepalli CD, Stillman AE, Raggi P. Epicardial adipose tissue and coronary artery plaque characteristics. Atherosclerosis 2010;210(1):150–154.

(79) Saad Z, El-Rawy M, Donkol RH, Boghattas S. Quantification of epicardial fat: Which method can predict significant coronary artery disease? World J Cardiol 2015 May 26;7(5):287–292.

(80) Shmilovich H, Dey D, Cheng VY, Rajani R, Nakazato R, Otaki Y, et al. Threshold for the upper normal limit of indexed epicardial fat volume: derivation in a healthy population and validation in an outcome-based study. Am J Cardiol 2011;108(11):1680–1685.

(81) Nakazato R, Rajani R, Cheng VY, Shmilovich H, Nakanishi R, Otaki Y, et al. Weight change modulates epicardial fat burden: a 4-year serial study with non-contrast computed tomography. Atherosclerosis 2012;220(1):139–144.

(82) Aldiss P, Davies G, Woods R, Budge H, Sacks HS, Symonds ME. 'Browning'the cardiac and peri-vascular adipose tissues to modulate cardiovascular risk. Int J Cardiol 2017;228:265–274.

(83) Ansaldo AM, Montecucco F, Sahebkar A, Dallegri F, Carbone F. Epicardial adipose tissue and cardiovascular diseases. Int J Cardiol 2019;278:254–260.

(84) Antonopoulos AS, Antoniades C. The role of epicardial adipose tissue in cardiac biology: classic concepts and emerging roles. J Physiol (Lond) 2017;595(12):3907–3917.

(85) Cheung L, Gertow J, Werngren O, Folkersen L, Petrovic N, Nedergaard J, et al. Human mediastinal adipose tissue displays certain characteristics of brown fat. Nutrition & diabetes 2013;3(5):e66.

(86) Després J. Body fat distribution and risk of cardiovascular disease: an update. Circulation 2012;126(10):1301–1313.

(87) Fantuzzi G, Mazzone T. Adipose tissue and atherosclerosis: exploring the connection. Arterioscler Thromb Vasc Biol 2007;27(5):996–1003.

(88) Guglielmo M, Lin A, Dey D, Baggiano A, Fusini L, Muscogiuri G, et al. Epicardial fat and coronary artery disease: role of cardiac imaging. Atherosclerosis 2021;321:30–38.

(89) Huang Cao ZF, Stoffel E, Cohen P. Role of perivascular adipose tissue in vascular physiology and pathology. Hypertension 2017;69(5):770–777.

(90) Mahabadi AA, Massaro JM, Rosito GA, Levy D, Murabito JM, Wolf PA, et al. Association of pericardial fat, intrathoracic fat, and visceral abdominal fat with cardiovascular disease burden: the Framingham Heart Study. Eur Heart J 2009;30(7):850–856.

(91) Corradi D, Maestri R, Callegari S, Pastori P, Goldoni M, Luong TV, et al. The ventricular epicardial fat is related to the myocardial mass in normal, ischemic and hypertrophic hearts. Cardiovascular Pathology 2004;13(6):313–316.

(92) Iacobellis G. Epicardial adipose tissue in endocrine and metabolic diseases. Endocrine 2014;46(1):8–15.

(93) Sacks HS, Fain JN. Human epicardial adipose tissue: a review. Am Heart J 2007;153(6):907–917.

(94) Marchington JM, Mattacks CA, Pond CM. Adipose tissue in the mammalian heart and pericardium: structure, foetal development and biochemical properties. Comp Biochem Physiol B 1989;94(2):225–232.

(95) Sawaguchi T, Nakajima T, Hasegawa T, Shibasaki I, Kaneda H, Obi S, et al. Serum adiponectin and TNFα concentrations are closely associated with epicardial adipose tissue fatty acid profiles in patients undergoing cardiovascular surgery. IJC heart & vasculature 2018;18:86–95.

(96) Iacobellis G. Epicardial adipose tissue in contemporary cardiology. Nature reviews cardiology 2022;19(9):593–606.

(97) Wang T, Lee W, Shih F, Huang C, Chen W, Lee Y, et al. Association of epicardial adipose tissue with coronary atherosclerosis is region-specific and independent of conventional risk factors and intra-abdominal adiposity. Atherosclerosis 2010;213(1):279–287.

(98) Chatterjee TK, Stoll LL, Denning GM, Harrelson A, Blomkalns AL, Idelman G, et al. Proinflammatory phenotype of perivascular adipocytes: influence of high-fat feeding. Circ Res 2009;104(4):541–549.

(99) Wang ZJ, Reddy GP, Gotway MB, Yeh BM, Hetts SW, Higgins CB. CT and MR imaging of pericardial disease. Radiographics 2003;23(suppl_1):S167–S180.

(100) Rabkin SW. Epicardial fat: properties, function and relationship to obesity. Obesity reviews 2007;8(3):253–261.

(101) Çetin M, Kocaman SA, Durakoğlugil ME, Erdoğan T, Ergül E, Dogan S, et al. Effect of epicardial adipose tissue on diastolic functions and left atrial dimension in untreated hypertensive patients with normal systolic function. J Cardiol 2013;61(5):359–364.

(102) Iacobellis G, Corradi D, Sharma AM. Epicardial adipose tissue: anatomic, biomolecular and clinical relationships with the heart. Nature clinical practice Cardiovascular medicine 2005;2(10):536–543.

(103) Pezeshkian M, Noori M, Najjarpour-Jabbari H, Abolfathi A, Darabi M, Darabi M, et al. Fatty acid composition of epicardial and subcutaneous human adipose tissue. Metabolic syndrome and related disorders 2009;7(2):125–132.

(104) Ho E, Shimada Y. Formation of the epicardium studied with the scanning electron microscope. Dev Biol 1978;66(2):579–585.

(105) Guauque-Olarte S, Gaudreault N, Piché M, Fournier D, Mauriège P, Mathieu P, et al. The transcriptome of human epicardial, mediastinal and subcutaneous adipose tissues in men with coronary artery disease. PloS one 2011;6(5):e19908.

(106) Sacks HS, Fain JN, Holman B, Cheema P, Chary A, Parks F, et al. Uncoupling protein-1 and related messenger ribonucleic acids in human epicardial and other adipose tissues: epicardial fat functioning as brown fat. The Journal of Clinical Endocrinology & Metabolism 2009;94(9):3611–3615.

(107) Piché M, Poirier P. Obesity, ectopic fat and cardiac metabolism. Expert Review of Endocrinology & Metabolism 2018;13(4):213–221.

(108) Barbatelli G, Murano I, Madsen L, Hao Q, Jimenez M, Kristiansen K, et al. The emergence of cold-induced brown adipocytes in mouse white fat depots is determined predominantly by white to brown adipocyte transdifferentiation. American Journal of Physiology-Endocrinology and Metabolism 2010;298(6):E1244–E1253.

(109) Xu F, Lin B, Zheng X, Chen Z, Cao H, Xu H, et al. GLP-1 receptor agonist promotes brown remodelling in mouse white adipose tissue through SIRT1. Diabetologia 2016;59:1059–1069.

(110) Wu J, Boström P, Sparks LM, Ye L, Choi JH, Giang A, et al. Beige adipocytes are a distinct type of thermogenic fat cell in mouse and human. Cell 2012;150(2):366–376.

(111) Lopaschuk GD. Metabolic abnormalities in the diabetic heart. Heart Fail Rev 2002;7(2):149–159.

(112) Chechi K, Blanchard P, Mathieu P, Deshaies Y, Richard D. Brown fat like gene expression in the epicardial fat depot correlates with circulating HDL-cholesterol and triglycerides in patients with coronary artery disease. Int J Cardiol 2013;167(5):2264–2270.

(113) Marchington JM, Pond CM. Site-specific properties of pericardial and epicardial adipose tissue: the effects of insulin and high-fat feeding on lipogenesis and the incorporation of fatty acids in vitro. Int J Obes 1990 Dec;14(12):1013–1022.

(114) Le Jemtel TH, Samson R, Ayinapudi K, Singh T, Oparil S. Epicardial adipose tissue and cardiovascular disease. Curr Hypertens Rep 2019;21:1–11.

(115) Jung HS, Park K, Cho YM, Chung SS, Cho HJ, Cho SY, et al. Resistin is secreted from macrophages in atheromas and promotes atherosclerosis. Cardiovasc Res 2006;69(1):76–85.

(116) Baker AR, Da Silva NF, Quinn DW, Harte AL, Pagano D, Bonser RS, et al. Human epicardial adipose tissue expresses a pathogenic profile of adipocytokines in patients with cardiovascular disease. Cardiovascular diabetology 2006;5(1):1–7.

(117) Shioji K, Moriguchi A, Moriwaki S, Manabe K, Takeuchi Y, Uegaito T, et al. Hypoadiponectinemia implies the development of atherosclerosis in carotid and coronary arteries. J Cardiol 2005;46(3):105–112.

(118) Wong HK, Tang F, Cheung TT, Cheung BM. Adrenomedullin and diabetes. World J Diabetes 2014 Jun 15;5(3):364–371.

(119) Iacobellis G, di Gioia CT, Cotesta D, Petramala L, Travaglini C, De Santis V, et al. Epicardial adipose tissue adiponectin expression is related to intracoronary adiponectin levels. Hormone and metabolic research 2009;41(03):227–231.

(120) Jain SH, Massaro JM, Hoffmann U, Rosito GA, Vasan RS, Raji A, et al. Cross-sectional associations bet ween abdominal and thoracic adipose tissue compartments and adiponectin and resistin in the Framingham heart study. Diabetes Care 2009;32(5):903–908.

(121) Prati F, Arbustini E, Labellarte A, Sommariva L, Pawlowski T, Manzoli A, et al. Eccentric atherosclerotic plaques with positive remodelling have a pericardial distribution: a permissive role of epicardial fat? A three-dimensional intravascular ultrasound study of left anterior descending artery lesions. Eur Heart J 2003;24(4):329–336.

(122) Schäffler A, Schölmerich J. Innate immunity and adipose tissue biology. Trends Immunol 2010;31(6):228–235.

(123) Sacks HS, Fain JN, Bahouth SW, Ojha S, Frontini A, Budge H, et al. Adult epicardial fat exhibits beige features. The Journal of Clinical Endocrinology & Metabolism 2013;98(9):E1448–E1455.

(124) Sacks H, Symonds ME. Anatomical locations of human brown adipose tissue: functional relevance and implications in obesity and type 2 diabetes. Diabetes 2013;62(6):1783–1790.

(125) Henningsson M, Brundin M, Scheffel T, Edin C, Viola F, Carlhäll C. Quantification of epicardial fat using 3D cine Dixon MRI. BMC Medical Imaging 2020;20:1–9.

(126) Karampetsou N, Alexopoulos L, Minia A, Pliaka V, Tsolakos N, Kontzoglou K, et al. Epicardial Adipose Tissue as an Independent Cardiometabolic Risk Factor for Coronary Artery Disease. Cureus 2022;14(6).

(127) Goossens GH, Bizzarri A, Venteclef N, Essers Y, Cleutjens JP, Konings E, et al. Increased adipose tissue oxygen tension in obese compared with lean men is accompanied by insulin resistance, impaired adipose tissue capillarization, and inflammation. Circulation 2011;124(1):67–76.

(128) Ojha S, Symonds ME, Budge H. Suboptimal maternal nutrition during early-to-mid gestation in the sheep enhances pericardial adiposity in the near-term fetus. Reproduction, Fertility and Development 2015;27(8):1205–1212.

(129) Iozzo P. Metabolic toxicity of the heart: insights from molecular imaging. Nutrition, Metabolism and Cardiovascular Diseases 2010;20(3):147–156.

(130) Roberts-Toler C, O'Neill BT, Cypess AM. Diet-induced obesity causes insulin resistance in mouse brown adipose tissue. Obesity 2015;23(9):1765–1770.

(131) Greenstein AS, Khavandi K, Withers SB, Sonoyama K, Clancy O, Jeziorska M, et al. Local inflammation and hypoxia abolish the protective anticontractile properties of perivascular fat in obese patients. Circulation 2009;119(12):1661–1670.

(132) Pang C, Gao Z, Yin J, Zhang J, Jia W, Ye J. Macrophage infiltration into adipose tissue may promote angiogenesis for adipose tissue remodeling in obesity. American Journal of Physiology-Endocrinology and Metabolism 2008;295(2):E313–E322.

(133) Henrichot E, Juge-Aubry CE, Pernin A, Pache J, Velebit V, Dayer J, et al. Production of chemokines by perivascular adipose tissue: a role in the pathogenesis of atherosclerosis? Arterioscler Thromb Vasc Biol 2005;25(12):2594–2599.

(134) Mancio J, Azevedo D, Saraiva F, Azevedo AI, Pires-Morais G, Leite-Moreira A, et al. Epicardial adipose tissue volume assessed by computed tomography and coronary artery disease: a systematic review and meta-analysis. European Heart Journal-Cardiovascular Imaging 2018;19(5):490–497.

(135) Iacobellis G, Assael F, Ribaudo MC, Zappaterreno A, Alessi G, Di Mario U, et al. Epicardial fat from echocardiography: a new method for visceral adipose tissue prediction. Obes Res 2003;11(2):304–310.

(136) Ahn S, Lim H, Joe D, Kang S, Choi B, Choi S, et al. Relationship of epicardial adipose tissue by echocardiography to coronary artery disease. Heart 2008 Mar;94(3):e7.

(137) Jeong J, Jeong MH, Yun KH, Oh SK, Park EM, Kim YK, et al. Echocardiographic epicardial fat thickness and coronary artery disease. Circulation Journal 2007;71(4):536–539.

(138) Sicari R, Sironi AM, Petz R, Frassi F, Chubuchny V, De Marchi D, et al. Pericardial rather than epicardial fat is a cardiometabolic risk marker: an MRI vs echo study. Journal of the American Society of Echocardiography 2011;24(10):1156–1162.

(139) Mustelier JV, Rego JOC, González AG, Sarmiento JCG, Riverón BV. Echocardiographic parameters of epicardial fat deposition and its relation to coronary artery disease. Arq Bras Cardiol 2011;97:122–129.

(140) Mookadam F, Goel R, Alharthi MS, Jiamsripong P, Cha S. Epicardial fat and its association with cardiovascular risk: a cross-sectional observational study. Heart Views 2010 Oct;11(3):103–108.

(141) Nelson AJ, Worthley MI, Psaltis PJ, Carbone A, Dundon BK, Duncan RF, et al. Validation of cardiovascular magnetic resonance assessment of pericardial adipose tissue volume. J Cardiovasc Magn Reson 2009;11(1):1–8.

(142) Eroglu S, Sade LE, Yildirir A, Bal U, Ozbicer S, Ozgul AS, et al. Epicardial adipose tissue thickness by echocardiography is a marker for the presence and severity of coronary artery disease. Nutrition, metabolism and cardiovascular diseases 2009;19(3):211–217.

(143) Iacobellis G, Leonetti F. Epicardial adipose tissue and insulin resistance in obese subjects. The journal of clinical endocrinology & metabolism 2005;90(11):6300–6302.

(144) Antonini-Canterin F, Pellegrinet M, Marinigh R, Favretto G. Role of cardiovascular ultrasound in the evaluation of obese subjects. Journal of cardiovascular echography 2014;24(3):67–71.

(145) Iacobellis G, Ribaudo MC, Assael F, Vecci E, Tiberti C, Zappaterreno A, et al. Echocardiographic epicardial adipose tissue is related to anthropometric and clinical parameters of metabolic syndrome: a new indicator of cardiovascular risk. The Journal of Clinical Endocrinology & Metabolism 2003;88(11):5163–5168.

(146) Iacobellis G, Willens HJ, Barbaro G, Sharma AM. Threshold values of high-risk echocardiographic epicardial fat thickness. Obesity 2008;16(4):887–892.

(147) Saura D, Oliva MJ, Rodriguez D, Pascual-Figal DA, Hurtado JA, Pinar E, et al. Reproducibility of echocardiographic measurements of epicardial fat thickness. Int J Cardiol 2010 Jun 11;141(3):311–313.

(148) Stocker TJ, Deseive S, Leipsic J, Hadamitzky M, Chen MY, Rubinshtein R, et al. Reduction in radiation exposure in cardiovascular computed tomography imaging: results from the PROspective multicenter registry on radiaTion dose Estimates of cardiac CT angIOgraphy iN daily practice in 2017 (PROTECTION VI). Eur Heart J 2018;39(41):3715–3723.

(149) Andreini D, Magnoni M, Conte E, Masson S, Mushtaq S, Berti S, et al. Coronary plaque features on CTA can identify patients at increased risk of cardiovascular events. JACC: Cardiovascular Imaging 2020;13(8):1704–1717.

(150) Lee JH, Han D, Danad I, ó Hartaigh B, Lin FY, Min JK. Multimodality imaging in coronary artery disease: focus on computed tomography. Journal of Cardiovascular Ultrasound 2016;24(1):7.

(151) Lesser JR, Flygenring BJ, Knickelbine T, Longe T, Schwartz RS. Practical approaches to overcoming artifacts in coronary CT angiography. Journal of cardiovascular computed tomography 2009;3(1):4–15.

(152) Dey D, Wong ND, Tamarappoo B, Nakazato R, Gransar H, Cheng VY, et al. Computer-aided non-contrast CT-based quantification of pericardial and thoracic fat and their associations with coronary calcium and metabolic syndrome. Atherosclerosis 2010;209(1):136–141.

(153) Budoff MJ, Shinbane JS. Cardiac CT imaging: diagnosis of cardiovascular disease. : Springer; 2016.

(154) Bucher AM, Schoepf UJ, Krazinski AW, Silverman J, Spearman JV, De Cecco CN, et al. Influence of technical parameters on epicardial fat volume quantification at cardiac CT. Eur J Radiol 2015;84(6):1062–1067.

(155) Abbara S, Desai JC, Cury RC, Butler J, Nieman K, Reddy V. Mapping epicardial fat with multi-detector computed tomography to facilitate percutaneous transepicardial arrhythmia ablation. Eur J Radiol 2006;57(3):417–422.

(156) Gorter PM, de Vos AM, van der Graaf Y, Stella PR, Doevendans PA, Meijs MF, et al. Relation of epicardial and pericoronary fat to coronary atherosclerosis and coronary artery calcium in patients undergoing coronary angiography. Am J Cardiol 2008;102(4):380–385.

(157) Tamarappoo B, Dey D, Shmilovich H, Nakazato R, Gransar H, Cheng VY, et al. Increased pericardial fat volume measured from noncontrast CT predicts myocardial ischemia by SPECT. JACC: Cardiovascular Imaging 2010;3(11):1104–1112.

(158) Austys D, Dobrovolskij A, Jablonskienė V, Dobrovolskij V, Valevičienė N, Stukas R. Epicardial adipose tissue accumulation and essential hypertension in non-obese adults. Medicina 2019;55(8):456.

(159) Dey D, Suzuki Y, Suzuki S, Ohba M, Slomka PJ, Polk D, et al. Automated quantitation of pericardiac fat from noncontrast CT. Invest Radiol 2008;43(2):145–153.

(160) Shahzad R, Bos D, Metz C, Rossi A, Kirişli H, van der Lugt A, et al. Automatic quantification of epicardial fat volume on non-enhanced cardiac CT scans using a multi-atlas segmentation approach. Med Phys 2013;40(9):091910.

(161) Barbosa JG, Figueiredo B, Bettencourt N, Tavares JMR. Towards automatic quantification of the epicardial fat in non-contrasted CT images. Comput Methods Biomech Biomed Engin 2011;14(10):905–914.

(162) Ding X, Terzopoulos D, Diaz-Zamudio M, Berman DS, Slomka PJ, Dey D. Automated pericardium delineation and epicardial fat volume quantification from noncontrast CT. Med Phys 2015;42(9):5015–5026.

(163) Norlén A, Alvén J, Molnar D, Enqvist O, Norrlund RR, Brandberg J, et al. Automatic pericardium segmentation and quantification of epicardial fat from computed tomography angiography. Journal of Medical Imaging 2016;3(3):034003.

(164) Nakazato R, Shmilovich H, Tamarappoo BK, Cheng VY, Slomka PJ, Berman DS, et al. Interscan reproducibility of computer-aided epicardial and thoracic fat measurement from noncontrast cardiac CT. Journal of cardiovascular computed tomography 2011;5(3):172–179.

(165) Commandeur F, Goeller M, Razipour A, Cadet S, Hell MM, Kwiecinski J, et al. Fully automated CT quantification of epicardial adipose tissue by deep learning: a multicenter study. Radiology: Artificial Intelligence 2019;1(6):e190045.

(166) Bastarrika G, Broncano J, Schoepf UJ, Schwarz F, Lee YS, Abro JA, et al. Relationship between coronary artery disease and epicardial adipose tissue quantification at cardiac CT: comparison between automatic volumetric measurement and manual bidimensional estimation. Acad Radiol 2010;17(6):727–734.

(167) Kim BJ, Kang JG, Lee SH, Lee JY, Sung KC, Kim BS, et al. Relationship of echocardiographic epicardial fat thickness and epicardial fat volume by computed tomography with coronary artery calcification: data from the CAESAR study. Arch Med Res 2017;48(4):352–359.

(168) Flüchter S, Haghi D, Dinter D, Heberlein W, Kühl HP, Neff W, et al. Volumetric assessment of epicardial adipose tissue with cardiovascular magnetic resonance imaging. Obesity 2007;15(4):870–878.

(169) Liu Z, Wang S, Wang Y, Zhou N, Shu J, Stamm C, et al. Association of epicardial adipose tissue attenuation with coronary atherosclerosis in patients with a high risk of coronary artery disease. Atherosclerosis 2019;284:230–236.

(170) Franssens BT, Nathoe HM, Leiner T, van der Graaf Y, Visseren FL, SMART Study Group. Relation between cardiovascular disease risk factors and epicardial adipose tissue density on cardiac computed tomography in patients at high risk of cardiovascular events. European journal of preventive cardiology 2017;24(6):660–670.

(171) Abazid RM, Smettei OA, Kattea MO, Sayed S, Saqqah H, Widyan AM, et al. Relation between epicardial fat and subclinical atherosclerosis in asymptomatic individuals. J Thorac Imaging 2017;32(6):378–382.

(172) Mahabadi AA, Balcer B, Dykun I, Forsting M, Schlosser T, Heusch G, et al. Cardiac computed tomography-derived epicardial fat volume and attenuation independently distinguish patients with and without myocardial infarction. PLoS One 2017;12(8):e0183514.

(173) Hell MM, Ding X, Rubeaux M, Slomka P, Gransar H, Terzopoulos D, et al. Epicardial adipose tissue volume but not density is an independent predictor for myocardial ischemia. Journal of cardiovascular computed tomography 2016;10(2):141–149.

(174) Goeller M, Tamarappoo BK, Kwan AC, Cadet S, Commandeur F, Razipour A, et al. Relationship between changes in pericoronary adipose tissue attenuation and coronary plaque burden quantified from coronary computed tomography angiography. European Heart Journal-Cardiovascular Imaging 2019;20(6):636–643.

(175) Sugiyama T, Kanaji Y, Hoshino M, Yamaguchi M, Hada M, Ohya H, et al. Determinants of pericoronary adipose tissue attenuation on computed tomography angiography in coronary artery disease. Journal of the American Heart Association 2020;9(15):e016202.

(176) Antonopoulos AS, Sanna F, Sabharwal N, Thomas S, Oikonomou EK, Herdman L, et al. Detecting human coronary inflammation by imaging perivascular fat. Science translational medicine 2017;9(398):eaal2658.

(177) Oikonomou EK, Marwan M, Desai MY, Mancio J, Alashi A, Centeno EH, et al. Non-invasive detection of coronary inflammation using computed tomography and prediction of residual cardiovascular risk (the CRISP CT study): a post-hoc analysis of prospective outcome data. The Lancet 2018;392(10151):929–939.

(178) Machann J, Thamer C, Schnoedt B, Haap M, Haring H, Claussen CD, et al. Standardized assessment of whole body adipose tissue topography by MRI. Journal of Magnetic Resonance Imaging: An Official Journal of the International Society for Magnetic Resonance in Medicine 2005;21(4):455–462.

(179) Mahajan R, Kuklik P, Grover S, Brooks AG, Wong CX, Sanders P, et al. Cardiovascular magnetic resonance of total and atrial pericardial adipose tissue: a validation study and development of a 3 dimensional pericardial adipose tissue model. J Cardiovasc Magn Reson 2013;15(1):73.

(180) Modern imaging of myocarditis: Possibilities and challenges. RöFo-Fortschritte auf dem Gebiet der Röntgenstrahlen und der bildgebenden Verfahren: © Georg Thieme Verlag KG; 2016.

(181) Lima JA, Desai MY. Cardiovascular magnetic resonance imaging: current and emerging applications. J Am Coll Cardiol 2004;44(6):1164–1171.

(182) Tanaka K, Fukuda D, Sata M. Roles of Epicardial Adipose Tissue in the Pathogenesis of Coronary Atherosclerosis—An Update on Recent Findings—. Circulation Journal 2020;85(1):2–8.

(183) Christen T, Sheikine Y, Rocha VZ, Hurwitz S, Goldfine AB, Di Carli M, et al. Increased glucose uptake in visceral versus subcutaneous adipose tissue revealed by PET imaging. JACC: Cardiovascular Imaging 2010;3(8):843–851.

(184) Love C, Tomas MB, Tronco GG, Palestro CJ. FDG PET of infection and inflammation. Radiographics 2005;25(5):1357–1368.

(185) Yuvaraj J, Cheng K, Lin A, Psaltis PJ, Nicholls SJ, Wong DT. The emerging role of CT-based imaging in adipose tissue and coronary inflammation. Cells 2021;10(5):1196.

(186) Mazurek T, Kobylecka M, Zielenkiewicz M, Kurek A, Kochman J, Filipiak KJ, et al. PET/CT evaluation of 18 F-FDG uptake in pericoronary adipose tissue in patients with stable

coronary artery disease: Independent predictor of atherosclerotic lesions' formation? Journal of Nuclear Cardiology 2017;24:1075–1084.

(187) Kwiecinski J, Dey D, Cadet S, Lee S, Otaki Y, Huynh PT, et al. Peri-coronary adipose tissue density is associated with 18F-sodium fluoride coronary uptake in stable patients with high-risk plaques. JACC: Cardiovascular Imaging 2019;12(10):2000–2010.

(188) Ohyama K, Matsumoto Y, Takanami K, Ota H, Nishimiya K, Sugisawa J, et al. Coronary adventitial and perivascular adipose tissue inflammation in patients with vasospastic angina. J Am Coll Cardiol 2018;71(4):414–425.

(189) Fainberg HP, Birtwistle M, Alagal R, Alhaddad A, Pope M, Davies G, et al. Transcriptional analysis of adipose tissue during development reveals depot-specific responsiveness to maternal dietary supplementation. Scientific Reports 2018;8(1):9628.

(190) Iozzo P, Lautamaki R, Borra R, Lehto H, Bucci M, Viljanen A, et al. Contribution of glucose tolerance and gender to cardiac adiposity. The Journal of Clinical Endocrinology & Metabolism 2009;94(11):4472–4482.

(191) Dey DK, Rothenberg E, Sundh V, Bosaeus I, Steen B. Height and body weight in the elderly. I. A 25-year longitudinal study of a population aged 70 to 95 years. Eur J Clin Nutr 1999;53(12):905–914.

(192) Perissinotto E, Pisent C, Sergi G, Grigoletto F, Enzi G, ILSA Working Group. Anthropometric measurements in the elderly: age and gender differences. Br J Nutr 2002;87(2):177–186.

(193) Duncan BB, Chambless LE, Schmidt MI, Szklo M, Folsom AR, Carpenter MA, et al. Correlates of body fat distribution: variation across categories of race, sex, and body mass in the atherosclerosis risk in communities study. Ann Epidemiol 1995;5(3):192–200.

(194) Willens HJ, Gomez-Marin O, Chirinos JA, Goldberg R, Lowery MH, Iacobellis G. Comparison of epicardial and pericardial fat thickness assessed by echocardiography in African American and non-Hispanic White men: a pilot study. Ethn Dis 2008;18(3):311–316.

(195) McClain J, Hsu F, Brown E, Burke G, Carr J, Harris T, et al. Pericardial adipose tissue and coronary artery calcification in the Multi-Ethnic Study of Atherosclerosis (MESA). Obesity 2013;21(5):1056–1063.

(196) Salami SS, Tucciarone M, Bess R, Kolluru A, Szpunar S, Rosman H, et al. Race and Epicardial Fat. Ethn Dis 2013;23(3):281–285.

(197) Natale F, Tedesco MA, Mocerino R, de Simone V, Di Marco GM, Aronne L, et al. Visceral adiposity and arterial stiffness: echocardiographic epicardial fat thickness reflects, better than waist circumference, carotid arterial stiffness in a large population of hypertensives. European Journal of Echocardiography 2009;10(4):549–555.

(198) Schejbal V. Epicardial fatty tissue of the right ventricle--morphology, morphometry and functional significance. Pneumologie 1989 Sep;43(9):490–499.

(199) de Vos AM, Prokop M, Roos CJ, Meijs MF, van der Schouw YT, Rutten A, et al. Peri-coronary epicardial adipose tissue is related to cardiovascular risk factors and coronary artery calcification in post-menopausal women. Eur Heart J 2008;29(6):777–783.

(200) Thanassoulis G, Massaro JM, O'Donnell CJ, Hoffmann U, Levy D, Ellinor PT, et al. Pericardial fat is associated with prevalent atrial fibrillation: the Framingham Heart Study. Circulation: Arrhythmia and Electrophysiology 2010;3(4):345–350.

(201) Lu C, Jia H, Wang Z. Association between epicardial adipose tissue and adverse outcomes in coronary heart disease patients with percutaneous coronary intervention. Biosci Rep 2019;39(5):BSR20182278.

(202) Costa RM, Neves KB, Tostes RC, Lobato NS. Perivascular adipose tissue as a relevant fat depot for cardiovascular risk in obesity. Frontiers in physiology 2018;9:253.

(203) Ridker PM, Antman EM. Pathogenesis and pathology of coronary heart disease syndromes. J Thromb Thrombolysis 1999;8:167–189.

(204) Wu Y, Zhang A, Hamilton DJ, Deng T. Epicardial fat in the maintenance of cardiovascular health. Methodist DeBakey cardiovascular journal 2017;13(1):20.

(205) Greif M, Becker A, von Ziegler F, Lebherz C, Lehrke M, Broedl UC, et al. Pericardial adipose tissue determined by dual source CT is a risk factor for coronary atherosclerosis. Arterioscler Thromb Vasc Biol 2009;29(5):781–786.

(206) Iacobellis G, Pistilli D, Gucciardo M, Leonetti F, Miraldi F, Brancaccio G, et al. Adiponectin expression in human epicardial adipose tissue in vivo is lower in patients with coronary artery disease. Cytokine 2005;29(6):251–255.

(207) Iacobellis G, Di Gioia CR, Di Vito M, Petramala L, Cotesta D, De Santis V, et al. Epicardial adipose tissue and intracoronary adrenomedullin levels in coronary artery disease. Hormone and metabolic research 2009;41(12):855–860.

(208) Iacobellis G. Epicardial fat: a new cardiovascular therapeutic target. Current opinion in pharmacology 2016;27:13–18.

(209) Iwayama T, Nitobe J, Watanabe T, Ishino M, Tamura H, Nishiyama S, et al. The role of epicardial adipose tissue in coronary artery disease in non-obese patients. J Cardiol 2014;63(5):344–349.

(210) Suganami T, Tanimoto-Koyama K, Nishida J, Itoh M, Yuan X, Mizuarai S, et al. Role of the Toll-like receptor 4/NF-κB pathway in saturated fatty acid–induced inflammatory changes in the interaction between adipocytes and macrophages. Arterioscler Thromb Vasc Biol 2007;27(1):84–91.

(211) Permana PA, Menge C, Reaven PD. Macrophage-secreted factors induce adipocyte inflammation and insulin resistance. Biochem Biophys Res Commun 2006;341(2):507–514.

(212) Zhang T, Yang P, Li T, Gao J, Zhang Y. Leptin expression in human epicardial adipose tissue is associated with local coronary atherosclerosis. Medical Science Monitor: International Medical Journal of Experimental and Clinical Research 2019;25:9913.

(213) Barandier C, Montani J, Yang Z. Mature adipocytes and perivascular adipose tissue stimulate vascular smooth muscle cell proliferation: effects of aging and obesity. American Journal of Physiology-Heart and Circulatory Physiology 2005;289(5):H1807–H1813.

(214) Zhang H, Zhang C. Regulation of microvascular function by adipose tissue in obesity and type 2 diabetes: evidence of an adipose-vascular loop. American journal of biomedical sciences 2009;1(2):133.

(215) Libby P, Tabas I, Fredman G, Fisher EA. Inflammation and its resolution as determinants of acute coronary syndromes. Circ Res 2014;114(12):1867–1879.

(216) Yudkin JS, Eringa E, Stehouwer CD. “Vasocrine” signalling from perivascular fat: a mechanism linking insulin resistance to vascular disease. The Lancet 2005;365(9473):1817–1820.

(217) Iacobellis G, Bianco AC. Epicardial adipose tissue: emerging physiological, pathophysiological and clinical features. Trends in Endocrinology & Metabolism 2011;22(11):450–457.

(218) Shimabukuro M, Hirata Y, Tabata M, Dagvasumberel M, Sato H, Kurobe H, et al. Epicardial adipose tissue volume and adipocytokine imbalance are strongly linked to human coronary atherosclerosis. Arterioscler Thromb Vasc Biol 2013;33(5):1077–1084.

(219) Golia E, Limongelli G, Natale F, Fimiani F, Maddaloni V, Russo PE, et al. Adipose tissue and vascular inflammation in coronary artery disease. World J Cardiol 2014 Jul 26;6(7):539–554.

(220) Echavarria-Pinto M, Hernando L, Alfonso F. From the epicardial adipose tissue to vulnerable coronary plaques. World J Cardiol 2013 Apr 26;5(4):68–74.

(221) Schlich R, Willems M, Greulich S, Ruppe F, Knoefel WT, Ouwens DM, et al. VEGF in the crosstalk between human adipocytes and smooth muscle cells: depot-specific release from visceral and perivascular adipose tissue. Mediators Inflamm 2013;2013.

(222) Antonopoulos AS, Tousoulis D. The molecular mechanisms of obesity paradox. Cardiovasc Res 2017;113(9):1074–1086.

(223) Vyas V, Blythe H, Wood EG, Sandhar B, Sarker S, Balmforth D, et al. Obesity and diabetes are major risk factors for epicardial adipose tissue inflammation. JCI insight 2021;6(16).

(224) Karastergiou K, Evans I, Ogston N, Miheisi N, Nair D, Kaski J, et al. Epicardial adipokines in obesity and coronary artery disease induce atherogenic changes in monocytes and endothelial cells. Arterioscler Thromb Vasc Biol 2010;30(7):1340–1346.

(225) Zhang J, Nie L, Razavian M, Ahmed M, Dobrucki LW, Asadi A, et al. Molecular imaging of activated matrix metalloproteinases in vascular remodeling. Circulation 2008;118(19):1953–1960.

(226) Northcott JM, Yeganeh A, Taylor CG, Zahradka P, Wigle JT. Adipokines and the cardiovascular system: mechanisms mediating health and disease. Can J Physiol Pharmacol 2012;90(8):1029–1059.

(227) Shibasaki I, Nishikimi T, Mochizuki Y, Yamada Y, Yoshitatsu M, Inoue Y, et al. Greater expression of inflammatory cytokines, adrenomedullin, and natriuretic peptide receptor-C in epicardial adipose tissue in coronary artery disease. Regul Pept 2010;165(2-3):210–217.

(228) Virmani R, Kolodgie FD, Burke AP, Finn AV, Gold HK, Tulenko TN, et al. Atherosclerotic plaque progression and vulnerability to rupture: angiogenesis as a source of intraplaque hemorrhage. Arterioscler Thromb Vasc Biol 2005;25(10):2054–2061.

(229) Elsanhoury A, Nelki V, Kelle S, Van Linthout S, Tschöpe C. Epicardial fat expansion in diabetic and obese patients with heart failure and preserved ejection fraction—a specific HFpEF phenotype. Frontiers in cardiovascular medicine 2021;8:720690.

(230) Demir B, Demir E, Acıksarı G, Uygun T, Utku IK, Gedikbasi A, et al. The association between the epicardial adipose tissue thickness and oxidative stress parameters in isolated metabolic syndrome patients: a multimarker approach. International Journal of Endocrinology 2014;2014.

(231) Langheim S, Dreas L, Veschini L, Maisano F, Foglieni C, Ferrarello S, et al. Increased expression and secretion of resistin in epicardial adipose tissue of patients with acute coronary syndrome. American Journal of Physiology-Heart and Circulatory Physiology 2010;298(3):H746–H753.

(232) Kim M, kyun Oh J, Sakata S, Liang I, Park W, Hajjar RJ, et al. Role of resistin in cardiac contractility and hypertrophy. J Mol Cell Cardiol 2008;45(2):270–280.

(233) Graveleau C, Zaha VG, Mohajer A, Banerjee RR, Dudley-Rucker N, Steppan CM, et al. Mouse and human resistins impair glucose transport in primary mouse cardiomyocytes, and oligomerization is required for this biological action. J Biol Chem 2005;280(36):31679–31685.

(234) Salgado-Somoza A, Teijeira-Fernández E, Fernández ÁL, González-Juanatey JR, Eiras S. Proteomic analysis of epicardial and subcutaneous adipose tissue reveals differences in proteins involved in oxidative stress. American Journal of Physiology-Heart and Circulatory Physiology 2010;299(1):H202–H209.

(235) Baker AR, Harte AL, Howell N, Pritlove DC, Ranasinghe AM, Da Silva NF, et al. Epicardial adipose tissue as a source of nuclear factor-κB and c-Jun N-terminal kinase mediated inflammation in patients with coronary artery disease. The Journal of Clinical Endocrinology & Metabolism 2009;94(1):261–267.

(236) Ishii T, Asuwa N, Masuda S, Ishikawa Y. The effects of a myocardial bridge on coronary atherosclerosis and ischaemia. The Journal of Pathology: A Journal of the Pathological Society of Great Britain and Ireland 1998;185(1):4–9.

(237) Chandalia M, Garg A, Vuitch F, Nizzi F. Postmortem findings in congenital generalized lipodystrophy. The Journal of Clinical Endocrinology & Metabolism 1995;80(10):3077–3081.

(238) Taguchi R, Takasu J, Itani Y, Yamamoto R, Yokoyama K, Watanabe S, et al. Pericardial fat accumulation in men as a risk factor for coronary artery disease. Atherosclerosis 2001;157(1):203–209.

(239) Ueno K, Anzai T, Jinzaki M, Yamada M, Jo Y, Maekawa Y, et al. Increased epicardial fat volume quantified by 64-multidetector computed tomography is associated with coronary atherosclerosis and totally occlusive lesions. Circulation Journal 2009;73(10):1927–1933.

(240) Hwang I, Park HE, Choi S. Epicardial adipose tissue contributes to the development of non-calcified coronary plaque: a 5-year computed tomography follow-up study. J Atheroscler Thromb 2017;24(3):262–274.

(241) Alam MS, Green R, de Kemp R, Beanlands RS, Chow BJ. Epicardial adipose tissue thickness as a predictor of impaired microvascular function in patients with non-obstructive coronary artery disease. Journal of Nuclear Cardiology 2013;20(5):804–812.

(242) Aydın AM, Kayalı A, Poyraz AK, Aydın K. The relationship between coronary artery disease and pericoronary epicardial adipose tissue thickness. J Int Med Res 2015;43(1):17–25.

(243) Demircelik MB, Yilmaz OC, Gurel OM, Selcoki Y, Atar IA, Bozkurt A, et al. Epicardial adipose tissue and pericoronary fat thickness measured with 64-multidetector computed tomography: potential predictors of the severity of coronary artery disease. Clinics 2014;69:388–392.

(244) McKenney ML, Schultz KA, Boyd JH, Byrd JP, Alloosh M, Teague SD, et al. Epicardial adipose excision slows the progression of porcine coronary atherosclerosis. Journal of cardiothoracic surgery 2014;9(1):1–11.

(245) Goeller M, Achenbach S, Marwan M, Doris MK, Cadet S, Commandeur F, et al. Epicardial adipose tissue density and volume are related to subclinical atherosclerosis, inflammation and major adverse cardiac events in asymptomatic subjects. Journal of cardiovascular computed tomography 2018;12(1):67–73.

(246) Nakanishi R, Slomka PJ, Rios R, Betancur J, Blaha MJ, Nasir K, et al. Machine learning adds to clinical and CAC assessments in predicting 10-year CHD and CVD deaths. Cardiovascular Imaging 2021;14(3):615–625.

(247) Greenland P, Blaha MJ, Budoff MJ, Erbel R, Watson KE. Coronary calcium score and cardiovascular risk. J Am Coll Cardiol 2018;72(4):434–447.

(248) Ramjattan NA, Lala V, Kousa O, Makaryus AN. Coronary CT angiography. 2017.

(249) Sarin S, Wenger C, Marwaha A, Qureshi A, Go BD, Woomert CA, et al. Clinical significance of epicardial fat measured using cardiac multislice computed tomography. Am J Cardiol 2008;102(6):767–771.

(250) Mahabadi AA, Lehmann N, Kälsch H, Robens T, Bauer M, Dykun I, et al. Association of epicardial adipose tissue with progression of coronary artery calcification is more pronounced in the early phase of atherosclerosis: results from the Heinz Nixdorf recall study. JACC: cardiovascular imaging 2014;7(9):909–916.

(251) Ding J, Kritchevsky SB, Harris TB, Burke GL, Detrano RC, Szklo M, et al. The association of pericardial fat with calcified coronary plaque. Obesity 2008;16(8):1914–1919.

(252) Djaberi R, Schuijf JD, van Werkhoven JM, Nucifora G, Jukema JW, Bax JJ. Relation of epicardial adipose tissue to coronary atherosclerosis. Am J Cardiol 2008;102(12):1602–1607.

(253) Bettencourt N, Toschke AM, Leite D, Rocha J, Carvalho M, Sampaio F, et al. Epicardial adipose tissue is an independent predictor of coronary atherosclerotic burden. Int J Cardiol 2012;158(1):26–32.

(254) Ding J, Kritchevsky SB, Hsu F, Harris TB, Burke GL, Detrano RC, et al. Association between non-subcutaneous adiposity and calcified coronary plaque: a substudy of the Multi-Ethnic Study of Atherosclerosis. Am J Clin Nutr 2008;88(3):645–650.

(255) Bos D, Shahzad R, van Walsum T, van Vliet LJ, Franco OH, Hofman A, et al. Epicardial fat volume is related to atherosclerotic calcification in multiple vessel beds. European Heart Journal-Cardiovascular Imaging 2015;16(11):1264–1269.

(256) Ahmadi N, Nabavi V, Yang E, Hajsadeghi F, Lakis M, Flores F, et al. Increased epicardial, pericardial, and subcutaneous adipose tissue is associated with the presence and severity of coronary artery calcium. Acad Radiol 2010;17(12):1518–1524.

(257) Nakanishi R, Rajani R, Cheng VY, Gransar H, Nakazato R, Shmilovich H, et al. Increase in epicardial fat volume is associated with greater coronary artery calcification progression in subjects at intermediate risk by coronary calcium score: a serial study using non-contrast cardiac CT. Atherosclerosis 2011;218(2):363–368.

(258) Keresztesi AA, Asofie G, Simion MA, Jung H. Correlation between epicardial adipose tissue thickness and the degree of coronary artery atherosclerosis. Turkish Journal of Medical Sciences 2018;48(1):40–45.

(259) Morita H, Fujimoto S, Kondo T, Arai T, Sekine T, Matsutani H, et al. Prevalence of computed tomographic angiography-verified high-risk plaques and significant luminal stenosis in patients with zero coronary calcium score. Int J Cardiol 2012;158(2):272–278.

(260) Ito T, Suzuki Y, Ehara M, Matsuo H, Teramoto T, Terashima M, et al. Impact of epicardial fat volume on coronary artery disease in symptomatic patients with a zero calcium score. Int J Cardiol 2013;167(6):2852–2858.

(261) Oka T, Yamamoto H, Ohashi N, Kitagawa T, Kunita E, Utsunomiya H, et al. Association between epicardial adipose tissue volume and characteristics of non-calcified plaques assessed by coronary computed tomographic angiography. Int J Cardiol 2012;161(1):45–49.

(262) Konishi M, Sugiyama S, Sugamura K, Nozaki T, Ohba K, Matsubara J, et al. Association of pericardial fat accumulation rather than abdominal obesity with coronary atherosclerotic plaque formation in patients with suspected coronary artery disease. Atherosclerosis 2010;209(2):573–578.

(263) Blankstein R, Ferencik M. The vulnerable plaque: Can it be detected with Cardiac CT? Atherosclerosis 2010 Aug;211(2):386–389.

(264) Okada K, Ohshima S, Isobe S, Harada K, Hirashiki A, Funahashi H, et al. Epicardial fat volume correlates with severity of coronary artery disease in nonobese patients. J Cardiovasc Med 2014;15(5):384–390.

(265) Motoyama S, Sarai M, Harigaya H, Anno H, Inoue K, Hara T, et al. Computed tomographic angiography characteristics of atherosclerotic plaques subsequently resulting in acute coronary syndrome. J Am Coll Cardiol 2009;54(1):49–57.

(266) Nakanishi K, Fukuda S, Tanaka A, Otsuka K, Jissho S, Taguchi H, et al. Persistent epicardial adipose tissue accumulation is associated with coronary plaque vulnerability and future acute coronary syndrome in non-obese subjects with coronary artery disease. Atherosclerosis 2014;237(1):353–360.

(267) Ito T, Nasu K, Terashima M, Ehara M, Kinoshita Y, Ito T, et al. The impact of epicardial fat volume on coronary plaque vulnerability: insight from optical coherence tomography analysis. European Heart Journal–Cardiovascular Imaging 2012;13(5):408–415.

(268) Kim TH, Yu SH, Choi SH, Yoon JW, Kang SM, Chun EJ, et al. Pericardial fat amount is an independent risk factor of coronary artery stenosis assessed by multidetector-row computed tomography: the Korean Atherosclerosis Study 2. Obesity 2011;19(5):1028–1034.

(269) Iwasaki K, Matsumoto T, Aono H, Furukawa H, Samukawa M. Relationship between epicardial fat measured by 64-multidetector computed tomography and coronary artery disease. Clin Cardiol 2011;34(3):166–171.

(270) Schlett CL, Ferencik M, Kriegel MF, Bamberg F, Ghoshhajra BB, Joshi SB, et al. Association of pericardial fat and coronary high-risk lesions as determined by cardiac CT. Atherosclerosis 2012;222(1):129–134.

(271) Nakazato R, Dey D, Cheng VY, Gransar H, Slomka PJ, Hayes SW, et al. Epicardial fat volume and concurrent presence of both myocardial ischemia and obstructive coronary artery disease. Atherosclerosis 2012;221(2):422–426.

(272) Mahabadi AA, Reinsch N, Lehmann N, Altenbernd J, Kälsch H, Seibel RM, et al. Association of pericoronary fat volume with atherosclerotic plaque burden in the underlying coronary artery: a segment analysis. Atherosclerosis 2010;211(1):195–199.

(273) Kim S, Chung J, Kwon B, Song S, Choi W. The associations of epicardial adipose tissue with coronary artery disease and coronary atherosclerosis. International heart journal 2014;55(3):197–203.

(274) Okura K, Maeno K, Okura S, Takemori H, Toya D, Tanaka N, et al. Pericardial fat volume is an independent risk factor for the severity of coronary artery disease in patients with preserved ejection fraction. J Cardiol 2015;65(1):37–41.

(275) Bo X, Ma L, Fan J, Jiang Z, Zhou Y, Zhang L, et al. Epicardial fat volume is correlated with coronary lesion and its severity. Int J Clin Exp Med 2015 Mar 15;8(3):4328–4334.

(276) Silaghi A, Piercecchi-Marti M, Grino M, Leonetti G, Alessi MC, Clement K, et al. Epicardial adipose tissue extent: relationship with age, body fat distribution, and coronaropathy. Obesity 2008;16(11):2424–2430.

(277) Sequeira DI, Ebert LC, Flach PM, Ruder TD, Thali MJ, Ampanozi G. The correlation of epicardial adipose tissue on postmortem CT with coronary artery stenosis as determined by autopsy. Forensic science, medicine, and pathology 2015;11:186–192.

(278) Verhagen SN, Visseren FL. Perivascular adipose tissue as a cause of atherosclerosis. Atherosclerosis 2011;214(1):3–10.

(279) Hajsadeghi F, Nabavi V, Bhandari A, Choi A, Vincent H, Flores F, et al. Increased epicardial adipose tissue is associated with coronary artery disease and major adverse cardiovascular events. Atherosclerosis 2014;237(2):486–489.

(280) Harada K, Amano T, Uetani T, Tokuda Y, Kitagawa K, Shimbo Y, et al. Cardiac 64-multislice computed tomography reveals increased epicardial fat volume in patients with acute coronary syndrome. Am J Cardiol 2011;108(8):1119–1123.

(281) Mahabadi AA, Berg MH, Lehmann N, Kälsch H, Bauer M, Kara K, et al. Association of epicardial fat with cardiovascular risk factors and incident myocardial infarction in the general population: the Heinz Nixdorf Recall Study. J Am Coll Cardiol 2013;61(13):1388–1395.

(282) Tanami Y, Jinzaki M, Kishi S, Matheson M, Vavere AL, Rochitte CE, et al. Lack of association between epicardial fat volume and extent of coronary artery calcification, severity of coronary artery disease, or presence of myocardial perfusion abnormalities in a diverse, symptomatic patient population: results from the CORE320 multicenter study. Circulation: Cardiovascular Imaging 2015;8(3):e002676.

(283) Van Meijeren AR, Ties D, de Koning ML, Van Dijk R, Van Blokland IV, Veloz PL, et al. Association of epicardial adipose tissue with different stages of coronary artery disease: A cross-sectional UK Biobank cardiovascular magnetic resonance imaging substudy. IJC Heart & Vasculature 2022;40:101006.

(284) Otaki Y, Rajani R, Cheng VY, Gransar H, Nakanishi R, Shmilovich H, et al. The relationship between epicardial fat volume and incident coronary artery calcium. Journal of cardiovascular computed tomography 2011;5(5):310–316.

(285) Romijn MA, Danad I, Bakkum MJ, Stuijfzand WJ, Tulevski II, Somsen GA, et al. Incremental diagnostic value of epicardial adipose tissue for the detection of functionally relevant coronary artery disease. Atherosclerosis 2015;242(1):161–166.

(286) Panda S, Vimala L, Livingstone R, Pearlin B, Irodi A, Joseph E, et al. Can epicardial and pericardial adipose tissue volume predict the presence and severity of coronary artery disease? Polish Journal of Radiology 2022;87(1):348–353.

(287) Muthalaly RG, Nerlekar N, Wong DT, Cameron JD, Seneviratne SK, Ko BS. Epicardial adipose tissue and myocardial ischemia assessed by computed tomography perfusion imaging and invasive fractional flow reserve. Journal of cardiovascular computed tomography 2017;11(1):46–53.

(288) Chaowalit N, Somers VK, Pellikka PA, Rihal CS, Lopez-Jimenez F. Subepicardial adipose tissue and the presence and severity of coronary artery disease. Atherosclerosis 2006;186(2):354–359.

(289) Faust IM, Johnson PR, Stern JS, Hirsch J. Diet-induced adipocyte number increase in adult rats: a new model of obesity. American Journal of Physiology-Endocrinology and Metabolism 1978;235(3):E279.

(290) Bruun JM, Lihn AS, Pedersen SB, Richelsen B. Monocyte chemoattractant protein-1 release is higher in visceral than subcutaneous human adipose tissue (AT): implication of macrophages resident in the AT. The Journal of clinical endocrinology & metabolism 2005;90(4):2282–2289.

(291) Weisberg SP, McCann D, Desai M, Rosenbaum M, Leibel RL, Ferrante AW. Obesity is associated with macrophage accumulation in adipose tissue. J Clin Invest 2003;112(12):1796–1808.

(292) Suganami T, Mieda T, Itoh M, Shimoda Y, Kamei Y, Ogawa Y. Attenuation of obesity-induced adipose tissue inflammation in C3H/HeJ mice carrying a Toll-like receptor 4 mutation. Biochem Biophys Res Commun 2007;354(1):45–49.

(293) Gorter PM, van Lindert AS, de Vos AM, Meijs MF, van der Graaf Y, Doevendans PA, et al. Quantification of epicardial and peri-coronary fat using cardiac computed tomography; reproducibility and relation with obesity and metabolic syndrome in patients suspected of coronary artery disease. Atherosclerosis 2008;197(2):896–903.

(294) Akyol B, Boyraz M, Aysoy C. Relationship of epicardial adipose tissue thickness with early indicators of atherosclerosis and cardiac functional changes in obese adolescents with metabolic syndrome. J Clin Res Pediatr Endocrinol 2013 Sep 10;5(3):156–163.

(295) Schusterova I, Leenen F, Jurko A, Sabol F, Takacova J. Epicardial adipose tissue and cardiometabolic risk factors in overweight and obese children and adolescents. Pediatric obesity 2014;9(1):63–70.

(296) Grundy SM, Brewer Jr HB, Cleeman JI, Smith Jr SC, Lenfant C. Definition of metabolic syndrome: report of the National Heart, Lung, and Blood Institute/American Heart Association conference on scientific issues related to definition. Circulation 2004;109(3):433–438.

(297) Aasum E, Hafstad AD, Severson DL, Larsen TS. Age-dependent changes in metabolism, contractile function, and ischemic sensitivity in hearts from db/db mice. Diabetes 2003;52(2):434–441.

(298) Belke DD, Larsen TS, Gibbs EM, Severson DL. Altered metabolism causes cardiac dysfunction in perfused hearts from diabetic (db/db) mice. American Journal of Physiology-Endocrinology and Metabolism 2000;279(5):E1104–E1113.

(299) Christoffersen C, Bollano E, Lindegaard ML, Bartels ED, Goetze JP, Andersen CB, et al. Cardiac lipid accumulation associated with diastolic dysfunction in obese mice. Endocrinology 2003;144(8):3483–3490.

(300) Zhou Y, Grayburn P, Karim A, Shimabukuro M, Higa M, Baetens D, et al. Lipotoxic heart disease in obese rats: implications for human obesity. Proceedings of the National Academy of Sciences 2000;97(4):1784–1789.

(301) Okyay K, Balcioglu AS, Tavil Y, Tacoy G, Turkoglu S, Abacı A. A relationship between echocardiographic subepicardial adipose tissue and metabolic syndrome. The International Journal of Cardiovascular Imaging 2008;24(6):577–583.

(302) Yorgun H, Canpolat U, Hazırolan T, Ateş AH, Sunman H, Dural M, et al. Increased epicardial fat tissue is a marker of metabolic syndrome in adult patients. Int J Cardiol 2013;165(2):308–313.

(303) Wang C, Hsu H, Hung W, Yu T, Chen Y, Chiu C, et al. Increased epicardial adipose tissue (EAT) volume in type 2 diabetes mellitus and association with metabolic syndrome and severity of coronary atherosclerosis. Clin Endocrinol (Oxf) 2009;70(6):876–882.

(304) Teijeira-Fernandez E, Eiras S, Grigorian-Shamagian L, Fernandez A, Adrio B, Gonzalez-Juanatey JR. Epicardial adipose tissue expression of adiponectin is lower in patients with hypertension. J Hum Hypertens 2008;22(12):856–863.

(305) Sironi AM, Pingitore A, Ghione S, De Marchi D, Scattini B, Positano V, et al. Early hypertension is associated with reduced regional cardiac function, insulin resistance, epicardial, and visceral fat. Hypertension 2008;51(2):282–288.

(306) McGavock JM, Lingvay I, Zib I, Tillery T, Salas N, Unger R, et al. Cardiac steatosis in diabetes mellitus: a 1H-magnetic resonance spectroscopy study. Circulation 2007;116(10):1170–1175.

(307) Iacobellis G, Barbaro G, Gerstein HC. Relationship of epicardial fat thickness and fasting glucose. Int J Cardiol 2008;128(3):424–426.

(308) Sardu C, D'Onofrio N, Torella M, Portoghese M, Loreni F, Mureddu S, et al. Pericoronary fat inflammation and Major Adverse Cardiac Events (MACE) in prediabetic patients with acute myocardial infarction: effects of metformin. Cardiovascular Diabetology 2019;18:1–11.

(309) Versteylen MO, Takx RA, Joosen IA, Nelemans PJ, Das M, Crijns HJ, et al. Epicardial adipose tissue volume as a predictor for coronary artery disease in diabetic, impaired fasting glucose, and non-diabetic patients presenting with chest pain. European Heart Journal–Cardiovascular Imaging 2012;13(6):517–523.

(310) Hasebe H, Yoshida K, Nogami A, Ieda M. Difference in epicardial adipose tissue distribution between paroxysmal atrial fibrillation and coronary artery disease. Heart Vessels 2020;35:1070–1078.

(311) Shin SY, Yong HS, Lim HE, Na JO, Choi CU, Choi JI, et al. Total and interatrial epicardial adipose tissues are independently associated with left atrial remodeling in patients with atrial fibrillation. J Cardiovasc Electrophysiol 2011;22(6):647–655.

(312) Zghaib T, Ipek EG, Zahid S, Balouch MA, Misra S, Ashikaga H, et al. Association of left atrial epicardial adipose tissue with electrogram bipolar voltage and fractionation: electrophysiologic substrates for atrial fibrillation. Heart Rhythm 2016;13(12):2333–2339.

(313) Doesch C, Suselbeck T, Leweling H, Fluechter S, Haghi D, Schoenberg SO, et al. Bioimpedance analysis parameters and epicardial adipose tissue assessed by cardiac magnetic resonance imaging in patients with heart failure. Obesity 2010;18(12):2326–2332.

(314) Khawaja T, Greer C, Chokshi A, Chavarria N, Thadani S, Jones M, et al. Epicardial fat volume in patients with left ventricular systolic dysfunction. Am J Cardiol 2011;108(3):397–401.

(315) Iacobellis G, Ribaudo MC, Zappaterreno A, Iannucci CV, Leonetti F. Relation between epicardial adipose tissue and left ventricular mass. Am J Cardiol 2004;94(8):1084–1087.

(316) Mureddu GF, Greco R, Rosato GF, Cella A, Vaccaro O, Contaldo F, et al. Relation of insulin resistance to left ventricular hypertrophy and diastolic dysfunction in obesity. Int J Obes 1998;22(4):363–368.

(317) Doesch C, Haghi D, Flüchter S, Suselbeck T, Schoenberg SO, Michaely H, et al. Epicardial adipose tissue in patients with heart failure. J Cardiovasc Magn Reson 2010;12(1):1–9.

(318) Liu J, Fox CS, Hickson DA, May WL, Ding J, Carr JJ, et al. Pericardial fat and echocardiographic measures of cardiac abnormalities: the Jackson Heart Study. Diabetes Care 2011;34(2):341–346.

(319) van Woerden G, Gorter TM, Westenbrink BD, Willems TP, van Veldhuisen DJ, Rienstra M. Epicardial fat in heart failure patients with mid-range and preserved ejection fraction. European journal of heart failure 2018;20(11):1559–1566.

(320) Abel ED, Doenst T. Mitochondrial adaptations to physiological vs. pathological cardiac hypertrophy. Cardiovasc Res 2011;90(2):234–242.

(321) Abrishami A, Eslami V, Baharvand Z, Khalili N, Saghamanesh S, Zarei E, et al. Epicardial adipose tissue, inflammatory biomarkers and COVID-19: Is there a possible relationship? Int Immunopharmacol 2021;90:107174.

(322) Slipczuk L, Castagna F, Schonberger A, Novogrodsky E, Sekerak R, Dey D, et al. Coronary artery calcification and epicardial adipose tissue as independent predictors of mortality in COVID-19. The International Journal of Cardiovascular Imaging 2021;37(10):3093–3100.

(323) Deng M, Qi Y, Deng L, Wang H, Xu Y, Li Z, et al. Obesity as a potential predictor of disease severity in young COVID-19 patients: a retrospective study. Obesity 2020;28(10):1815–1825.

(324) Launbo N, Zobel EH, von Scholten BJ, Færch K, Jørgensen PG, Christensen RH. Targeting epicardial adipose tissue with exercise, diet, bariatric surgery or pharmaceutical interventions: a systematic review and meta-analysis. Obesity Reviews 2021;22(1):e13136.

(325) Steinberg D. The statins in preventive cardiology. N Engl J Med 2008;359(14):1426–1427.

(326) Ray KK, Cannon CP. The potential relevance of the multiple lipid-independent (pleiotropic) effects of statins in the management of acute coronary syndromes. J Am Coll Cardiol 2005;46(8):1425–1433.

(327) Kang J, Kim Y, Park JJ, Kim S, Kang S, Cho YJ, et al. Increased epicardial adipose tissue thickness is a predictor of new-onset diabetes mellitus in patients with coronary artery disease treated with high-intensity statins. Cardiovascular Diabetology 2018;17:1–9.

(328) Park J, Park YS, Kim YJ, Lee IS, Kim JH, Lee J, et al. Effects of statins on the epicardial fat thickness in patients with coronary artery stenosis underwent percutaneous coronary intervention: comparison of atorvastatin with simvastatin/ezetimibe. Journal of Cardiovascular Ultrasound 2010;18(4):121–126.

(329) Alexopoulos N, Melek BH, Arepalli CD, Hartlage G, Chen Z, Kim S, et al. Effect of intensive versus moderate lipid-lowering therapy on epicardial adipose tissue in hyperlipidemic post-menopausal women: a substudy of the BELLES trial (Beyond Endorsed Lipid Lowering with EBT Scanning). J Am Coll Cardiol 2013;61(19):1956–1961.

(330) Raggi P, Gadiyaram V, Zhang C, Chen Z, Lopaschuk G, Stillman AE. Statins reduce epicardial adipose tissue attenuation independent of lipid lowering: a potential pleiotropic effect. Journal of the American Heart Association 2019;8(12):e013104.

(331) Parisi V, Petraglia L, D'Esposito V, Cabaro S, Rengo G, Caruso A, et al. Statin therapy modulates thickness and inflammatory profile of human epicardial adipose tissue. Int J Cardiol 2019;274:326–330.

(332) Tokubuchi I, Tajiri Y, Iwata S, Hara K, Wada N, Hashinaga T, et al. Beneficial effects of metformin on energy metabolism and visceral fat volume through a possible mechanism of fatty acid oxidation in human subjects and rats. PloS one 2017;12(2):e0171293.

(333) Ziyrek M, Kahraman S, Ozdemir E, Dogan A. Metformin monotherapy significantly decreases epicardial adipose tissue thickness in newly diagnosed type 2 diabetes patients. Revista Portuguesa de Cardiologia 2019;38(6):419–423.

(334) Sacks HS, Fain JN, Cheema P, Bahouth SW, Garrett E, Wolf RY, et al. Inflammatory genes in epicardial fat contiguous with coronary atherosclerosis in the metabolic syndrome and type 2 diabetes: changes associated with pioglitazone. Diabetes Care 2011;34(3):730–733.

(335) Grosso AF, de Oliveira SF, Higuchi MdL, Favarato D, Dallan LAdO, da Luz PL. Synergistic anti-inflammatory effect: simvastatin and pioglitazone reduce inflammatory markers of plasma and epicardial adipose tissue of coronary patients with metabolic syndrome. Diabetology & metabolic syndrome 2014;6(1):1–8.

(336) Distel E, Penot G, Cadoudal T, Balguy I, Durant S, Benelli C. Early induction of a brown-like phenotype by rosiglitazone in the epicardial adipose tissue of fatty Zucker rats. Biochimie 2012;94(8):1660–1667.

(337) Jonker JT, Lamb HJ, Van der Meer RW, Rijzewijk LJ, Menting LJ, Diamant M, et al. Pioglitazone compared with metformin increases pericardial fat volume in patients with type 2 diabetes mellitus. The Journal of Clinical Endocrinology & Metabolism 2010;95(1):456–460.

(338) Vallon V, Verma S. Effects of SGLT2 inhibitors on kidney and cardiovascular function. Annu Rev Physiol 2021;83:503–528.

(339) Bolinder J, Ljunggren Ö, Kullberg J, Johansson L, Wilding J, Langkilde AM, et al. Effects of dapagliflozin on body weight, total fat mass, and regional adipose tissue distribution in patients with type 2 diabetes mellitus with inadequate glycemic control on metformin. The Journal of Clinical Endocrinology & Metabolism 2012;97(3):1020–1031.

(340) Bouchi R, Terashima M, Sasahara Y, Asakawa M, Fukuda T, Takeuchi T, et al. Luseogliflozin reduces epicardial fat accumulation in patients with type 2 diabetes: a pilot study. Cardiovascular Diabetology 2017;16:1–9.

(341) Fukuda T, Bouchi R, Terashima M, Sasahara Y, Asakawa M, Takeuchi T, et al. Ipragliflozin reduces epicardial fat accumulation in non-obese type 2 diabetic patients with visceral obesity: a pilot study. Diabetes Therapy 2017;8:851–861.

(342) Sato T, Aizawa Y, Yuasa S, Fujita S, Ikeda Y, Okabe M. The effect of dapagliflozin treatment on epicardial adipose tissue volume and P-wave indices: an ad-hoc analysis of the previous randomized clinical trial. J Atheroscler Thromb 2020;27(12):1348–1358.

(343) Anker SD, Butler J, Filippatos GS, Jamal W, Salsali A, Schnee J, et al. Evaluation of the effects of sodium–glucose co-transporter 2 inhibition with empagliflozin on morbidity and mortality in patients with chronic heart failure and a preserved ejection fraction: rationale for and design of the EMPEROR-Preserved Trial. European journal of heart failure 2019;21(10):1279–1287.

(344) Iacobellis G, Mohseni M, Bianco SD, Banga PK. Liraglutide causes large and rapid epicardial fat reduction. Obesity 2017;25(2):311–316.

(345) Dutour A, Abdesselam I, Ancel P, Kober F, Mrad G, Darmon P, et al. Exenatide decreases liver fat content and epicardial adipose tissue in patients with obesity and type 2 diabetes: a prospective randomized clinical trial using magnetic resonance imaging and spectroscopy. Diabetes, Obesity and Metabolism 2016;18(9):882–891.

(346) Beiroa D, Imbernon M, Gallego R, Senra A, Herranz D, Villarroya F, et al. GLP-1 agonism stimulates brown adipose tissue thermogenesis and browning through hypothalamic AMPK. Diabetes 2014;63(10):3346–3358.

(347) Pastel E, McCulloch LJ, Ward R, Joshi S, Gooding KM, Shore AC, et al. GLP-1 analogue-induced weight loss does not improve obesity-induced AT dysfunction. Clin Sci 2017;131(5):343–353.

(348) Mulvihill EE, Varin EM, Ussher JR, Campbell JE, Bang KA, Abdullah T, et al. Inhibition of dipeptidyl peptidase-4 impairs ventricular function and promotes cardiac fibrosis in high fat–fed diabetic mice. Diabetes 2016;65(3):742–754.

(349) Iacobellis G, Camarena V, Sant DW, Wang G. Human epicardial fat expresses glucagon-like peptide 1 and 2 receptors genes. Hormone and Metabolic Research 2017;49(08):625–630.

(350) Lima-Martínez MM, Paoli M, Rodney M, Balladares N, Contreras M, D'Marco L, et al. Effect of sitagliptin on epicardial fat thickness in subjects with type 2 diabetes and obesity: a pilot study. Endocrine 2016;51:448–455.

(351) Iacobellis G, Mohseni M, Bianco S. Liraglutide causes massive and rapid reduction of cardiac fat independent of weight loss in type 2 diabetes. The 75th American Diabetes Association, Scientific Sessions, LBA-5785, Boston, USA 2015.

(352) Iacobellis G, Villasante Fricke AC. Effects of semaglutide versus dulaglutide on epicardial fat thickness in subjects with type 2 diabetes and obesity. Journal of the Endocrine Society 2020;4(4):bvz042.

(353) Elisha B, Azar M, Taleb N, Bernard S, Iacobellis G, Rabasa-Lhoret R. Body composition and epicardial fat in type 2 diabetes patients following insulin detemir versus insulin glargine initiation. Hormone and metabolic research 2016;48(01):42–47.

(354) Konwerski M, Gąsecka A, Opolski G, Grabowski M, Mazurek T. Role of epicardial adipose tissue in cardiovascular diseases: a review. Biology 2022;11(3):355.

(355) Christensen RH, Wedell-Neergaard A, Lehrskov LL, Legaard GE, Dorph E, Larsen MK, et al. Effect of aerobic and resistance exercise on cardiac adipose tissues: secondary analyses from a randomized clinical trial. JAMA cardiology 2019;4(8):778–787.

(356) Fernandez-del-Valle M, Gonzales JU, Kloiber S, Mitra S, Klingensmith J, Larumbe-Zabala E. Effects of resistance training on MRI-derived epicardial fat volume and arterial stiffness in women with obesity: a randomized pilot study. Eur J Appl Physiol 2018;118:1231–1240.

(357) Kahl KG, Kerling A, Tegtbur U, Gützlaff E, Herrmann J, Borchert L, et al. Effects of additional exercise training on epicardial, intra-abdominal and subcutaneous adipose tissue in major depressive disorder: A randomized pilot study. J Affect Disord 2016;192:91–97.

(358) Konwerski M, Postuła M, Barczuk-Falęcka M, Czajkowska A, Mróz A, Witek K, et al. Epicardial adipose tissue and cardiovascular risk assessment in ultra-marathon runners: a pilot study. International journal of environmental research and public health 2021;18(6):3136.

(359) Saco-Ledo G, Valenzuela PL, Castillo-García A, Arenas J, León-Sanz M, Ruilope LM, et al. Physical exercise and epicardial adipose tissue: a systematic review and meta-analysis of randomized controlled trials. Obesity Reviews 2021;22(1):e13103.

(360) Gepner Y, Shelef I, Schwarzfuchs D, Zelicha H, Tene L, Yaskolka Meir A, et al. Effect of distinct lifestyle interventions on mobilization of fat storage pools: CENTRAL magnetic resonance imaging randomized controlled trial. Circulation 2018;137(11):1143–1157.

(361) Snel M, Jonker JT, Hammer S, Kerpershoek G, Lamb HJ, Meinders AE, et al. Long-term beneficial effect of a 16-week very low calorie diet on pericardial fat in obese type 2 diabetes mellitus patients. Obesity 2012;20(8):1572–1576.

(362) Kim M, Tanaka K, Kim M, Matuso T, Endo T, Tomita T, et al. Comparison of epicardial, abdominal and regional fat compartments in response to weight loss. Nutrition, Metabolism and Cardiovascular Diseases 2009;19(11):760–766.

(363) Kim M, Tomita T, Kim M, Sasai H, Maeda S, Tanaka K. Aerobic exercise training reduces epicardial fat in obese men. J Appl Physiol 2009;106(1):5–11.

(364) Iacobellis G, Singh N, Wharton S, Sharma AM. Substantial changes in epicardial fat thickness after weight loss in severely obese subjects. Obesity 2008;16(7):1693–1697.

(365) Gaborit B, Jacquier A, Kober F, Abdesselam I, Cuisset T, Boullu-Ciocca S, et al. Effects of bariatric surgery on cardiac ectopic fat: lesser decrease in epicardial fat compared to visceral fat loss and no change in myocardial triglyceride content. J Am Coll Cardiol 2012;60(15):1381–1389.

(366) Hannukainen JC, Lautamäki R, Pärkkä J, Strandberg M, Saunavaara V, Hurme S, et al. Reversibility of myocardial metabolism and remodelling in morbidly obese patients 6 months after bariatric surgery. Diabetes, Obesity and Metabolism 2018;20(4):963–973.

(367) Graziani F, Leone AM, Cialdella P, Basile E, Della Bona R, Iaconelli A, et al. Effects of bariatric surgery on cardiac remodeling: clinical and pathophysiologic implications. Eur Heart J 2013;34(suppl_1):4356.

(368) Altin C, Erol V, Aydin E, Yilmaz M, Tekindal MA, Sade LE, et al. Impact of weight loss on epicardial fat and carotid intima media thickness after laparoscopic sleeve gastrectomy: a prospective study. Nutrition, Metabolism and Cardiovascular Diseases 2018;28(5):501–509.

(369) Willens HJ, Byers P, Chirinos JA, Labrador E, Hare JM, de Marchena E. Effects of weight loss after bariatric surgery on epicardial fat measured using echocardiography. Am J Cardiol 2007;99(9):1242–1245.

(370) Rabkin SW, Campbell H. Comparison of reducing epicardial fat by exercise, diet or bariatric surgery weight loss strategies: a systematic review and meta-analysis. Obesity reviews 2015;16(5):406–415.

(371) Funk S, Kermer J, Doganguezel S, Schwenke C, von Knobelsdorff-Brenkenhoff F, Schulz-Menger J. Quantification of the left atrium applying cardiovascular magnetic resonance in clinical routine. Scandinavian Cardiovascular Journal 2018;52(2):85–92.

(372) Kawel N, Nacif M, Zavodni A, Jones J, Liu S, Sibley CT, et al. T1 mapping of the myocardium: intra-individual assessment of the effect of field strength, cardiac cycle and variation by myocardial region. J Cardiovasc Magn Reson 2012;14(1):1–10.

(373) Hudsmith LE, Petersen SE, Tyler DJ, Francis JM, Cheng AS, Clarke K, et al. Determination of cardiac volumes and mass with FLASH and SSFP cine sequences at 1.5 vs. 3 Tesla: a validation study. Journal of Magnetic Resonance Imaging: An Official Journal of the International Society for Magnetic Resonance in Medicine 2006;24(2):312–318.

(374) Knuuti J, Wijns W, Saraste A, Capodanno D, Barbato E, Funck-Brentano C, et al. 2019 ESC Guidelines for the diagnosis and management of chronic coronary syndromes: The Task Force for the diagnosis and management of chronic coronary syndromes of the European Society of Cardiology (ESC). Eur Heart J 2020;41(3):407–477.

(375) Task Force Members, Montalescot G, Sechtem U, Achenbach S, Andreotti F, Arden C, et al. 2013 ESC guidelines on the management of stable coronary artery disease: the Task Force on the management of stable coronary artery disease of the European Society of Cardiology. Eur Heart J 2013;34(38):2949–3003.

(376) Bax JJ, Baumgartner H, Ceconi C, Dean V, Fagard R, Funck-Brentano C, et al. Third universal definition of myocardial infarction. J Am Coll Cardiol 2012;60(16):1581–1598.

(377) Thygesen K, Alpert JS, Jaffe AS, Chaitman BR, Bax JJ, Morrow DA, et al. Fourth universal definition of myocardial infarction (2018). J Am Coll Cardiol 2018;72(18):2231–2264.

(378) Campeau L. Letter: Grading of angina pectoris. Circulation 1976 Sep;54(3):522–523.

(379) Rampidis GP, Benetos G, Benz DC, Giannopoulos AA, Buechel RR. A guide for Gensini Score calculation. Atherosclerosis 2019;287:181–183.

(380) Neeland IJ, Patel RS, Eshtehardi P, Dhawan S, McDaniel MC, Rab ST, et al. Coronary angiographic scoring systems: an evaluation of their equivalence and validity. Am Heart J 2012;164(4):547–552. e1.

(381) Gensini GG. A more meaningful scoring system for determining the severity of coronary heart disease. Am J Cardiol 1983;51:606.

(382) Prasad K. Current status of primary, secondary, and tertiary prevention of coronary artery disease. International Journal of Angiology 2021;30(03):177–186.

(383) Nuttall FQ. Body mass index: obesity, BMI, and health: a critical review. Nutrition today 2015;50(3):117.

(384) DuBois D. A formula to estimate the approx-imate surface area if height and weight be known. Arch Intern Med 1916;17:863–871.

(385) Bois D. A formula to estimate the approximate surface area if height and weight be known. 1916. Nutrition 1989;5:303.

(386) Parsaee M, Faghihi SH, Vasheghani A. Assciation between epicardial fat thickness and premature coronary artery disease. 2014.

(387) Kamal D, Abd ElMoteleb AM, Samir R, Saeed M. Epicardial fat thickness can predict severity and multivessel distribution in Egyptian patients with atherosclerotic coronary artery stenosis. The Egyptian Heart Journal 2018;70(4):323–327.

(388) Tekin I, Edem E. Association of epicardial fat tissue with coronary artery disease and left ventricle diastolic function indicators. Medical science monitor: international medical journal of experimental and clinical research 2018;24:6367.

(389) Meenakshi K, Rajendran M, Srikumar S, Chidambaram S. Epicardial fat thickness: A surrogate marker of coronary artery disease–Assessment by echocardiography. Indian Heart J 2016;68(3):336–341.

(390) Erkan AF, Tanindi A, Kocaman SA, Ugurlu M, Tore HF. Epicardial adipose tissue thickness is an independent predictor of critical and complex coronary artery disease by Gensini and syntax scores. Texas Heart Institute Journal 2016;43(1):29–37.

(391) Ghaderi F, Eshraghi A, Shamloo AS, Mousavi S. Assosiation of epicardial and pericardial fat thickness with coronary artery disease. Electronic physician 2016;8(9):2982.

(392) Shemirani H, Meysam Khoshavi M. Correlation of echocardiographic epicardial fat thickness with severity of coronary artery disease-an observational study. Anatolian Journal of Cardiology/Anadolu Kardiyoloji Dergisi 2012;12(3).

(393) Yañez-Rivera TG, Baños-Gonzalez MA, Ble-Castillo JL, Torres-Hernandez ME, Torres-Lopez JE, Borrayo-Sanchez G. Relationship between epicardial adipose tissue, coronary

artery disease and adiponectin in a Mexican population. Cardiovascular ultrasound 2014;12:1–6.

(394) Iacobellis G, Lonn E, Lamy A, Singh N, Sharma AM. Epicardial fat thickness and coronary artery disease correlate independently of obesity. Int J Cardiol 2011 Feb 3;146(3):452–454.

(395) Shambu SK, Desai N, Sundaresh N, Babu MS, Madhu B, Gona OJ. Study of correlation between epicardial fat thickness and severity of coronary artery disease. Indian Heart J 2020;72(5):445–447.

(396) Maimaituxun G, Shimabukuro M, Fukuda D, Yagi S, Hirata Y, Iwase T, et al. Local Thickness of Epicardial Adipose Tissue Surrounding the Left Anterior Descending Artery Is a Simple Predictor of Coronary Artery Disease—New Prediction Model in Combination With Framingham Risk Score—. Circulation Journal 2018;82(5):1369–1378.

(397) Gać P, Macek P, Poręba M, Kornafel-Flak O, Mazur G, Poręba R. Thickness of epicardial and pericoronary adipose tissue measured using 128-slice MSCT as predictors for risk of significant coronary artery diseases. Irish Journal of Medical Science (1971-) 2021;190:555–566.

(398) Bachar GN, Dicker D, Kornowski R, Atar E. Epicardial adipose tissue as a predictor of coronary artery disease in asymptomatic subjects. Am J Cardiol 2012;110(4):534–538.

(399) Alnaggar MF, Samy NI, Abdalzez WF. Epicardial fat measured by multidetector computed tomography and coronary artery disease. Menoufia Medical Journal 2020;33(1):303–308.

(400) Refaat M, Abo Elezz MO, Helmy IM, Helal AFMI, El-shazly IM. Diagnostic value of Multi Detector Computed Tomography in Assessment of Epicardial Adipose Tissue with Coronary Artery Disease. Benha Medical Journal 2023.

(401) Khurana R, Yadav A, Buxi T, Sawhney J, Rawat KS, Ghuman SS. Correlation of epicardial fat quantification with severity of coronary artery disease: A study in Indian population. Indian Heart J 2018;70:S140–S145.

(402) Shehata SM, Zaiton FM, Warda MA. Role of MDCT in evaluation of epicardial fat volume as an independent risk factor for coronary atherosclerosis. The Egyptian Journal of Radiology and Nuclear Medicine 2018;49(2):329–337.

(403) Taha DA, El Shafey RAA, Hamesa MF, Abu-Dewan KAE, Nagy HA. Relationship between epicardial fat volume measured by multi-detector computed tomography and coronary artery disease. Egyptian Journal of Radiology and Nuclear Medicine 2021;52:1–16.

(404) Merelo-Nicolás M, Consuegra-Sánchez L, Pinar-Bermúdez E, Wasniewski S, León-Allocca RA, Ramos-Ruiz P, et al. Relationship of epicardial adipose tissue with coronary artery disease, cardiovascular risk factors and patient outcomes. REC: CardioClinics 2022;57(3):165–171.

(405) Wu F, Chou K, Huang Y, Wu M. The relation of location-specific epicardial adipose tissue thickness and obstructive coronary artery disease: systemic review and meta-analysis of observational studies. BMC cardiovascular disorders 2014;14(1):1–10.

8 Tabular curriculum vitae

Andrej Dobrovolskij

BERUFSERFAHRUNG

[05.12.2023–Aktuell] **Facharzt (Radiologie)**

Gemeinschaftsklinikum Mittelrhein (Kemperhof)

Ort: Koblenz | Land: Deutschland

[01.01.2019–04.12.2023] **Arzt in Weiterbildung (Radiologie)**

Gemeinschaftsklinikum Mittelrhein (Kemperhof)

Ort: Koblenz | Land: Deutschland

[27.04.2018–07.12.2018] **Herzsportarzt**

GO-IN Bautzen

Ort: Bautzen | Land: Deutschland

[02.11.2017–14.11.2018] **Arzt in Weiterbildung (Innere Medizin)**

Oberlausitz-Kliniken Bautzen. Medizinische Klinik I und II

Ort: Bautzen | Land: Deutschland

[05.02.2017–20.05.2017] **Internatur**

Universitätsklinikum Santariškės

Ort: Vilnius | Land: Litauen

28.04.2017-21.05.2017. III. Abteilung für Intensivmedizin
27.03.2017-27.04.2017. Zentrum für Kinder - und Jugendmedizin
03.03.2017-26.03.2017. Zentrum für Gynäkologie und Geburtshilfe
06.02.2017-02.03.2017. Abteilungen für Anästhesiologie.

Famulatur

01.07.2016-31.07.2016. Universitätsklinikum Santariškės. Zentrum für Radiologie und Nuklearmedizin, Vilnius, Litauen

01.08.2016-28.08.2016. Helios Klinik Cuxhaven. Klinik für Anästhesiologie, Intensivmedizin, Notfallmedizin und Schmerztherapie, Cuxhaven, Deutschland

03.08.2015-31.08.2015. Universitätsklinikum Santariškės. Abteilungen für Anästhesiologie und Intensivmedizin, Vilnius, Litauen

ALLGEMEINE UND BERUFLICHE BILDUNG

[30.03.2020–Aktuell] **Promotion**

Johannes Gutenberg-Universität Mainz

Ort: Mainz | Land: Deutschland

Kurse:

- Literaturverwaltung mit EndNote (1 CP)
- Effektive Suche medizinischer Literatur in PubMed (1 CP)
- Lesestrategien und Zeitmanagement (1 CP)
- Rohtexten und Überarbeiten (1 CP)
- Einführung in Klinische Studien (2 CP)
- Gute wissenschaftliche Praxis (1 CP)
- Academic Writing in English (2 CP)
- Tierexperimentelle Eingriffe an Versuchstieren (2 CP)
- Wissenschaftliches Schreiben für Peer-Reviewed Journals (1 CP)
- Führungskräfte kompakt (2 CP)
- Zielgerichtete Kommunikation und Konfliktklärung (2 CP)
- Grundlagenworkshop Projektmanagement: Erfolgreich das Promotionsprojekt managen (2 CP)
- Intercultural Communication (2 CP)

[02.11.2017–Aktuell] **Approbation als Arzt**

Landesdirektion Sachsen

Ort: Dresden | Land: Deutschland

[31.08.2011–26.06.2017] **Master der Medizin**

Universität Vilnius, Fakultät für Medizin

Ort: Vilnius | Land: Litauen

Abschlussnote: 1,3 (nach Konvertierung der Noten durch JGU, Mainz)

Abschlussarbeit: Thickness and Volume of Epicardial Adipose Tissue: Risk Assessment of Essential Hypertension

Durchschnittsnote - 9,29 (maximum - 10) Internaturprüfung – 10

Wissenschaftliche Arbeiten:

- Häufigkeit des Auftretens akzessorischer Nierenarterien, ihre Anatomie sowie Unterschiede des Auftretens bei den Geschlechten

- Bewertung akzessorischer Nierenarterien als mögliche Risikofaktoren für das Auftreten einer essentiellen Hypertonie. Muss man sie wirklich fürchten?
- Dicke und Volumen des epikardischen Fettgewebes: Risikobewertung einer essentiellen Hypertonie
- Einfluss der Tageszeit bei orthotopischen Lebertransplantationen
- Auftreten eines Postreperfusionssyndroms bei orthotopischen Lebertransplantationen
- Der Einfluss von Hypotonie auf die Sauerstoffversorgung des Gehirns beim Operieren im Sitzen: Vergleich zweier verschiedener Narkosearten
- Der Einfluss von Vollnarkose mit zusätzlicher regionaler Betäubung und die Dauer von Operation und Klinikaufenthalt bei Schulterarthroskopien
- Identifizierung der die intraartikuläre Visualisierung bei einer arthroskopischen Schulteroperation beeinflussenden Faktoren

[23.07.2015–14.09.2015] Kurs: Statistik in der Medizin

Universität Stanford

Ort: Stanford | Land: Vereinigten Staaten

Abschluss mit Auszeichnung

[31.08.1999–13.07.2011] Abschlusszeugnis

Naujamiestis - Mittelschule

Ort: Vilnius | Land: Litauen

Abschluss mit Auszeichnung

[31.08.2007–22.05.2011] Fachorientierte musikalische Ausbildung

"Ažuoliukas" Musikschule

Ort: Vilnius | Land: Litauen

Abschluss mit Auszeichnung

[31.08.1999–22.05.2007] Musikalische Grundausbildung

"Ažuoliukas" Musikschule

Ort: Vilnius | Land: Litauen

Abschluss mit Auszeichnung

PUBLIKATIONEN

[2025] Mental Health First Aid Knowledge among Students in Lithuania (accepted manuscript)

Quellenangabe: Archives of Psychiatry Research

[2019] Epicardial Adipose Tissue Accumulation and Essential Hypertension in Non-Obese Adults

Quellenangabe: Austys D, Dobrovolskij A, Jablonskienė V, Dobrovolskij V, Valevičienė N, Stukas R. Epicardial Adipose Tissue Accumulation and Essential Hypertension in Non-Obese Adults. Medicina (Kaunas). 2019 Aug 9;55(8):456. doi: 10.3390/medicina55080456. PMID: 31405056; PMCID: PMC6723255.

KONFERENZEN (VORTRÄGE)

[13.07.2022–17.07.2022] **European Congress of Radiology (ECR) 2022** | Wien (Österreich)

Poster: Indexation Techniques of Epicardial Adipose Tissue in Prediction of Coronary Artery Disease

[03.03.2021–07.03.2021] **European Congress of Radiology (ECR) 2021** | Wien (Österreich)

Vortrag: Measurement Techniques of Epicardial Adipose Tissue in the Diagnosis of Coronary Heart Disease

[15.07.2020–19.07.2020] **European Congress of Radiology (ECR) 2020** | Wien (Österreich)

Vortrag: Increased Epicardial Adipose Tissue Accumulation as a Predictor for Essential Hypertension in non-obese Adults

[11.09.2019–14.09.2019] **38th European Society of Regional Anesthesia (ESRA) Congress** | Bilbao (Spanien)

Vortrag: Cerebral Oxygenation using near-infrared Spectroscopy in beach-chair Position during Shoulder Arthroscopy under different Anaesthesia Types

[11.05.2018–12.05.2018] **IV Annual International Conference of the Baltic Society of Regional Anaesthesia** | Jurmala (Lettland)

Vortrag: Cerebral Oxygenation using near-infrared Spectroscopy in bear-chair Position during Shoulder Arthroscopy under different Anaesthesia Types

Einer der drei besten Vorträge der Konferenz

[05.05.2017–06.05.2017] **III Annual International Conference of the Baltic Society of Regional Anaesthesia** | Pärnu (Estland)

Vortrag: Influence of Anaesthesia Choice for the Intra-articular Shoulder Field Visualization

Einer der drei besten Vorträge der Konferenz

[20.04.2017–22.04.2017] **12th Bialystok International Medical Congress for Young Scientists** | Bialystok (Polen)

Vortrag: Identification of the Factors affecting Intra-articular Visualization during Shoulder Arthroscopic Surgery

[05.04.2017–05.04.2017] **Rīga Stradiņš University (RSU) International Student Conference** | Riga (Lettland)

Vortrag: Postreperfusion Syndrome during Orthotopic Liver Transplantation

Vortrag: Impact of a Composite Inhalational and Regional Anesthesia to the Optimization of Perioperative Period during Shoulder Arthroscopy

[09.11.2016–12.11.2016] **9th European Public Health Conference (EPH)** | Wien (Österreich)

Vortrag: Epicardial Adipose Tissue in Patients with Coronary Artery Disease: Healthy vs. Unhealthy Lifestyle

[14.06.2016–19.06.2016] **Evolutionary Medicine: Pre-existing Mechanisms and Patterns of Current Health Issue** | Vilnius (Litauen)

Vortrag: Accumulation of Epicardial Adipose Tissue: Myocardial Infarction versus Chronic Ischemia

SPRACHKENNTNISSE

Muttersprache(n): Litauisch und Russisch

Sprache(n):

Litauisch

Hören C2; **Lesen** C2; **Schreiben** C2; **Zusammenhängendes sprechen** C2; **An Gesprächen teilnehmen** C2

Russisch

Hören C2; **Lesen** C2; **Schreiben** C2; **Zusammenhängendes sprechen** C2; **An Gesprächen teilnehmen** C2

Englisch

Hören C2; **Lesen** C2; **Schreiben** C2; **Zusammenhängendes sprechen** C1; **An Gesprächen teilnehmen** C1

Deutsch

Hören C1; **Lesen** C1; **Schreiben** C1; **Zusammenhängendes sprechen** C1; **An Gesprächen teilnehmen** C1

Stufen: A1 und A2: Elementar; B1 und B2: Selbstständig; C1 und C2: Kompetent